

Report No. CSS05-09
June 1, 2006



Center for Sustainable Systems
University of Michigan

**Life Cycle Assessment of the 33 kW
Photovoltaic System on the Dana Building
at the University of Michigan:
Thin Film Laminates, Multi-crystalline Modules, and Balance of
System Components**

Sergio Pacca, Deepak Sivaraman and Gregory A. Keoleian

**Life Cycle Assessment of the 33 kW Photovoltaic System on the
Dana Building at the University of Michigan:
Thin Film Laminates, Multi-crystalline Modules, and Balance of System
Components**

Sergio Pacca, Deepak Sivaraman and Gregory A. Keoleian
Center for Sustainable Systems

University of Michigan
Ann Arbor

June 1, 2006

A report of the Center for Sustainable Systems
Report No. CSS05-09

Document Description

LIFE CYCLE ASSESSMENT OF THE 33 kW PHOTOVOLTAIC SYSTEM ON THE
DANA BUILDING AT THE UNIVERSITY OF MICHIGAN: THIN FILM LAMINATES,
MULTI-CRYSTALLINE MODULES, AND BALANCE OF SYSTEM COMPONENTS

Sergio Pacca, Deepak Sivaraman and Gregory A. Keoleian

Center for Sustainable Systems, Report No. CSS05-09

University of Michigan, Ann Arbor, Michigan

June 1, 2006

87 pp., 16 tables, 44 figures, 11 appendices

This document is available online at: <http://css.snre.umich.edu>

Center for Sustainable Systems
School of Natural Resources and Environment
University of Michigan
440 Church Street, Dana Building
Ann Arbor, MI 48109-1041
Phone: 734-764-1412
Fax: 734-647-5841
Email: css.info@umich.edu
Web: <http://css.snre.umich.edu>

Acknowledgements

The installation of a large photovoltaic system on the roof of the Dana building was made possible through the support of:

Wege Foundation
United Solar Ovonix LLC
Ballard Power Systems
University of Michigan

We would also like to thank:

- Dr. Subhendu Guha, Allan Greg, and Alen Cheng from United Solar Ovonix LLC for providing us with material and energy data for the United Solar modules and assisting with the design and installation of the data acquisition system (DAS)
- Glenn Kowalske and Jurgen Juziuk from Ballard Power Systems for their assistance in data collection and life cycle modeling of the inverter
- David Spitzley and Geoffrey Lewis for sharing the data collected previously at United Solar Ovonix LLC
- Yoshiko Hill and William O'Dell for providing technical data and specifications for the PV system, and managing the installation and commissioning of the PV System
- William Weakley and Richard Wickboldt for their timely response to questions regarding the University of Michigan Campus Power Plant (CPP)
- Philip Ray for helping us with the hardware required for the working of the PV DAS

Deepak Sivaraman is very grateful for his 2004/2005 graduate student research assistantship provided in conjunction with the project.

TABLE OF CONTENTS

1.	Purpose of the Study	8
2.	Literature Review of Life Cycle Assessment of Photovoltaic Systems	9
2.1.	Factors Driving the Results of PV LCA	11
2.1.1.	Technological Options	11
2.1.2.	Incoming Solar Radiation	14
2.1.3.	Balance of the System (BOS)	14
2.1.4.	Installation Type	15
2.1.5.	Conversion Efficiency Trend	18
2.1.6.	Lifetime of the System	18
3.	Methods	20
3.1.	Life Cycle Assessment of the Photovoltaic System	20
3.1.1.	Photovoltaic System Characterization	21
3.1.2.	Functional Unit	22
3.1.3.	Assumptions	23
3.1.4.	United Solar Thin Film Amorphous Modules	23
3.1.5.	Kyocera Multi-crystalline Modules	30
3.1.6.	Balance of the System	32
3.1.6.1.	Balance of the System - Kyocera Modules	33
3.1.6.2.	Balance of the System - UNI-SOLAR Modules	35
3.1.7.	Common Balance of the System Components	35
3.1.7.1.	Combiner Box	35
3.1.7.2.	Inverter	36
3.1.8.	Installation	38
3.2.	Power and Solar Radiation Availability	39
3.2.1.	Solar Radiation Calculation and Module Position	40
3.2.2.	Expected Electrical Output	43
3.3.	Inventory of Electricity Supply for the Dana Building	45
3.3.1.	Campus Power Plant (CPP)	45
3.3.2.	Compensatory Heating System for PV	48

4.	Results and Discussion	49
4.1.	Primary Energy Consumption.....	49
4.2.	Environmental Emissions and Impacts.....	51
4.3.	Environmental Footprint of the Three PV Modules	52
4.4.	Net Energy Ratio.....	54
4.5.	Energy Pay Back Time	56
4.5.1.	Kyocera Modules' Pay Back Time With and Without the Frame	59
4.6.	Pollution Prevention Benefits	61
4.7.	Sensitivity Analysis of Pollution Prevention Benefits.....	64
4.8.	Life Cycle Impact Assessment Results.....	65
4.8.1.	Human Health Benefits:.....	65
4.8.2.	Ecological Benefits:	67
4.9.	Unique Scenario.....	71
4.10.	Cost Comparison of PV Technologies.....	72
5.	Conclusions.....	74
6.	Outreach Resources	77
6.1.	PV Technology Description.....	77
6.2.	Renewable Energy in the US	79
6.3.	Benefits of Renewable Energy Use	80
6.4.	Data Acquisition System and Lobby Display.....	80
6.5.	Theoretical vs. Actual Data Comparison and Comparison with NREL Data.....	83
7.	References.....	85
	Appendix 1: Bill of Materials	A-1
	Appendix 2: UNI-SOLAR Shingle ASR128 Specifications	A-2
	Appendix 3: UNI-SOLAR PVL Specifications.....	A-3
	Appendix 4: KC120 Specification Sheet.....	A-4
	Appendix 5: Solar Radiation in Detroit, MI	A-5
	Appendix 6: System Layout.....	A-6
	Appendix 7: PVL Installation and Cable Connections.....	A-7
	Appendix 8: Junction Box and BOS for Kyocera Modules.....	A-8
	Appendix 9: UNI-SOLAR BOS Components	A-12
	Appendix 10: Energy Requirement for Hoisting Equipment	A-13
	Appendix 11: Level Diagrams	A-14

LIST OF FIGURES

Figure 1: Net Energy Ratio of the System's Arrays	3
Figure 2: Energy Pay Back Time of the System's Arrays	4
Figure 3: HTP Reduced over Three Operating Periods	5
Figure 4: Greenhouse Gas Emission Reductions Due to the Use of the PV System.....	6
Figure 5: PV Modules Learning Curve (1976-1992): Cost vs. Module Sales.....	13
Figure 6: Materials and Energy Input in Alternative PV Installations (kg/kWpeak)	16
Figure 7: Electricity Costs and CO ₂ Emissions Versus System Lifetime.....	19
Figure 8: Level 1 Diagram of Photovoltaic Modules Installed in the Dana Building.	21
Figure 9: Structure of United-Solar's Triple Junction Thin Film Cell	24
Figure 10: Cross-section of a Photovoltaic Device Comprising 3 p-i-n-type Cells	25
Figure 11: Multiple Deposition Chambers for Production of Amorphous PV Cells.....	27
Figure 12: Aluminum Frame of KC120 (cross sections).....	31
Figure 13: Level Diagram of Balance of the System (BOS) components	34
Figure 14: Inverter's Efficiency as a Function of Its Capacity Use.....	36
Figure 15: Motion of the Earth about the Sun and Location of Tropics.....	39
Figure 16: Scheme Showing a_m and t	42
Figure 17: Present Electricity Sources for the Dana Building.....	45
Figure 18: Central Power Plant Cogeneration Diagram	47
Figure 19: Compensatory System for Dana Building.....	48
Figure 20: Total Land Area Impacts per Module of the Three PV Modules.....	53
Figure 21: Total Land Area Impacts of the Three PV Modules Installed	54
Figure 22: Net Energy Ratio of the PV System for 10, 20 and 30 Years	55
Figure 23: Net Energy Ratio (NER) of the PV Modules for Two Inverter Cases	56
Figure 24: Energy Pay Back Time of PV Modules for the Two Inverter Cases	58
Figure 25: Energy Pay Back Time of the PV Modules and The Entire System.....	58
Figure 26: Impact of Frame on the E-PBT of Kyocera Modules and the System	60
Figure 27: The NER of Kyocera Modules With and Without the Frame	60
Figure 28: Share of Avoided Air Emissions from Each of the Displaced Sources	65
Figure 29: Human Cancer Impacts Reduced Due to Generation of PV Electricity.....	66

Figure 30: Global Warming Impact Reduced Due to Generation of PV Electricity	68
Figure 31: Smog Formation Impact Reduced Due to Generation of PV Electricity	68
Figure 32: Acid Rain Impact Reduced Due to Generation of PV Electricity	69
Figure 33: Global Warming Impact Reduced Due to Generation of PV Electricity	70
Figure 34: Smog Formation Impact Reduced Due to Generation of PV Electricity	70
Figure 35: Acid Rain Impact Reduced Due to Generation of PV Electricity	71
Figure 36: NER of PVL136 Considering Two Alternative Energy Sources.....	72
Figure 37: Cost Comparison of Major Components of the PV System.....	73
Figure 38: Comparison of E-PBT Results in this Report and Previous Assessment.....	75
Figure 39: Direct Solar Radiation Map.....	78
Figure 40: The Role of Renewable Energy Consumption in the US Energy Supply	79
Figure 41: PV System Data Flow Chart	81
Figure 42: Layout of the Display in the SNRE's Lobby	82
Figure 43: Energy Output Comparison : NREL vs. PV DAS.....	84
Figure 44: Theoretical vs. Actual Energy Output for May 18 th , 2005.....	84

LIST OF TABLES

Table 1: Impact Categories and Their Respective Subcategories.....	2
Table 2: Published Carbon Dioxide Emissions per Kilowatt-hour for PV Systems.....	10
Table 3: Characteristic Parameters in a PV Installation	11
Table 4: Energy Input into System Components	15
Table 5: Module's Type and Characteristics*	21
Table 6: Information on Material Inputs in Manufacture of a ASR128 Module.....	29
Table 7: Material and Energy Requirements per Multi-Crystalline KC120 Module	33
Table 8: Type, Mass and Source Database for Materials Used in the Inverter	37
Table 9: PV System Characteristics and Annual Output	44
Table 10: CPP Fuel Consumption and Power Production Summary 2003 - 2004	46
Table 11: Breakdown of the Total Energy Input into the PV System.	49
Table 12: Primary Energy Consumption per Area for 3 PV Modules.....	50
Table 13: Primary Energy Consumption per Peak Power (W_p) for 3 PV Modules.....	50
Table 14: Criteria Air Pollutants and Greenhouse Gas Emissions of the PV System	51
Table 15: Power to Area Ratio of the Three PV Modules.....	53
Table 16: Total Mass of Air Pollutant Emissions Reduced by the PV System	63

Executive Summary

The photovoltaic (PV) system on the roof of the School of Natural Resources and Environment (SNRE) serves as another model for the installation of PV systems in urbanized areas, which could play a major role in energy self sufficiency and security while solving the nation's greenhouse gas emission problem.

The goals of the project were (1) to provide renewable electricity to the School of Natural Resources and Environment; (2) to serve as a demonstration site for two alternative PV technologies – amorphous and multi-crystalline – in a relatively large installation, which also includes a 30 kW inverter; (3) to support research and provide historical system performance data.

Among the potential benefits of PV in substitution for fossil fuel based electricity are the reduction of greenhouse gas emissions which impact the global climate; the reduction of criteria pollutant emissions such as nitrogen oxides (NO_x), sulfur dioxide (SO_2), and carbon monoxide (CO) which cause health problems and damage the environment; and finally, the reduction of toxic emissions which cause human and ecological harm.

No electricity generation is free from harmful air emissions and the comparison and quantification of potential environmental benefits attained from the use of renewable energy systems requires the application of life cycle assessment (LCA). The production of the PV modules also consumes energy and materials which are also responsible for the release of harmful substances. In this report, we use a LCA methodology to weigh the benefits of replacing electricity from the grid and from the central campus power plant against the environmental releases that result from manufacture of the PV modules.

The report evaluates a 33 kilowatt peak (kW_p) PV system which is comprised of 88 KC120 multi-crystalline modules manufactured by Kyocera rated at 120 watts of peak power (W_p) each, 132 PV laminates (PVL136) rated at 136 W_p each, and 75 PVL62 rated at 62 W_p each. The laminates are manufactured by UNI-SOLAR using thin film technology. The total power of the KC120 array corresponds to 10,560 W_p , the total power of the PVL136 array corresponds to 17,952 W_p , and the total power of the PVL62 array corresponds to 4,650 W_p . Therefore, the KC120, PVL136, and PVL62 are responsible, respectively, for 32%, 54%, and 14% of the total power output of the PV

system. Although the total power of the system sums to 33kW, the maximum power output is limited by the capacity of the inverter which corresponds to 30kW.

A comprehensive model was developed to evaluate the energy and environmental performance of the PV system. The LCA characterizes manufacture and installation of the amorphous and multi-crystalline modules, manufacture of the inverter and all the ancillary material that comprises the balance of the system (BOS), and includes: hardware, cables, combiner boxes, and mounting structures.

The prediction of the life cycle electrical output of the PV system takes into account the local available solar radiation, the conversion efficiency of the modules, and their position. The model created to determine the lifetime electrical output of the system is based on the Bird Clear Sky Model from the National Renewable Energy Laboratory (NREL). According to results from this model, 44,848 kWh are produced by the entire system per year. The lifetime of the system is assumed to be 20 years, which corresponds to the warranty of the amorphous modules.

The results of the LCA of the PV system are compared to the emissions of greenhouse gas, criteria pollutants, and toxic emissions from the electricity generation technologies that provide electricity to SNRE. Therefore, this study also includes an inventory of the emissions from the natural gas fueled campus power plant (CPP) and the regional electricity grid. Several impact categories are assessed in this report (Table 1).

Table 1: Impact Categories and Their Respective Subcategories

Impact category	Subcategories
Life cycle energy conversion efficiency	- Energy pay back time (E-PBT) - Net energy ratio (NER)
Life cycle criteria air pollutant emissions	- Carbon monoxide (CO) - Particulate matter (PM ₁₀) - Nitrogen oxides (NO _x) - Sulfur dioxide (SO ₂) - Lead (Pb) - Hydrocarbons (C _x H _y)
Greenhouse gas emissions	- Carbon dioxide (CO ₂) - Methane (CH ₄)

One metric widely applied in assessing electricity generation technologies is the net energy ratio (NER). Figure 1 shows the NER of the three modules used in the system and the system average value based on a 20-year period of analysis. Calculation of the system's NER takes into account energy and material input in manufacture of the BOS components and the inverter. In the case of the NER for single modules, the manufacturing energy input for the inverter was allocated based on the share of electricity output for each array.

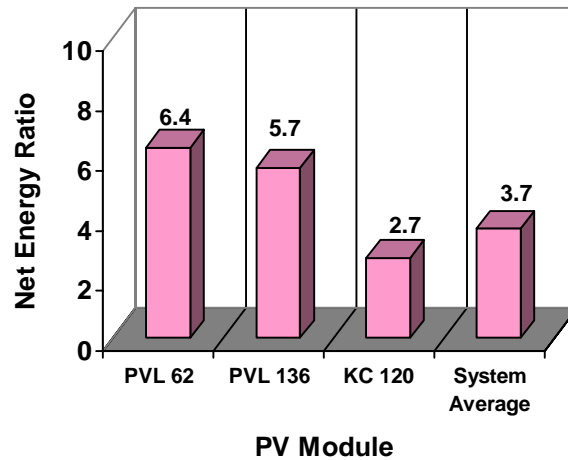


Figure 1: Net Energy Ratio of the System's Arrays

The NER compares the primary energy input over the life cycle of the electricity generation system to its electrical energy output.ⁱ When NER is applied to renewable energy sources it also represents the leveraging capacity of the source because it computes the amount of renewable energy obtained through the consumption of fossil fuels, which accounts for the majority of the energy inputs in the production of the renewable energy system. The higher the NER, the greater is the fossil fuel leveraging capacity of the energy system. In contrast to the NER, the energy payback time (E-PBT) measures the time period required for an electricity generation system to offset the amount of primary energy input in the system, which usually comes from non renewable sources. The E-PBT of the system is based on the same assumptions regarding the BOS and the inverter's energy and material inputs.

ⁱ The NER applied in the study does not account for solar radiation as primary energy.

Figure 2 shows the energy payback time for different arrays of the system and the system's average E-PBT. The E-PBT of the KC120 is higher because of its higher energy intensity during manufacturing compared to the PVL modules, and due to the need of an aluminum supporting structure for the modules. The KC120 modules are installed with the same tilt angle as the PVL modules on the standing seam for comparison purposes. However, because they require a metallic mounting structure they could have been positioned at a tilt angle that would increase their electrical output. We estimate that 15% more power could be produced if the modules are positioned at an angle that corresponds to the local latitude (42°N). This would make the KC120 array more competitive with the PVL array, which currently lacks the capability of being adjusted at an optimal angle to maximize the incoming solar radiation.

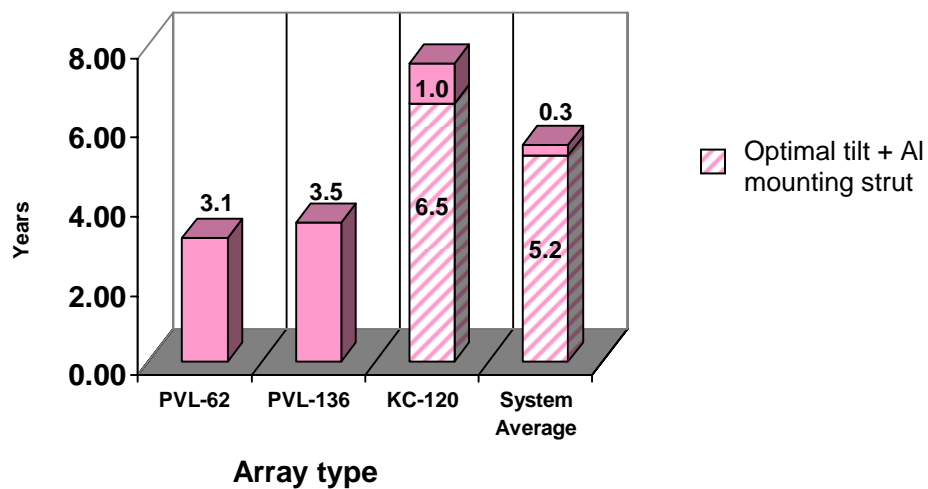


Figure 2: Energy Pay Back Time of the System's Arrays

In addition to leveraging fossil resources, the PV system avoids the environmental and health impacts associated with fossil fueled power plants. However, because part of the PV system output substitutes for electricity produced at a combined heat and power (CHP) facility, which also delivers steam to the buildings, the installation of the PV system would demand a compensatory system to supply the same level of service. The quantification of the avoided emissions is based on emissions released by the systems that traditionally supply electricity to the building less emissions due to manufacture and

installation of the PV system and emissions due to the operation of a hypothetical compensatory system.

The energy mix originally supplied to the building consists of 67% of electricity generated at the Campus Power Plant (CPP) and 33% of energy from the East Central Area Reliability Coordination Agreement (ECAR) electrical grid, which contains 90% coal and 10% nuclear energy. For each kWh generated by the CPP (CHP plant), 13.4 ft³ of natural gas are consumed.

The modeling of the environmental performance of the PV system is based on two different scenarios. The ‘Net Emissions’ scenario assumes that the PV system substitutes for the actual energy supplied to the Dana Building, consisting of electricity and steam produced at the CPP and electricity delivered by the ECAR grid. This scenario assumes the use of a compensatory system to produce steam, which consists of a boiler with the same characteristics of the CPP but at a much smaller scale. The ‘Net Emissions*’ scenario assumes that the PV system substitutes for the electricity provided by the ECAR grid, and does not take into account the compensatory system.

Several compounds, released during the extraction, transportation, and combustion of fossil fuels are highly toxic and carcinogenic. The potential impact of those compounds can be represented using the human toxicity potential (HTP) method, which renders the aggregated potential reduction of human cancer due to the substitution of electricity from the PV system for electricity from fossil fueled plants (Figure 3).

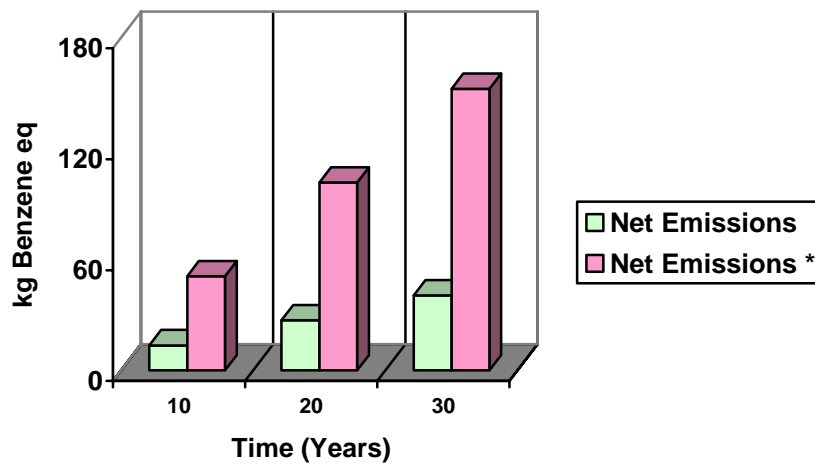


Figure 3: HTP Reduced over Three Operating Periods

The reduction of toxic releases by the PV system due to the displacement of fossil fuels also provides significant benefits to the global environment. The cumulative greenhouse emission reductions for 3 different time horizons due to the installation of the PV system are reported in Figure 4 as metric tons of CO₂ equivalent, which are calculated based on 100 year global warming potentials (GWP).

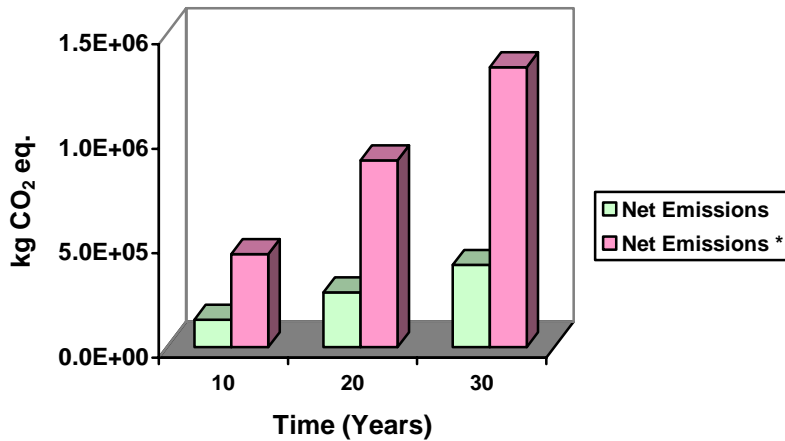


Figure 4: Greenhouse Gas Emission Reductions Due to the Use of the PV System

Finally, the project’s outreach effort conveys the benefits of PV renewable energy use to both students and the general public visiting SNRE. A data acquisition system (DAS) installed in the building monitors the real-time output of the PV system and each one of its arrays. The DAS calculates the cumulative air emissions avoided such as: carbon dioxide, sulfur dioxide, nitrogen oxides, and mercury. It also calculates resource consumption savings such as: coal, uranium, and natural gas. The DAS also compares the current output of the PV system to the corresponding energy load in the building, and tracks the best hour for weekdays and weekend days in which the highest share of electricity consumed in the building was met by the PV system.

In summary, installation of the PV system brings about valuable human health and environmental benefits compared to nonrenewable technologies available for supplying power to the Dana building. It is undoubtedly a significant part of the greening of the Dana building, which can serve as an example for the University and the City of Ann Arbor. On a sunny day in mid-May 2005 the PV system met 23% of the power

demand of the Dana Building. The pursuit of higher shares of power coming from the system can encourage energy conservation in the building.

1. Purpose of the Study

In 2004, a 33 kW rated photovoltaic (PV) system was installed on the roof of the Dana Building, which houses the School of Natural Resources & Environment (SNRE) and the Center for Sustainable Systems (CSS). This PV system is a key element of the “Greening of Dana Building” project, which was initiated in 1999 and led to the gold Leadership in Energy and Environmental Design (LEED) certification in 2005. The installation of the PV system, which was completed in 2005, is a unique opportunity to conduct a comprehensive life cycle assessment (LCA) and evaluate the performance of PV technologies. Moreover, because the system is on the roof of SNRE, its installation has also an educational facet. Consequently, four distinct goals characterize this study:

1. Evaluating the life cycle energy and environmental performance of the system, comparing two different PV technologies, and collecting measured electricity output data for future research.
2. Determining the net reductions in air emissions released as a result of using electricity generated from the building integrated photovoltaic (BIPV) system, which displaces fossil fueled based electricity.
3. Facilitating an educational outreach effort that will create an increased awareness about green energy generated from the PV system and its potential for leveraging fossil fuels and reducing air emissions.
4. Providing documentation regarding the monitoring of the PV system.

No electricity generation option is free from environmental impacts. A comprehensive environmental characterization of the available options requires the use of LCA. This is especially important in the case of PV systems that are emission free during their operation phase. Several LCAs of electricity generation systems including PV have been published (Table 2), and a literature review of these studies provides useful background content for this study.

This report is organized in the following way. Initially, a literature review of LCAs applied to photovoltaic systems is presented. Next, methods used in the research are presented and discussed. We start by presenting the LCA of the PV system, the data collection methods, and the LCA methods used in modeling the PV system. Next, we

describe the model used to estimate the solar radiation available for the PV array that is used to determine the total electrical output of the system. The amount of energy produced over the lifetime of the PV system is important to normalize the results of the LCA on a per electricity output basis so that they become comparable to other energy sources. Next, we present the methods used in the quantification of the avoided emissions due to the displacement of electricity supplied by the campus thermal power plant and the regional grid. Next, we present the results of the assessment based on several environmental indicators. Finally, we present outreach materials that will be used to educate building users and visitors about the project.

2. Literature Review of Life Cycle Assessment of Photovoltaic Systems

Solar photovoltaic (PV) modules convert solar energy directly into electricity. Although several published life cycle assessments (LCA) quantify the life cycle energy input of PV installations, and their environmental releases such as CO₂ emissions, normalized by electricity output, these studies are difficult to compare. That is, different studies use different methods, draw on different boundary conditions, rely on different data sources and inventory methods, model different PV technologies at different locations, and consider different lifetimes and analytical periods. Thus, the range of values published is quite large. Table 2 shows a compilation of studies that quantified CO₂ emissions of PV systems. Variability in the results may be linked to the boundary setting of each analysis, energy mix used in material manufacturing in each system and also differences in production processes used to manufacture the PV system. Because different PV technologies have different energy conversion efficiencies, this aspect of PV systems also affects the final results of the assessment.

Table 2: Published Carbon Dioxide Emissions per Kilowatt-hour for PV Systems¹

Author	year	Characteristics	gCO₂/kWh
Fritsche	1989	n.a.	32.0
Meridien Corp.	1989	central station PV plant	6.5
San Martin	1989	central station PV plant	5.4
Kreith	1990	central PV system 100 MW	24.0
Uchiyama	1992	PV	201.3
Nieuwlaar	1996	roof integrated system - 30 m ² amorphous cells	47.0
Komiyama ²	1996	Japan – polycrystalline	143.0
Komiyama	1996	Indonesia – polycrystalline	132.0
Dones	1998	PV p-Si (CH) – 100 yr. GWP	189.0
Dones	1998	PV m-Si (CH) – 100 yr. GWP	114.0
IEA	1998	mc-Si	87.0
Frankl	1998	monocrystalline silicon PV power plant	200.0
Kato	1998	single-crystalline silicon	83.0
Kato	1998	polycrystalline silicon (poly-Si) PV module - future technology	20.0
Kato	1998	amorphous silicon (a-Si) PV module - future technology	17.0
Lewis and Keoleian ³	1999	Thin film (amorphous) build integrated system in Detroit, MI. 20 year lifetime.	187.8
Alsema	2000	thin film (amorphous) grid connected roof top systems (1700 kWh m ⁻² yr ⁻¹) 30 yr. lifetime	50.0
Alsema	2000	monocrystalline grid connected roof top systems (1700 kWh m ⁻² yr ⁻¹) 30 yr. lifetime	60.0
Greijer	2000	dye sensitized solar cell (ncDSC) 20 yrs. Lifetime - 2190 kWh m ⁻² yr ⁻¹ – 500 MW plant - amorphous – Efficiency = 7% and process energy = 100 kWh m ⁻²	19.0
Greijer	2000	dye sensitized solar cell (ncDSC) 20 yrs. Lifetime - 2190 kWh m ⁻² yr ⁻¹ – 500 MW plant - amorphous	47.0
Greijer	2000	efficiency = 12% and process energy = 220 kWh m ⁻²	22.0
Greijer	2000	efficiency = 9% and process energy = 180 kWh m ⁻²	25.0
Oliver	2000	building integrated grid connected 12% module efficiency poly-crystalline	120.0
Oliver	2000	centralized Plant 12% module efficiency poly-crystalline	170.0
Nomura	2001	concentration design using a polycrystalline solar-cell - grid connected - near future technology	190.0
Nomura	2001	concentration design using a polycrystalline solar-cell - grid connected - short run technology	133.0
Nomura	2001	concentration design using a polycrystalline solar-cell - grid connected - long run technology	104.0
Ganon&Uchiyama	2002	n.a.	13.0
Meier	2002	building integrated PV system	39.0
Ito	2003	polycrystalline 12.8% efficiency	44.0

2.1. Factors Driving the Results of PV LCA

In summary, a set of parameters is responsible for the variability in the performance of different installations. Aside from the level of incoming solar radiation, which depends on the latitude and the characteristics of the local air mass and reflects a natural characteristic of the site selected for the installation of the modules, other parameters are simple choices made by the user of the system which sometimes are technology dependent, and other times are driven according to the purpose of the system. Some of these parameters are listed in Table 3 and discussed in the next paragraphs.

Table 3: Characteristic Parameters in a PV Installation

Technology	System configuration
Module's technology	Array area
Module's efficiency	Tilt angle and/or orientation
Tracking system	Mounting structure
Components' lifetime	Stand alone vs. grid connected
	Installation scale
	Other balance of the system (BOS) components

2.1.1. Technological Options

Currently, PV module production follows three types of technologies: mono-crystalline, multi-crystalline, and thin film (amorphous). The manufacture of crystalline PV modules is more energy intensive than the manufacture of amorphous modules. The primary energy required for the fabrication of crystalline PV modules has been reported to be 2.9 to 3.8 times greater than the input for the same unit area of thin film modules⁴. Primary energy requirements for manufacturing crystalline modules were found to range between 2,400 and 7,600 MJ m⁻² for multi-crystalline (mc-Si) modules and between 5,300 and 16,500 MJ m⁻² for mono-crystalline (sc-Si) modules, whereas the manufacturing energy requirement for thin film modules ranges from 710 to 1,980 MJ/m².⁴

Although the energy required for manufacturing PV modules is more a function of the modules' area than its power⁴, some studies report the manufacturing energy

normalized by the power output. For example, manufacture of an 11.2% efficient mono-crystalline module requires 9,683 kWh/kWp of electricity, whereas manufacture of a 10.3% efficiency multi-crystalline module requires 12,723 kWh/kWp.⁵ Assuming Standard Test Conditions, which corresponds to $1,000 \text{ W m}^{-2}$ of solar radiation, these values equate to $3,904 \text{ MJ m}^{-2}$ and $4,718 \text{ MJ m}^{-2}$ respectively.

The primary energy input into the manufacturing phase affects the energy payback time of the modules, the higher the input primary energy the longer the pay back time and vice versa. The source of the energy mix is one of the factors that strongly influences the amount of emissions released (emissions released are also dependent in the type of materials used) during manufacture of the PV system's components. Most greenhouse gas emissions associated with PV systems (80 to 90%) are linked to electricity requirements for the fabrication of modules. Because the energy mix is critical in influencing its greenhouse gas emissions, the substitution of renewable electricity for fossil fuel based electricity in manufacturing the modules is expected to reduce the emissions from the energy usage by significant amounts⁶. In addition, the energy consumed to produce the machinery used to make PV modules is not negligible. The equipment manufacturing energy and overhead energy combined can be 10.9% and 25% of the total module manufacturing energy for multi-crystalline and thin film modules, respectively⁷. This energy consumption was not considered in this study.

Of course, the energy conversion efficiency of the modules also affects the energy pay back time of PV systems. The energy conversion efficiency measures the ratio between the electricity output of the panel and the incoming solar radiation perpendicular to the surface of the module, and is expressed as a percentage. The efficiency of a module is a function of the technology used; therefore, different brands, vintages, and types of modules have different efficiencies. The energy conversion efficiency of the PV modules often degrades over time. Improving both the energy conversion efficiency of the modules and their manufacturing efficiency, that is, reducing energy and materials inputs, affects the life cycle cost (total cost of the electricity generated from the PV system) of the electricity produced by PV installations. The continuous growth of the PV industry has benefited from both practices that affect the penetration of the technology in

the market and the electricity cost. Such evolution in the industry is usually demonstrated by a learning curve (Figure 5).

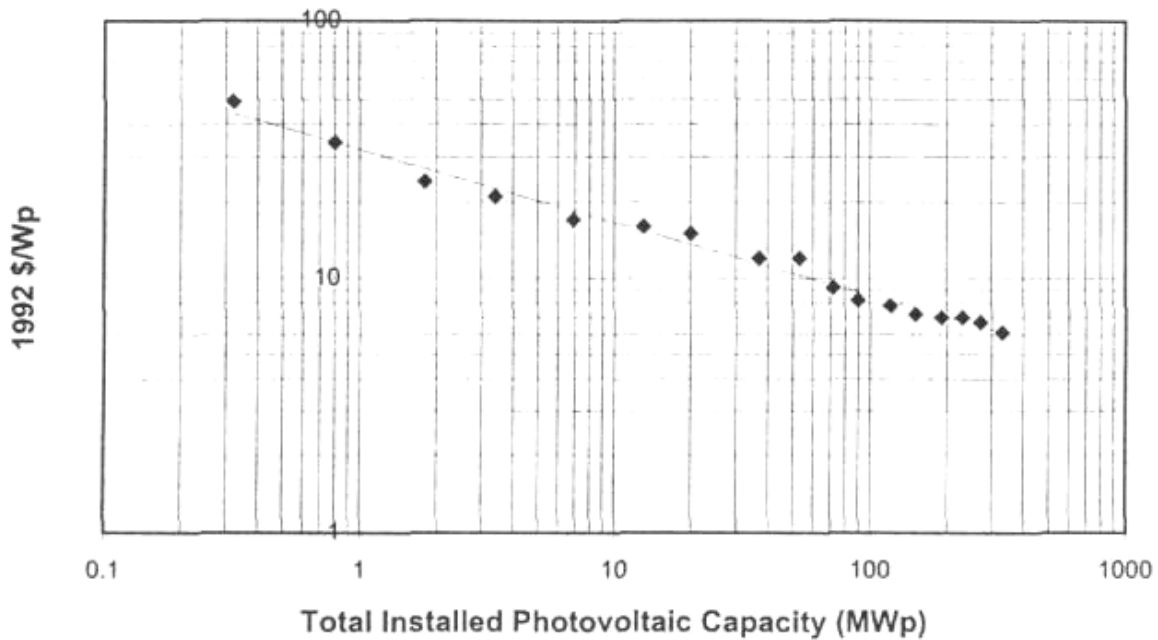


Figure 5: PV Modules Learning Curve (1976-1992): Cost vs. Module Sales⁸

Manufacture of the crystalline cells involves the production of silicon wafers from electronic grade silicon. About 60% of the silicon is currently discarded due to quality concerns detected between the production of electronic grade silicon and the wafers, which are the assemblies used in crystalline modules. Manufacture of the multi-crystalline silicon wafers consume 3,200 MJ/m² and because of a more controlled crystallization process manufacture of the mono-crystalline silicon wafers consume 4,700 MJ/m²⁷. Thus the high silicon losses and the significant amounts of energy consumed during the production of the crystallized silicon negatively affect the E-PBT of the modules and their life-cycle emissions.

Technological innovations are constantly improving the efficiency of the modules and reducing their manufacturing costs. The electricity consumption per peak power during module manufacturing (9,683 kWh/kW_p for mono-crystalline cells, 12,723 kWh/kW_p for multi-crystalline cells) and the process heat / primary energy content of materials required (13,255 MJ/kW_p for mono-crystalline cells, 16,038 MJ/kW_p for multi-

crystalline cells) during manufacturing are expected to decrease with time, according to an 1998 study by Frankl.⁵ A reduction of 70.2% and 85% reduction in electricity consumption and 80.2% and 83% reduction in the process heat / primary energy content of materials are predicted for mono-crystalline and multi-crystalline cells, respectively. Multi-crystalline cells are also expected to have the best environmental profile in the future. When compared to the mono-crystalline cells, the multi-crystalline cells despite having lower cell efficiencies (16% when compared to 18%), are still expected to have comparable module efficiencies (approximately 14%), consume significantly less electricity and reduce air pollutant emissions during the manufacturing stage.⁵

2.1.2. Incoming Solar Radiation

Because the electricity output of a module depends on how much solar radiation reaches the surface of the module, the position of the module with respect to the sun is important. The electricity produced by the module depends on the orientation of the module's face and the angle with the horizontal plane. Modules may be mounted on a frame that tracks the position of the sun over time and increases the amount of incoming radiation. While some of the arrays move only along one axis based on a frame filled with refrigerant gas, other tracking systems move along four axes and are powered by a small electric motor. In this case some electricity generated by the system is consumed during its operation⁹.

The choice of the tilt angle depends not only on the maximization of the energy output of the modules, which varies with the seasons of the year, but also on the economic and environmental cost of the structures to support the modules.

2.1.3. Balance of the System (BOS)

The Balance of the System (BOS) is the term used to refer to all the other components in the PV installation besides the modules. The BOS depends on the type of application and local conditions, and includes the structure to support the modules and the installation hardware. Batteries to store and deliver energy during load periods, as well as inverters might be necessary if the system is connected to a network that operates with alternate current (AC). Cables to interconnect modules and arrays to batteries and

inverters are also part of the BOS. Batteries have emission impacts throughout their life cycle and potential disposal concerns at their end of life. The assessment of the energy, carbon, and other emissions associated with the BOS should also be part of a comprehensive LCA. Table 4 shows energy inputs into some of the components used in the BOS from a previous investigation.

Table 4: Energy Input into System Components⁴

Aluminum module frame	MJ/m ²	500
Array support – central plant	MJ/m ²	1800
Array support – rooftop	MJ/m ²	700
Inverter (3 kW)	MJ/W	1

Whenever energy to be recovered in the future is stored or converted, some losses occur; therefore, there are some efficiency losses associated with these practices that need to be included in the analysis. Accordingly, it is estimated that 25% of energy is lost in the system through BOS conversion efficiency losses, which accounts for inverter and storage losses⁷.

The inverter, a very important component of the balance of system (BOS), converts the direct current (DC) generated by the PV modules into alternating current (AC) that can be used by the building. Lewis and Keoleian (2003) modeled the structural components, certain electronic components, printed wiring board (PWB) fabrication process and the transportation of the inverter. The study found that the inverter contributed to 18% CO₂, 16% lead, 11% NO_x, 4% particulates and 46% of the SO₂ emissions released during the entire life cycle of the PV system.¹⁰

2.1.4. Installation Type

The user's requirements of the installation can also influence the system's performance. While some PV systems are stand-alone systems that can only supply energy for small consumers, others are grid-connected. The scale of grid-connected systems is variable and affects the BOS of the system and its respective material requirements⁶.

Figure 6 shows a comparison of energy and material inputs of six different configurations of grid-connected systems using mono-crystalline (m-Si) and multi-crystalline (p-Si) PV modules⁶. Efficiencies of the m-Si and p-Si modules modeled are 16.5% and 14%, respectively. Roof modules produced 860 kWh per year per kW_p, whereas the 100 kW plant produced 1,000 kWh per year per kW_p, and the 500 kW plant produced 1,200 kWh per year per kW_p.

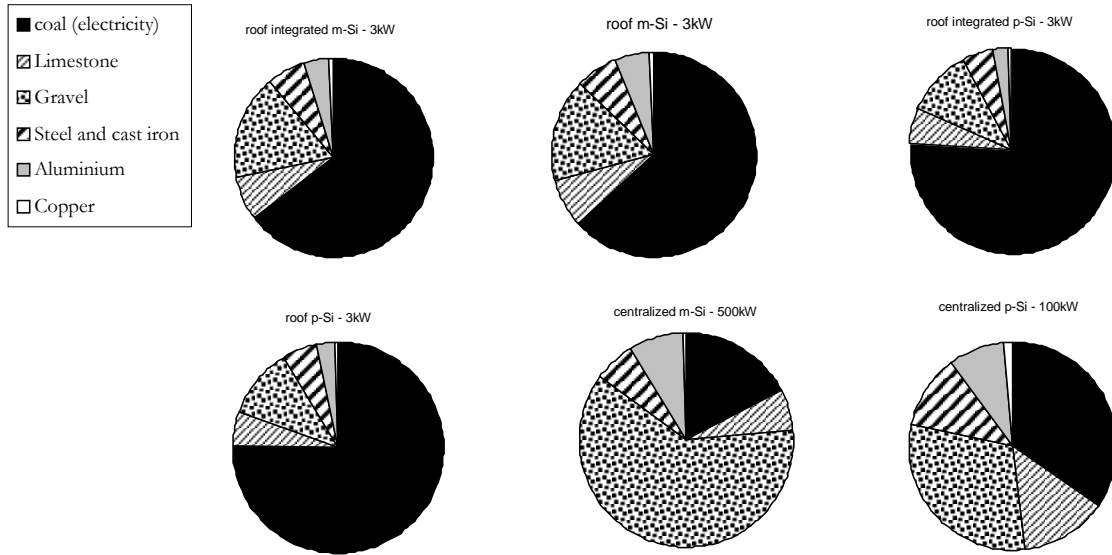


Figure 6: Materials and Energy Input in Alternative PV Installations (kg/kWpeak)⁶

The share of coal is more significant in systems installed on roof tops because manufacture of PV modules requires a significant amount of electricity and energy, which usually depends on coal combustion. In addition, roof top systems use less material for the installation of the modules. Installation materials, which include construction materials, comprise other inputs such as concrete, which account for a significant share of the materials input in centralized land based systems. As mentioned before in section 2.1.1, the electricity consumption per peak power during module manufacturing (9,683 kWh/kW_p for mono-crystalline cells, 12,723 kWh/kW_p for multi-crystalline cells) and the process heat/primary energy content of materials required (13,255 MJ/kW_p for mono-crystalline cells, 16,038 MJ/kW_p for multi-crystalline cells) during manufacturing are comparatively higher for multi-crystalline cells. Consequently,

the amount of coal consumed is greater in the systems using multi-crystalline modules than in systems using mono-crystalline modules.

According to Alsema (2000), different mounting options affect the amount of energy input into the systems; thus, the energy pay back time for a rooftop system is typically 2.5 to 3 years, whereas the pay back time for a ground mounted system is 4 years.⁴ The ground mounted PV system involves the installation of additional support structures to help generate the maximum possible electricity from the system. However, from the energy pay back time estimates it is evident that the structures used to support the modules consume significant amounts of energy and also are responsible for GHG emissions. Indeed, concrete and steel used in the construction of the structures to support the modules are responsible for a considerable amount of energy input in some PV installations ($1,100 \text{ MJ/m}^2$)⁵. The use of an existing structure, such as an existing building roof, to support the modules also reduces the environmental impacts of this electricity generation alternative since the structure serves other functions in addition to supporting the modules. One advantage of using a special structure to support the modules is that they can be positioned in order to maximize the amount of effective solar radiation received; and therefore, the amount of electricity output of the modules.

Building-integrated PV (BIPV) are PV modules/laminates integrated in the building envelop such as PV shingles.¹⁰ While rooftop modules are placed on an existing structure through the use of simple frames to hold a set of modules, stand-alone systems demand manufacture and installation of special frames on the ground to hold an array, which includes a set of modules.

Although small producers may own grid-connected systems, the aggregation of several small suppliers in a network may result in a significant energy source, which could be comparable to centralized power plants. When a large number of individual modules are connected to the grid the scale of the system could be comparable with the capacity of a centralized PV power plant where all modules are located side by side in the same place. However, there are additional advantages to a network system, including its resilience to massive power outages that are characteristic in large-scale centralized systems, and the elimination of power transmission and distribution losses when modules

are installed close to consumers.¹¹ In a recent study, transmission and distribution losses for the state of Michigan were calculated as 9.58% of the power delivered to the grid.¹²

The scale of grid-connected systems varies, and although a collection of small modules may match the energy produced in a larger installation, there are some advantages due to economies of scale in the construction of large-scale centralized systems. One advantage of a centralized system is that the materials used in the facility can be reused, recovered, and recycled more readily than if they were in dispersed installations.¹³ Changing the position of the panels to maximize the amount of incoming radiation may also be easier in a centralized plant. In Japan, large-scale centralized plants (100 MW) are expected to be constructed over the next couple of years.¹¹ Presently, the largest PV installation with 32,740 modules totaling 4 MW of installed capacity is located in the southern state of Bavaria in Germany.¹⁴

2.1.5. Conversion Efficiency Trend

A comparison between crystalline and amorphous technologies shows that more efficient crystalline modules consume more energy during manufacturing than less efficient amorphous modules⁷. However, the output of amorphous modules diminishes over time more dramatically than the efficiency of crystalline modules.¹⁵ The output of amorphous modules typically declines about 25% over the first few months of exposure to the sun due to the Staebler-Wronski effect¹⁶, but then the efficiency tends to stabilize and minimal decay in the efficiency rates are observed after this point for the life-cycle of the PV. Another study by National Academy of Engineering reports that the power output of amorphous silicon modules decrease by 15-40% during the first few months of operation (due to Staebler-Wronski effect) after which the power output stabilizes itself¹⁷.

2.1.6. Lifetime of the System

A LCA compares material and energy input and various emissions to the energy generated over a certain period, which usually equals to the lifetime of a major component of the system. In the case of PV systems, the crystalline modules have an expected life time of 25 to 30 years⁵ and the UNI-SOLAR thin film modules have a life time warranty for 20 years¹⁸. While some parameters are determined by the system

designer, others are circumstantial, that is, they depend on local characteristics or natural conditions. The lifetime of the modules is an important parameter that affects both the electricity costs and the amount of reduced CO₂ emissions (Figure 7).

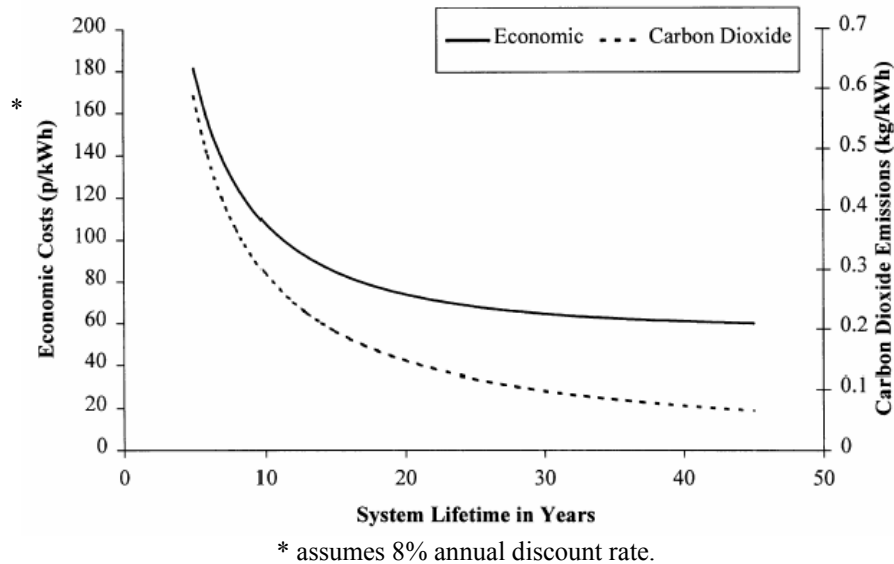


Figure 7: Electricity Costs and CO₂ Emissions Versus System Lifetime¹⁹

The PV industry is increasingly beginning to recognize the value of the life cycle approach to reduce GHG emissions of the electricity generation systems and improve manufacturing, design and end-of-life of the facilities¹³. The reduction of GHG emissions over the life-cycle of the system depends both on improving conversion efficiency of solar radiation to electricity and using efficient and low emission energy sources. In addition, energy and material amounts input in the PV system should be minimized.²⁰ Retrofitting PV installations seems also beneficial since part of the old structure could be reused and new modules could be more efficient and embed less carbon emissions over their life-cycle.

3. Methods

The LCA of PV systems is an important tool to quantify the potential environmental advantage of using solar technologies versus more traditional technologies, especially the ones relying on non renewable fossil fuel sources. One step in the production of the LCA results is the normalization of the environmental burdens by the electricity output of the system.

The first methods section describes the LCA of the PV system, the characterization of the components and the data collection for each one including the energy consumption for the installation of the system and its respective environmental impacts. The second methods section of this report shows how to determine the solar resource availability for a given geographic location and the most appropriate way to position a module to maximize its electricity output. The last part of the methods section describes the other power systems that supply electricity for the university, and their respective environmental implications.

3.1. Life Cycle Assessment of the Photovoltaic System

The LCA of the PV system is used to determine all life cycle material and energy inputs in the system, which is later, normalized by its expected electricity output, which in turn depends on the solar radiation model described in section 3.2.1.

The following section (Figure 8) presents the various life cycle stages considered in this study. The life cycle of the PV system consists of the manufacture of three different photovoltaic modules (Kyocera KC120 crystalline modules, UNI-SOLAR PVL62 and PVL136 thin film laminates), the transport of the modules to Dana Building (Ann Arbor, MI) from San Diego, CA, and the amount of energy consumed during installation of the modules and the BOS components.

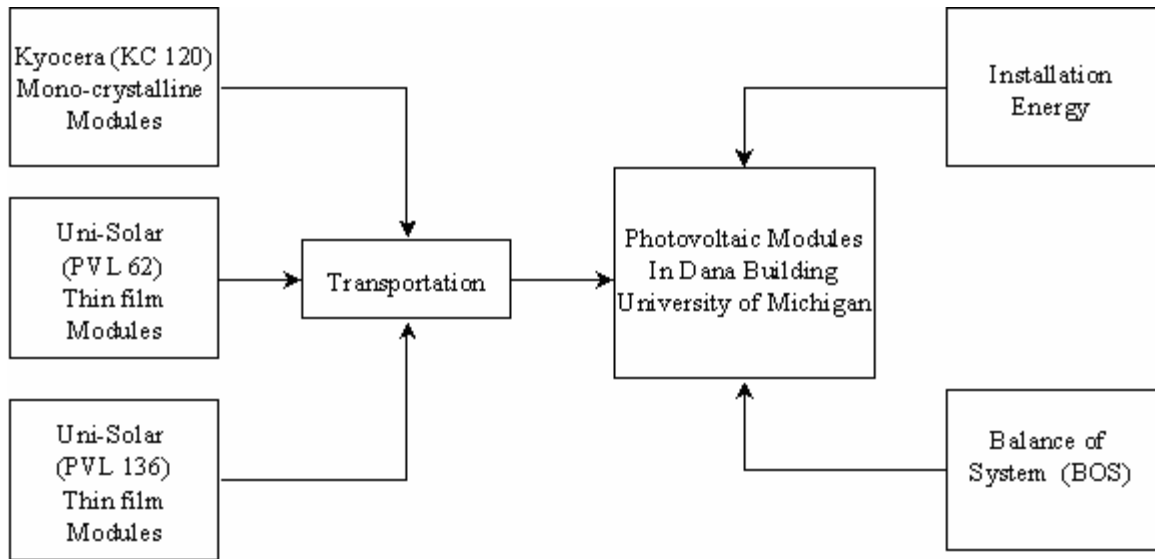


Figure 8: Level 1 Diagram of Photovoltaic Modules Installed in the Dana Building.

3.1.1. Photovoltaic System Characterization

The installation of a 33kW photovoltaic system on the roof of Dana Building provides a valuable opportunity to perform a LCA of this renewable energy technology. The system comprises two different photovoltaic technologies: amorphous and multi-crystalline. Thin film amorphous modules manufactured by United Solar Ovonic Corporation (Auburn Hills, MI) are used in the system in addition to multi-crystalline modules manufactured by the Kyocera Corporation (Table 5). The thin film amorphous laminates used in the system differ in size and power output. The photovoltaic laminate (PVL) 62 is rated at 62 W of peak power (W_p) and the PVL 136 is rated at 136 W_p .

Table 5: Module's Type and Characteristics*

Model	Type	Number of modules	Power	Area per module	Total area	Total power
KC120	Multi-crystalline	88	120 W	0.93 m ²	82 m ²	10,560 W
PVL136	Thin film	132	136 W	2.16 m ²	285 m ²	17,952 W
PVL62	Thin film	75	62 W	1.03 m ²	77 m ²	4,650 W

*more details are shown in the specification sheets in appendices 2 and 3

In addition to different PV technologies and types of modules the installation of the arrays on the roof of the building also differs. All modules are on the south side of the building; however, 77 PVL136 modules and 72 PVL62 modules are placed on the steel standing seam with a 12° tilt angle. The rest of the PVL modules are mounted on the lower part of the roof, glued on the rubber membrane. This part of the roof has a tilt angle of 8° with respect to the horizontal plane. There are two arrays with 44 KC120 crystalline modules each, which are mounted on an aluminum structure. The tilt of these modules is similar to the standing seam (12°) A detailed system layout is shown in appendix 6 and its level diagram is presented in appendix 11.

3.1.2. Functional Unit

The comparison of the performance of the system is assessed based on a per kWh functional unit. That is, the life cycle energy and material inputs in the system and the respective quantified environmental emissions are normalized based on the total expected electricity output of the system after considering the conversion losses such as the use of the inverter.

The indicator used in this study expresses the net reduction in air emissions released. In the case of the Dana Building the electricity generated by the PV system displaces an equivalent amount of electricity and steam currently generated from conventional fossil fuel based resources (later explained in detail in section 3.3). Hence the indicator, the net air emissions reduced per kWh (g/kWh) of conventional electricity displaced was determined and presented. The report also shows emission factors separately for each one of the two technologies used in the system.

In the following section we present and compare the LCA of the two competing PV technologies. An emphasis is placed on the manufacturing phase and corresponding material and energy consumption.

3.1.3. Assumptions

A number of assumptions were used in this study. A list of assumptions used is provided below.

- 1) All of the air emissions from the combined heat and power (CHP) facility on campus were due to electricity generation and steam production
- 2) Because part of the PV system output substitutes for electricity generated by a CHP facility, emissions due to the production of 9.5 psi steam are deducted from the weighted emissions of the traditional supply system in the 'Net Emissions' scenario.
- 3) The conversion efficiency of the multi-crystalline Kyocera modules is constant over time, whereas the conversion efficiency of the PVL degrades at a 1.1% annual rate.
- 4) The US average energy mix is used even if the final energy consumption takes place in regions with peculiar energy mixes.
- 5) Maintenance and substitution of parts in the system are ignored even when the period of analysis is extended up to 30 years.
- 6) Energy and material input data in the fabrication of a multi-crystalline module represents the production of the KC120 module (Phylipsen and Alsema 1995).

3.1.4. United Solar Thin Film Amorphous Modules

The two types of thin film photovoltaic laminates (PVL) installed differ in their respective power and size. There are 75 PVL62 modules with dimensions (length vs. breadth) of 102.75 inches by 15.5 inches, which are rated at 62W each. In addition there are 132 PVL136 modules with dimensions (length vs. breadth) of 216.6 inches by X 15.5 inches, which are rated at 136 W each (Appendix 1). The PVL62 and PVL136 modules both have an expected conversion efficiency of approximately 6.6% and 6.3%, respectively. These values slightly differ for both the thin film modules and were obtained from the technical specification sheets of both the thin film laminates based on their electrical specifications. (See Appendix 3)

Modules of the PVL series contain triple junction cells, which are made in a continuous roll-to-roll deposition on a stainless steel sheet. This process allows the continuous production of PV, which lowers its manufacturing costs. The thin film modules are based on a tri layered structure, which is manufactured through the deposition of gases containing silicon on a substrate inside a special chamber.

Each one of the three layers absorbs distinct wavelengths of light (blue, green, red). The modules are covered by a transparent conductive oxide film, encapsulated in stabilized polymers, and have an adhesive film on their back to facilitate their installation (Figure 9).

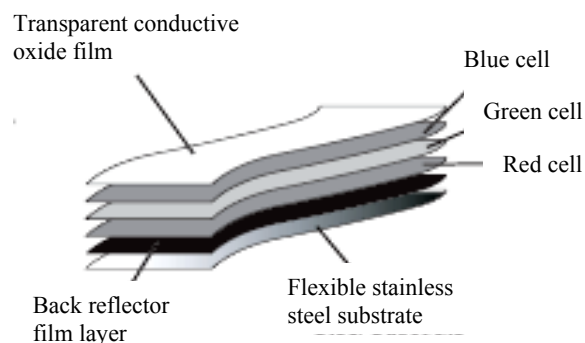


Figure 9: Structure of United-Solar’s Triple Junction Thin Film Cell

Each layer contains a p-i-n type cell, which is formed by three layers of amorphous, semiconductor alloys superposed. The p-type semiconductor layer is light absorptive and has high conductivity. Semiconductor layers are characterized by an adjusted wave length threshold for solar photoresponse, high light absorption, low dark conductivity and high photoconductivity, including sufficient amounts of a band gap adjusting element or elements to optimize the band gap for the particular cell application. Therefore, the layers are band gap adjusted to provide cell 12a with the lowest band gap (red), cell 12c with the highest band gap (blue), and cell 12b with a band gap between the other two (green) (Figure 10). The n-type semiconductor layers are characterized by low light absorption, high conductivity alloy layers. The thickness of the n-type layers is in the range of about 25 to 100 angstroms. The thickness of the band gap adjusted, amorphous intrinsic alloy layers can be between 2,000 to 3,000 angstroms. The thickness of p-type layers can be between 50 to 200 angstroms. Due to the shorter diffusion length

of the holes, the p-type layers generally will be as thin as possible. Further, the outermost layer, here the n-type layer, will be as thin as possible to avoid absorption of light since it does not include the band gap adjusting element.

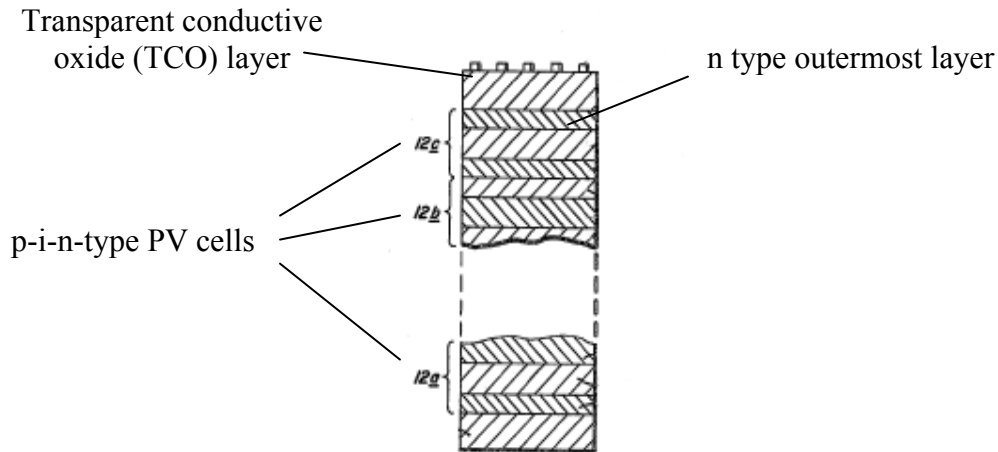


Figure 10: Cross-section of a Photovoltaic Device Comprising 3 p-i-n-type Cells²¹

The production of thin film modules does not require the formation of silicon crystals and the production of wafers, which constitute a more energy intensive process than the use of gaseous silicon deposition. The output of a typical high volume process comprises a large area roll of substrate material coated with multiple semiconductor layers. In order to fabricate a practical device, it is generally necessary to cut the large sized material output of the roll-to-roll process into various laminates optimized for a particular voltage and power requirements. Processing steps typically include:

- cutting the large area material into individual laminates,
- testing the individual laminates,
- applying current collecting structures such as collector grids and bus bars to the individual laminates,
- assembling the devices into power generating modules, and
- affixing protective and/or support structures to the modules.²²

A large scale production of tandem p-i-n-type photovoltaic cells demands the deposition of successive layers of amorphous semiconductor alloys onto a substrate material in a plurality of dedicated deposition chambers (Figure 11). The substrate is

usually stainless steel that is continuously and sequentially fed through the chamber for building up the active PV layers.²¹

Usually the manufacturing process involves the production of two amorphous photovoltaic laminates and the deposition of gas comprises the following steps:

- effecting a vacuum in the deposition chambers through which the substrate is advanced;
- heating the chambers to warm the substrate and reaction gas mixtures;
- introducing the reaction gas mixtures into the chambers in such a manner that the gas mixtures in each compartment is free from contamination
- moving the substrate through the plasma region of each deposition chamber for depositing the gas mixtures onto the substrate; and
- maintaining the substrate temperature, the speed of substrate travel, the substrate tension, the mixtures of reaction gases, the pressure differentials between adjacent chambers, and the vacuum pressures, whereby tandem, amorphous, photovoltaic solar cells are continuously produced on the web of substrate material.

The substrate's plate moves continuously across the chain of deposition chambers, and the feeding of the plate is controlled by a set of moving rolls. The position of the steering idler roller is controlled through a mechanical linkage by a servo-motor located outside of the deposition chamber, and connected to the mechanical linkage by means of a rotary vacuum seal.²¹

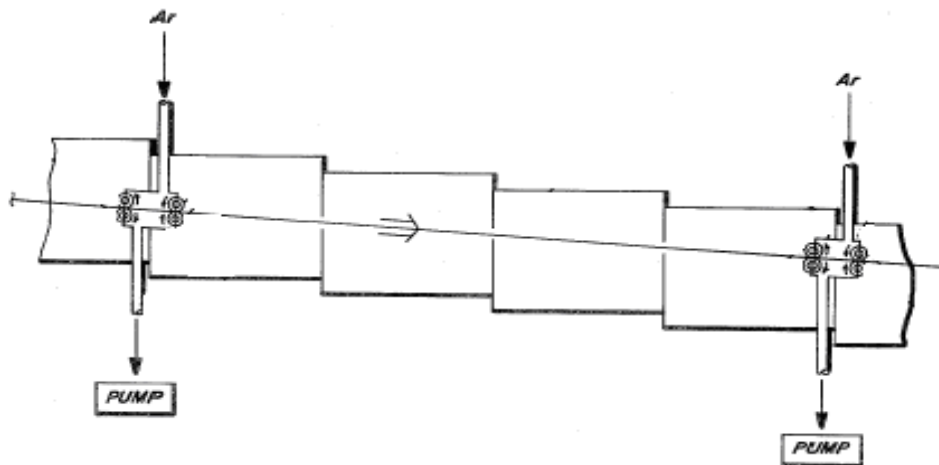


Figure 11: Multiple Deposition Chambers for Production of Amorphous PV Cells

Following the deposition of the semiconductor alloy layers, an extra deposition step is performed in a separate environment. In this step, a TCO (transparent conductive oxide) layer is added. This layer, which is characterized by low resistivity, high electrical conductivity and high transparency, is usually made of indium tin oxide (ITO), cadmium stannate (Cd_2SnO_4) or doped tin oxide (SnO_2).

Manufacturing the PVL modules requires various materials and energy inputs. In this report it is assumed that manufacture of the PVL requires material inputs similar to the manufacture of the ASR128, which is also a triple junction module. Table 6 shows the material and energy inputs for manufacturing one ASR128 module²³. This information, which was previously collected from UNI-SOLAR, is used to model the life cycle primary energy input and the corresponding environmental outputs due to the production of the PVLs used in the system.

Because the size and the power of the PVL modules differ from the size and power of the ASR128 module, and yet they have the same three layered structure, the ratio between the area of the PVL modules and the ASR128 was used to determine the amount of materials in the PVL modules. Each ASR has 219.6 inches of length by 16 inches of width, and the exposed area of the module corresponds to 23 ft² or 3,312 square inches (Appendix 2).

The area of each PVL62 and each PVL136 modules is 1,593 and 3,348 square inches, respectively. Consequently, the area ratios used to determine the material inputs for one PVL62 and one PVL136 are 0.48 and 1.01 times the material inputs into one ASR128, respectively. Both the wires and the wire insulation material were not taken into account because the PVLs are connected through quick connect cables, which are modeled as part of the BOS. Although the area of the ASR128 and the area of the PVL136 are similar, the PVL136 yields 8 watts of additional peak power compared to the ASR128 output.

The energy input in manufacture of the modules was obtained directly from the manufacturer. The production of 8.1 MW of PVL requires 6,917,120 kWh of electricity and 816,500 ft³ of natural gas²⁴. These values are used to determine the energy inputs into the ASR128 modules based on its corresponding peak power value.

Table 6: Information on Material Inputs in Manufacture of a ASR128 Module

No	Material	Mass (grams)	LCI Source	Material's Energy Intensity (MJ/kg)	Transportation Mass-Distance (metric tons-km)	Transportation Mode	Transportation LCI Source
1	Aluminum	32.44	BUWAL 250	134.00	8.67E-03	Ocean freighter	Franklin
2	Hydrogen	49.53	BUWAL 250	190.00	1.69E-02	Ocean freighter	Franklin
3	Monosilane	8.11	UPM Report (Energy)	756.00	8.67E-03	Ocean freighter	Franklin
4	Oxygen	1.10	BUWAL 250	5.6	3.33E-03	Diesel locomotive	Franklin
5	Phosphine	0.17	UPM Report (Energy)	107.00	1.18E-03	Ocean freighter	Franklin
6	Stainless steel	2,184.25	IDEMAT	26.2	4.51E-04	Diesel locomotive	Franklin
7	High density polyethylene (HDPE)	2,490.91	BUWAL 250	74.00	1.82E-04	Ocean freighter	Franklin
8	Tefzel	278.96	UPM Report (Energy)	21.00	6.99E-05	Diesel locomotive	Franklin
9	Glass fiber	81.08	IDEMAT	8.7	6.91	Ocean freighter	Franklin
10	Madico (PE)	702.50	BUWAL 250	78.8	3.27	Diesel locomotive	Franklin
11	Duraseal (PE)	147.73	BUWAL 250	78.8	0.43	Ocean freighter	Franklin
12	Busbar (Cu)	140.32	ETH	69.4	2.56E-01	N.A	N.A
13	Solder tin	22	IDEMAT	121.2	1.21E-01	N.A	N.A
14	Solder lead	5.94	ETH	121.2	N.A	N.A	N.A
15	Wire (Cu)	11.20	ETH	N.A	N.A	N.A	N.A
16	Wire insulation (rubber)	5.45	ETH	N.A	N.A	N.A	N.A
17	Water	89,929.20	ETH	6.3E-03	N.A	N.A	N.A
18	Low density polyethylene (LDPE)	41.79	BUWAL 250	80.8	N.A	N.A	N.A

In addition, the transport distances for several material inputs in manufacture of the ASR128 and the corresponding transportation modes used and their fuel consumption were used in the calculation of the life cycle primary energy consumption.

The conversion of the material inputs in the PVL modules into primary energy inputs was done using various life cycle inventory (LCI) databases, which are included in the SimaPro software. Table 6 shows a list of the inputs in one ASR128 module, their respective mass, and the LCI information used to model the primary energy input and the environmental releases associated with each material. The primary energy consumption values per kg of material (MJ/kg) for materials such as monosilane, phosphine, TefzelTM, were obtained from the above mentioned study²⁵. The energy consumption to produce the required mass of these 3 materials to manufacture the two thin film modules (PVL62 and PVL136) was assessed and further modeled in SimaPro using the ‘US Primary Energy’ module to calculate the resource consumption and process emissions. The remainder materials are directly modeled in SimaPro using built in LCA process blocks. A level diagram of the PVL modules is presented in appendix 11.

The assessment of the primary energy consumed in the purification of silicon was based on the mass percent of Si in each of the compounds containing Si combined with the primary energy consumption for winning and purification of Si.⁷

The installation of the PVL modules does not require a special structure, and the modules are placed directly on the roof of the building, and the electrical connections are made through quick connect terminals, which are part of the PVLs. (see pictures in appendix 7 for more details).

3.1.5. Kyocera Multi-crystalline Modules

The multi crystalline system consists of two arrays of Kyocera modules (Appendix 4). There are 88 KC120 modules in total, and each one has the following dimensions (L x B: 58 in x 26 in). The modules are placed on aluminum structures of 11 modules each. Therefore, there are a total of 8 arrays within the whole system. Each module contains a junction box for the electrical connection with the other modules. The modules are mounted on an aluminum frame structure, which supports the arrays.

Materials and energy requirements for this part of the system are detailed in the balance of the system (BOS) section.

The manufacture of multi-crystalline modules differs from manufacture of thin film modules, because they require the production of silicon crystals. However, multi-crystalline modules do not require perfect crystals such as the ones used in the production of mono-crystalline modules; and therefore, they can be produced at lower costs.⁷

Multi-crystalline modules are rigid and contain an aluminum frame. The aluminum frame of the KC120 module has a total volume of 54.6 cubic inches²⁶. Figure 12 shows the cross sections of the frame used in one module.

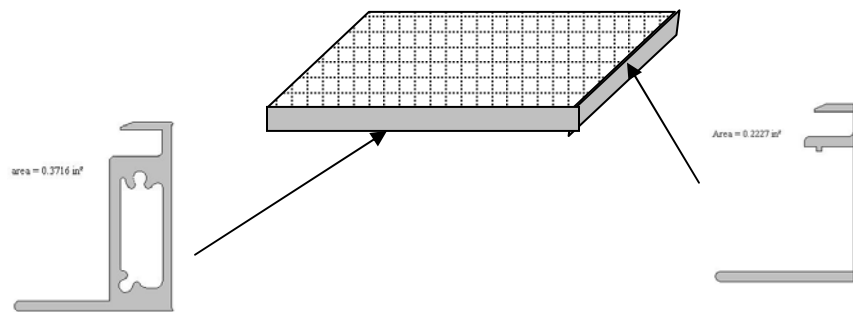


Figure 12: Aluminum Frame of KC120 (cross sections)

The inventory of the life cycle energy inputs in the production of a KC120 module was based on two previous studies related to the manufacture of a generic multi-crystalline module^{7,27}. Philipsen and Alsema, 1995 reported the material composition (kg/m^2) and process energy requirements (in kWh/m^2) for the manufacture of a single multi-crystalline module in Europe. The functional unit of that assessment is on a per m^2 basis. The dimensions of the KC120 module used in this study are 56.1 in x 25.67 in (0.93 m^2)²⁸. Hence the reported material and energy values both on a per m^2 basis are multiplied by a factor of 0.93 to calculate the energy requirements for a single KC120 multi-crystalline module in this study. After calculating the material mass per module, the materials are then modeled in SimaPro. Although we assume that the KC120 modules are produced in Tijuana, Mexico,²⁹ the reported energy values from the previous study are adapted to U.S. conditions. In fact, Tijuana is not connected to Mexico's power

grid but rather connected to the electrical power grid of Southern California.³⁰ Thus, the energy (electricity) requirements for the module was modeled in SimaPro using the U.S average electricity fuel mix from the Franklin database.

Table 7 presents material and energy requirements for one KC120 multi-crystalline module. In this previous study, the multi-crystalline PV modules considered have a conversion efficiency of 13%. In contrast, the Kyocera KC120 modules installed in Dana Building have a conversion efficiency of 12.9%. The aluminum frame of the KC120 modules is modeled separately.

Material input for the aluminum frame was calculated based on the AutoCAD diagrams for the KC120 module²⁸. Based on the AutoCAD drawing the volume of the aluminum frame was calculated and multiplied by the density of aluminum to get the final material mass (Figure 12)³¹. The mass of aluminum was modeled in SimaPro based on the aluminum with 25% of recycled content from the BUWAL LCI database. A level diagram of the KC120 is presented in appendix 11.

Final emissions and life cycle energy are reported for the KC120 arrays on the roof of the Dana building, which also includes the supporting aluminum structure that is modeled as part of the BOS and the inverter.

3.1.6. Balance of the System

The balance of the system (BOS) comprises structures and equipment that are needed to support the modules and deliver the electricity to the local network. Figure 13 shows a diagram of the components and inputs into the BOS.

The two photovoltaic technologies installed require different BOS components; therefore, we access the BOS of each one separately. However, because the arrays are part of a common system, part of the BOS such as the combiner boxes and the inverter are discussed in a general BOS section (3.1.6). A detailed level diagram of the BOS is presented in appendix 11.

Table 7: Material and Energy Requirements per Multi-Crystalline KC120 Module

No	Materials	Mass (kg)	Energy Intensity. (MJ/kg)	Energy (MJ)	LCI Source*
1	Argon	0.58	2.00	1.15	ETH / Alsema
2	Hydro fluoric acid	0.10	22.50	2.30	ETH / Alsema
3	Sodium hydroxide	0.53	9.51	5.04	ETH / Alsema
4	Sulfuric acid	0.39	1.25	0.49	BUWAL / Alsema
5	HDPE	1.04	74.00	77.00	BUWAL / Alsema
6	Glass	7.49	13.90	104.08	BUWAL / Alsema
7	Aluminum	1.73E-04	134.00	2.32E-02	BUWAL / Alsema
8	Tin	0.02	228.00	4.92	IDEMAT / Alsema
9	Copper	0.02	69.40	1.50	ETH / Alsema
10	Polyester	1.06	2.39	2.53	IDEMAT / Alsema
11	Ammonia	0.01	12.90	0.10	BUWAL / Alsema
12	Nitrogen	0.09	3.15	0.27	ETH / Alsema
13	Charcoal	0.62	1.98	1.23	ETH / Alsema
14	Coal	0.94	30.60	28.71	ETH / Alsema
15	Coke	0.62	49.50	30.81	ETH / Alsema
16	Wood	2.19	0.04	0.10	ETH / Alsema
17	Silicium carbide	1.15	74.40	85.71	IDEMAT / Alsema
18	Tedlar	5.02	18.59	62.28	Franklin / Alsema
19	Aluminum	2.35	134.00	314.90	BUWAL / Alsema
20	Silicon	4.45	84.60	376.46	IDEMAT / Alsema
21	Aluminum	0.05	134.00	6.22	BUWAL / Alsema
22	Process energy			3019.25	IDEMAT / Alsema
Total				4125.1	

* The material and energy values were adopted from Phylipsen and Alsema 1995 and modeled using the various LCI databases mentioned.

3.1.6.1. Balance of the System - Kyocera Modules

The BOS for the Kyocera modules consists of junction boxes attached to the back of each module, wires, and the aluminum mounting structure. The mounting structure for the KC120 has a Two Seas Metalwork model GR 11, which consists of a set of aluminum struts. The dimensions of the vertical struts and the weight of the major components are detailed in appendix 6. The total aluminum volume is 300.63 in³. In addition there are

other aluminum parts: T shaped connectors and inside bar connectors. The total mass of aluminum required for manufacture of the mounting structure is estimated at 47.68 kg.

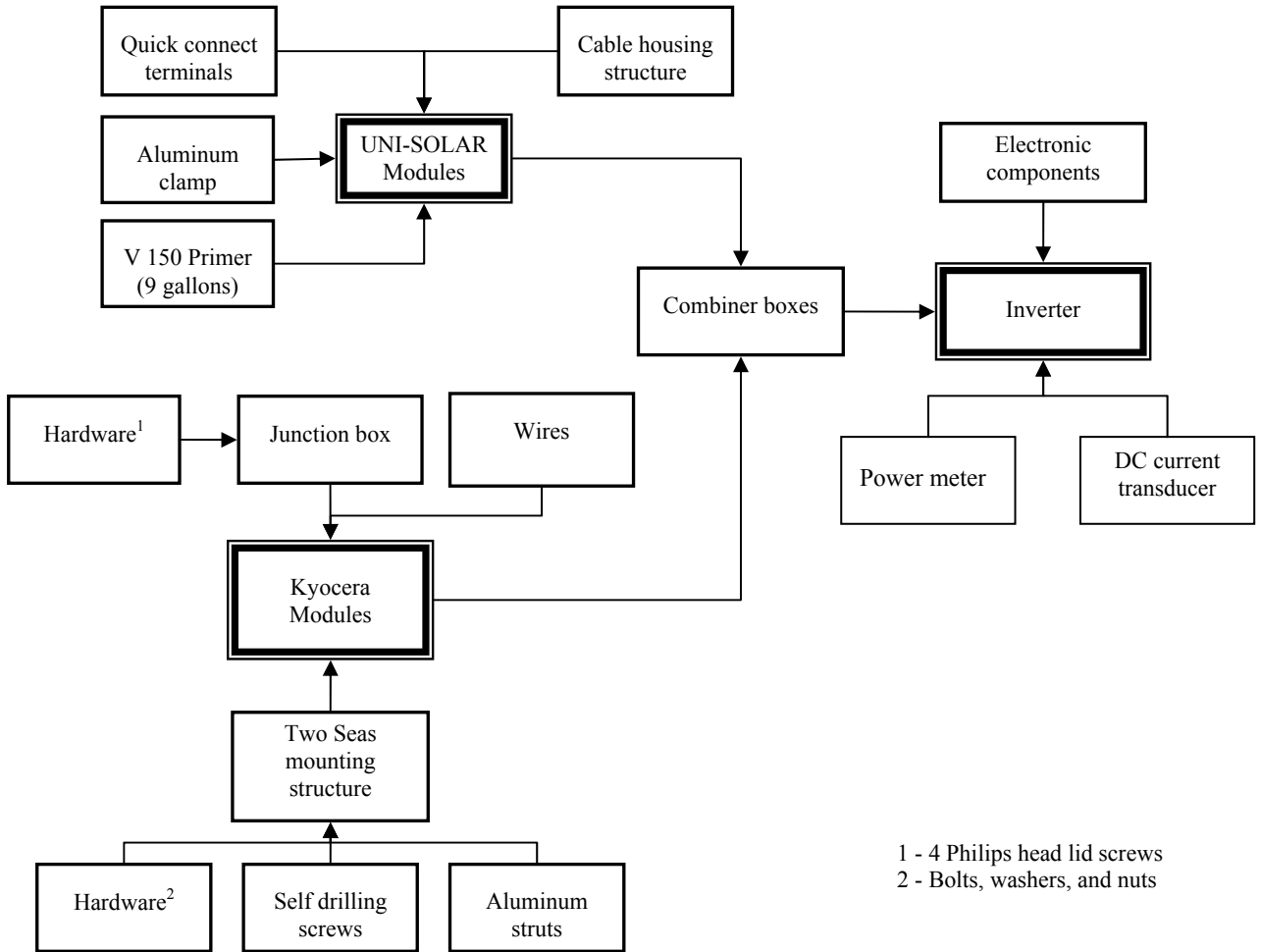


Figure 13: Level Diagram of Balance of the System (BOS) components

Each T shaped connector has 5 stainless steel bolts and nuts and 2 washers, and each inside bar connectors has 8 bolts and nuts, and 2 washers. The volume of each ASTM F 593 stainless steel hex cap nuts used in the supporting structure is 2 cm³. The mass of the total number of nuts, bolts, and washers used in the mounting structure is 12.14 kg (Appendix 6). About 7,700 MJ are consumed in the production of the mounting structure for the Kyocera modules.

3.1.6.2. Balance of the System - UNI-SOLAR Modules

The BOS of the UNI-SOLAR modules is less material intensive than the BOS of the multi-crystalline modules because these modules are mounted directly on the existing roof structure. However, because of the energy intensity of the materials used in some of the components the primary energy requirements may be substantial. For instance, about 10,400 MJ of primary energy are consumed in manufacture of the cable housing for the PVL modules.

Each UNI-SOLAR PVL136 module mounted on the seam has one aluminum clamp to hold the cable housing. All aluminum clamps are furnished with stainless steel bolts and washers (3/8" diameter x 5/8" length: bolt head size is 9/16"). The estimated aluminum volume of the clamp is 3.5 cm³. The volume of the 77 clamps used amounts to 57 cm³ (Appendix 7).

3.1.7. Common Balance of the System Components

In addition to BOS that is specific to the two different technologies there are also components that are required for the operation of the whole system. Combiner boxes consolidate the direct current (DC) output from the arrays whereas the inverter converts DC power into alternate current (AC).

3.1.7.1. Combiner Box

The combiner box is a device that combines the output of multiple high voltage solar electric (PV) source circuits. There are 3 combiner boxes on the roof of Dana. One combiner box draws power from the multi-crystalline modules (Kyocera), and the other 2 combiner boxes draw power from the thin film (UNI-SOLAR) arrays. The combiner boxes are high voltage PV array combiner boxes with 8 inputs and they are supplied by Connect Energy³². The boxes are rated at 600V(DC), have 10 PV input circuits with each circuit having the capacity to accept up to 8 input wire connections. The biggest advantage with the combiner box is the fact that it has the capacity to accept a number of input connections, yet only a pair of wires is required to connect the combiner box output

to the inverter. This results in considerably less wires being installed. The combiner box used on the roof of Dana Building is shown in Appendix 8. Manufacture of each one of the three combiner boxes required 330 MJ of primary energy.

3.1.7.2. Inverter

A 30 kW Ecostar™ Power Converter inverter manufactured by Ballard Power Systems (Dearborn, MI) is installed in Dana Building to convert the direct current (DC) generated by the PV system into alternating current (AC) that can be used to power the building. According to the manufacturer the maximum efficiency of the equipment occurs at 75% of its capacity (23 kW).³³ Figure 14 shows how the efficiency of the inverter changes with the electrical load. In the calculations in the report, we assumed a 95% conversion efficiency, which corresponds to the peak efficiency with transformer at 75% of output.³³ The data for the bill of materials for the inverter was collected directly from the facility located in Dearborn, Michigan. The inventory of the inverter included structural components, printed circuit boards, certain electronic components, wiring materials, nuts/bolts, packaging and transportation.

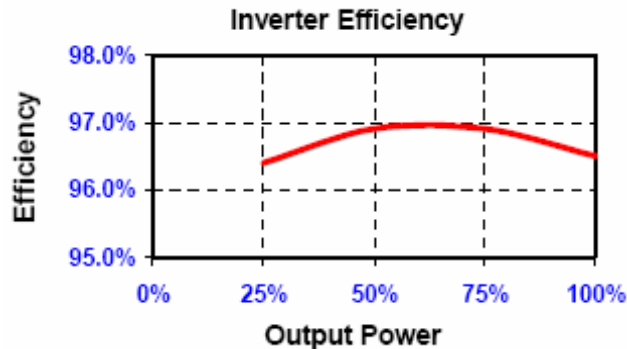


Figure 14: Inverter’s Efficiency as a Function of Its Capacity Use

The dimensions of the structural components were determined from the mechanical drawings of the components provided by the facility. All of the structural components were made of steel (AISI C1010). A total of 216 lb of steel was used for manufacturing the structural components after considering a stamping loss of 10%³⁴. The mass of the busbar (copper), heat exchanger and fan housing (both made of aluminum),

terminal block components (Polyethylene) and the inverter packaging (wood) were determined. After the mass of the materials going into a single inverter was determined, the energy consumption and the corresponding air emissions due to manufacture of the materials were determined by modeling the components using built in databases in SimaPro. Table 8 provides the type and amount of material that go into manufacture of one inverter along with the source database that was used in SimaPro to model the components. A detailed level diagram of the inverter is presented in appendix 11.

Table 8: Type, Mass and Source Database for Materials Used in the Inverter

Material	Mass (lb)	Source Database
Steel	216.0	Franklin
Aluminum	98.7	BUWAL
Copper	23.2	ETH-ESU
Polyethylene	5.3	BUWAL 250
Circuit boards	3.0	IDEMAT
Wood (Packaging)	107.9	IDEMAT
All other electronic components	n.a.	EIOLCA
Nuts and bolts	n.a.	EIOLCA

n.a. not available

SimaPro was also used to model three printed circuit boards, with 84 square inches of total area and weighing one pound each.

In addition, a list of the number of nuts and bolts (made of zinc plated steel) that go into the manufacture of one inverter was obtained from the facility. The cost of the number of nuts and bolts used was determined from the company that manufactured these components (McMaster-Carr, <http://www.mcmaster.com/>). A total of \$ 17.67 of nuts and bolts was determined to go into the manufacture of an inverter. The dollar value was then adjusted to equivalent 1997 values using the consumer price index (CPI) and the energy consumption for manufacturing the components was determined using the NAICS sector # 332720 (Turned product and screw, nut and bolt manufacturing) in EIOLCA. Six transducers were also modeled using the EIOLCA sector “all other electronic component manufacturing” and a cost of \$31.5 per unit.³⁵ Manufacture of the inverter demanded 15,100 MJ of primary energy.

The transportation of the inverter from the Dearborn facility to University of Michigan in Ann Arbor was also modeled. The transportation distance by road (distance 36.6 miles) was obtained from MapQuest and modeled using data for the truck from the ETH-ESU database in SimaPro.

3.1.8. Installation

The installation of the system consists of transportation of the modules from the factory to the installation site (Dana Building) and further the installation of the modules on to the roof of the building. The modules were transported in a Volvo FH 12 diesel truck coming from San Diego, CA to Ann Arbor, MI via Toledo, MI. The road distances were obtained from MapQuest³⁶ with the total distance traveled being 2,854.4 miles. The truck's mileage was 33 liters/100Km.³⁷

The total weight of the packages with thin film modules was 3460 lbs, whereas the total weight of the multi-crystalline modules was 6905.15 lbs. The total weight hoisted from the ground level to the roof of the three story building was 10,365.15 lbs. The equipment used was a Sterling truck with a Terex hoist (TC 4792). The truck was powered by a caterpillar engine (CAT 3126), and the performance of the engine during the hoisting of the packages was surveyed. The work load for each lift 384.44 lbs demanded 15,000 rpm for 45s. In order to hoist a total of 10,365 lbs, the hoist had to repeat the cycle 27 times (10,365 lbs / 384.4 lbs). The rest of the time the engine was idling at a 7,500 rpm. The total working time was approximately half an hour and the estimated energy consumption was approximately 3,000 MJ. (Details are presented in appendix 10).

Some modules, which were installed on the rubber membrane, required the use of primer (see appendix 7). The primer is used to clean up the surface before the application of the modules. About 8 gallons of Versico V150 primer, which is a toluene based product, were used for this purpose during the installation of modules on the membrane. The associated energy consumption (1,910 MJ) and air emissions due to the production of toluene are determined using SimaPro.

3.2. Power and Solar Radiation Availability

The amount of electricity produced by a PV system is directly proportional to the amount of solar radiation received by the arrays, which depends on the module's position relative to the sun. The geocentric position of the sun varies according to the latitude and the time of the year due to the tilt of the earth's rotation axis and its orbit around the sun. Figure 15 shows the position of the earth for the solstice of summer on the south and north hemispheres. During these days a module positioned flat on the tropics will receive the solar beams perpendicular to its surface at noon. During the same days if the module is positioned on the equator (latitude zero) it should be tilted by $23\frac{1}{2}^\circ$ to receive the sun beams perpendicular to its surface.

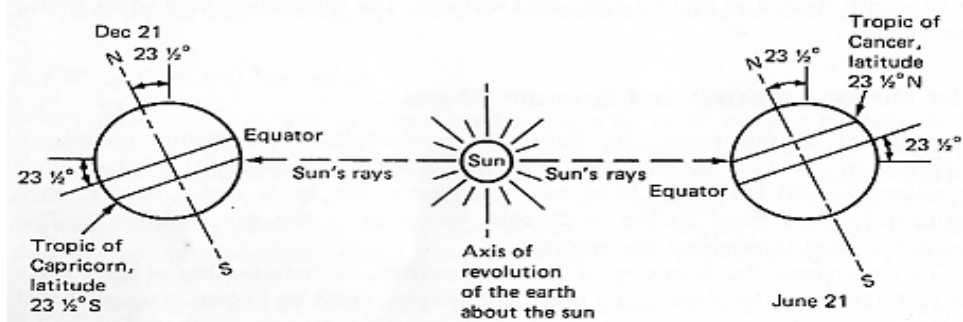


Figure 15: Motion of the Earth about the Sun and Location of Tropics³⁸

Solar beams reaching the module perpendicular to its surface are the most effective ones. Therefore, positioning the module in order to maximize the amount of solar radiation received perpendicular to its surface is fundamental to maximize the electrical output of the array.

The solar flux on the earth's surface perpendicular to the solar rays is $1,372 \text{ W/m}^2$. However, because of the tilt of the earth's axis ($23^\circ.43'$), the latitude of the globe which is exposed parallel to the solar rays varies seasonally. Moreover, for latitudes higher than the tropics ($23\frac{1}{2}^\circ$) sun beams will never reach the earth perpendicularly to its surface.

The geocentric position of the sun also varies according to the season of the year and the time of the day. Therefore, if the position of the sun is known, the module may be positioned to maximize its electricity output over a given period.

3.2.1. Solar Radiation Calculation and Module Position

In order to estimate the annual amount of electricity produced by solar modules it is necessary to know the total amount of solar radiation that reaches a module positioned at a specific location, tilt angle, and magnetic orientation. The total solar radiation combines the power from direct beams on the module's surface, the diffuse radiation, and the radiation reflected from the land surface back to the module's surface (albedo).

In order to quantify the amount of solar radiation, a model, which is based on the *Bird Clear Sky Model*³⁹ from the National Renewable Energy Laboratory (NREL), was created in an electronic spreadsheet.

The *Bird Clear Sky Model* calculates the available solar radiation over discrete time intervals during a year for a given location and date. It is a broadband algorithm which produces estimates of clear sky direct beam, hemispherical diffuse, and total hemispherical solar radiation on a horizontal surface. The excel spreadsheet (<http://rredc.nrel.gov/solar/models/clearsky/>) implementation of the model was done by Daryl Myers. The model is based on comparisons with results from more rigorous models available to calculate direct and diffuse solar radiation. It is composed of simple algebraic expressions with 10 user provided inputs. Model results should be expected to agree within $\pm 10\%$ with more rigorous models. The model computes hourly average solar radiation for every hour of the year, based on the 10 user input parameters; however variable atmospheric parameters such as aerosol optical depth, ozone, water vapor are fixed for the entire year.

This model calculates the solar radiation available on the roof of the Dana building. The exact coordinates of the location are obtained from a website, which uses the zip code as a reference.⁴⁰ The results for the zip code 48109 are Latitude North 42.2909, and Longitude West 83.7144 (-83.7144).

The Bird model calculates:

- Earth's declination in degrees (δ),
- Solar zenith angle in degrees (Z),
- Hour angle in degrees (H),
- Direct radiation normal to the beam at the earth surface (B) in W/m^2 ,
- Direct radiation incident upon a horizontal surface W/m^2 ,
- Global radiation incident upon a horizontal surface W/m^2 ,
- Diffuse radiation incident upon a horizontal surface (D_0) W/m^2 .

Because the output of the Bird model consists of the beam received at a horizontal surface due south, it is necessary to adjust the radiation according to the module's tilt (t) and azimuth (a_m) (Figure 16). The intensity on a tilted surface in W/m^2 is calculated based on equation 1:

$$I_{(tilt)} = B * \cos(i) + D_t + R_t \quad (1)$$

Where:

B is the direct radiation normal to the beam at the earth surface,

D_t is the diffuse sky radiation on a tilted module,

R_t is the reflected ground radiation in field of view of the tilted module.

Equation 2 is used to calculate the incidence angle beam i , on a tilted surface with an orientation other than due south:³⁸

$$i = \arccos[\cos(a_s - a_m) \times \cos \alpha \times \sin t + \sin \alpha \times \cos t] \quad (2)$$

Where:

a_s is the azimuth of the sun in degrees,

a_m is the azimuth of the module in degrees,

α is the solar altitude angle in degrees,

t is the tilt angle of the module in degrees.

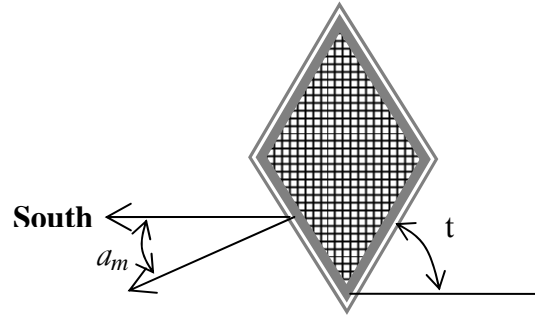


Figure 16: Scheme Showing a_m and t

The solar azimuth (a_s) in degrees is calculated based on the equation 3:⁴¹

$$a_s = \arcsin\left(\frac{\cos \delta \times \sin H}{\sin Z}\right) \quad (3)$$

Where:

δ is the Earth's declination,

H is the hour angle,

Z is the sun's zenith.

The diffuse sky radiation on a tilted module is calculated using equation 4.

$$D_t = 0.5 \times D_0 (1 + \cos t) \times \left[1 + \sin\left(\frac{t}{2}\right)^3 \right] \times [1 + \cos i^2 \times \sin Z^3] \quad (4)$$

Where:

Z is the sun's zenith angle in degrees,

t is the tilt angle of the module in degrees,

i is the incidence angle beam.

The reflected ground radiation in the field of view of the tilted module (R_t) in W/m^2 is calculated using equation 5.⁴²

$$R_t = 0.5 * D_0 * A * (1 - \cos(t)) \quad (5)$$

Where:

D_0 is the diffuse radiation incident upon a horizontal surface in W/m^2 ,

A is the ground albedo (0.2),⁴²

t is the tilt angle of the module in degrees.

Most of the parameters used in the equations above can also be determined for a specific time of the day and location using the website <http://www.susdesign.com/sunangle/>

3.2.2. Expected Electrical Output

The expected electrical output of the system depends on the amount of solar radiation received, the position of the modules and their respective efficiency. The efficiency of the modules is calculated based on the information provided in the specification sheets (appendices 3 and 4).

During testing, modules are exposed to a power intensity equivalent to $1,000 W/m^2$.

Thus, the efficiency of the module (η) is calculated using equation 6:

$$\eta = \frac{\text{module's rated power (W)}}{\text{module's area (m}^2\text{)} \times 1,000 W/m^2} \quad (6)$$

The amount of solar radiation depends on the position of the modules. All modules are positioned due south; however, 77 PVL136 modules and 72 PVL62 modules are placed on the steel standing seam with a 12° tilt angle. The rest of the PVL modules are mounted on the lower part of the roof, glued on the rubber membrane. This part of the roof has a tilt angle of 8° with respect to the horizontal plane. There are two arrays with 44 KC120 crystalline modules each, which are mounted on an aluminum structure. The tilt of these modules is similar to the standing seam position (12°).

By combining the output of the solar radiation model with the technical specification for the modules it is possible to determine the annual output of the system. Table 9 shows the information used to model the energy output of the system and its expected annual electricity generation. The total electricity output of the system in one year is 44,848 kWh. The actual output of the system after the 5% inverter loss during the conversion of direct current into alternating current is estimated at 42,555 kWh.

According to the Solar Radiation Data Manual for Flat-Plate and Concentrating Collectors published by the National Renewable Energy Laboratory (NREL), a module is generally exposed to the maximum yearly solar radiation when it is tilted by an angle equal to the local latitude. The performance can be optimized during the winter if the angle is 15° greater than the latitude and during the summer if the angle is 15° less than the latitude.⁴³

Table 9: PV System Characteristics and Annual Output

Module's location	Tilt angle	Annual solar radiation	Number of modules	Module's model	Area per module	Total area	Module's efficiency	Total annual output (DC)
standing seam	12 °	1,359 kWh/m ²	75	PVL62	1.03 m ²	77 m ²	6.62%	6,950 kWh
			77	PVL136	2.16 m ²	166 m ²	6.30%	14,240 kWh
rubber membrane	8 °	1,241 kWh/m ²	55	PVL136	2.16 m ²	119 m ²	6.30%	9,288 kWh
aluminum array	12 °	1,359 kWh/m ²	88	KC120	0.93 m ²	82 m ²	12.92%	14,370 kWh
DC Total								44,848 kWh

A module located in Detroit, MI (latitude N 42.42 and longitude W 83.02) due south tilted at an angle that equals the site latitude minus 15 degrees (27.42°) receives an amount of annual solar radiation that corresponds to 1,570 kWh/m² (Appendix 5). The total system output based on this position of the arrays would correspond to 52,825 kWh, which is 15% more than the amount predicted with the actual position of the arrays. Usually, between 15-40% more energy could be produced if systems were optimally oriented and tilted.¹⁹

3.3. Inventory of Electricity Supply for the Dana Building

The current electricity sources for the Dana building are the campus power plant (CPP), and the East Central Area Reliability Coordination Agreement (ECAR) grid energy fuel mix. The share of each source varies but on average 67% of the energy is produced by the Campus Power Plant (CPP) and 33% is purchased from the ECAR grid⁴⁴.

The installation of the thin film and multi-crystalline PV arrays will diversify the electricity supply sources for the Dana Building (Figure 17). The substitution of renewable energy for the CPP and ECAR sources brings about tangible environmental benefits such as improvement in air quality and fossil fuel resource conservation. Such environmental benefits realized due to the displacement of electricity generated from CPP and ECAR by PV electricity will be quantified and presented.

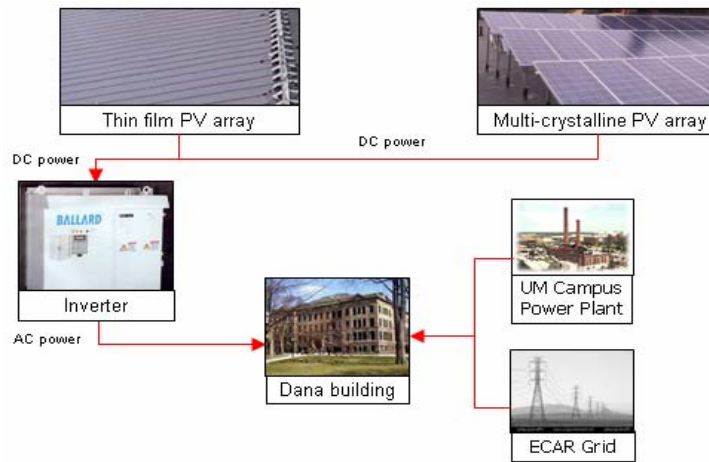


Figure 17: Present Electricity Sources for the Dana Building

3.3.1. Campus Power Plant (CPP)

The Central Power Plant is a combined heat and power (CHP) facility located on the central campus of the University of Michigan. In 2003/2004 the total output of the plant was 2.6 billion pounds of steam. The “Fuel Consumption and Power Production for the period 2003/2004 is shown on Table 10.

Table 10: CPP Fuel Consumption and Power Production Summary 2003 - 2004⁴⁵

Category (unit)	Jul-03	Aug-03	Sep-03	Oct-03	Nov-03	Dec-03	Jan-04	Feb-04	Mar-04	Apr-04	May-04	Jun-04	Total	
Fuel	Gas (CCF)	3,841,840	4,147,260	3,715,530	2,820,760	2,875,890	3,672,990	2,730,540	3,790,260	2,744,540	2,499,190	3,070,880	3,652,490	39,562,170
	Oil (Bals)	0	0	0	0	20,254	72,990	454,567	58,387	0	0	368	10,354	616,920
400# Steam (KLB)	258,775	266,741	244,171	187,565	196,758	202,043	215,600	263,147	182,859	166,991	194,151	238,930	2,617,731	
Gross Generation (KWH)	14,515,000	18,226,000	16,612,000	13,163,000	13,704,000	15,219,000	15,727,000	18,182,000	11,022,000	9,692,000	13,360,000	16,917,000	176,339,000	
Station Power (KWH)	(1,441,000)	(1,583,000)	(1,458,000)	(1,384,000)	(1,324,000)	(1,313,000)	(1,564,000)	(1,632,000)	(1,396,000)	(1,430,000)	(1,449,000)	(1,600,000)	(17,574,000)	
Net Generation (KWH)	13,074,000	16,643,000	15,154,000	11,779,000	12,380,000	13,906,000	14,163,000	16,550,000	9,626,000	8,262,000	11,911,000	15,317,000	158,765,000	
Purchased Power (KWH)	7,028,000	7,336,000	9,408,000	9,380,000	9,044,000	5,992,000	4,396,000	4,592,000	9,240,000	12,488,000	9,408,000	8,631,000	96,943,000	
Power Sold (KWH)	0	(14)	0	0	(404)	(1,802)	(54,709)	(86,203)	0	0	0	0	(143,132)	
Net Power Distribution (KWH)	20,102,000	23,978,986	24,562,000	21,159,000	21,423,596	19,896,198	18,504,291	21,055,797	18,866,000	20,750,000	21,319,000	23,948,000	255,564,868	

The energy input in the CPP is used to determine the natural gas volume required to produce steam and electricity, which is then compared to the output of the PV system. The operation of the CPP is also important to calculate the emissions avoided due to the production of photovoltaic energy. The average boiler efficiency of the plant is 83%.⁴⁴

After producing electricity in a turbine, the waste heat is recovered in a boiler producing steam, which is further added to the steam produced in a conventional boiler (Figure 18). A fraction of the steam is used to produce more electricity in a turbine, and the remaining steam goes into the tunnels that are connected to the steam network of the University of Michigan. Consequently, the amount of useful energy output from the facility is maximized.

The steam supplied to heat the buildings is of two types; 80% is supplied at 9.5 psi, and 20% is supplied at 63 psi.⁴⁴ Based on thermodynamic properties the heat content of the two steam types is 1,165.8 Btu/lb and 1,201.8 Btu/lb respectively.⁴⁴ The total heat content from the two types of steam is thus calculated. Based on the natural gas energy density of 1034 Btu/ft³ the volume of natural gas required to produce the total amount of steam is calculated assuming the same 83% boiler efficiency. The corresponding monthly electricity output of the CPP is used to normalize the volume of natural gas per kWh of electricity produced. A detailed energy flow diagram of the plant is presented in Figure 18.

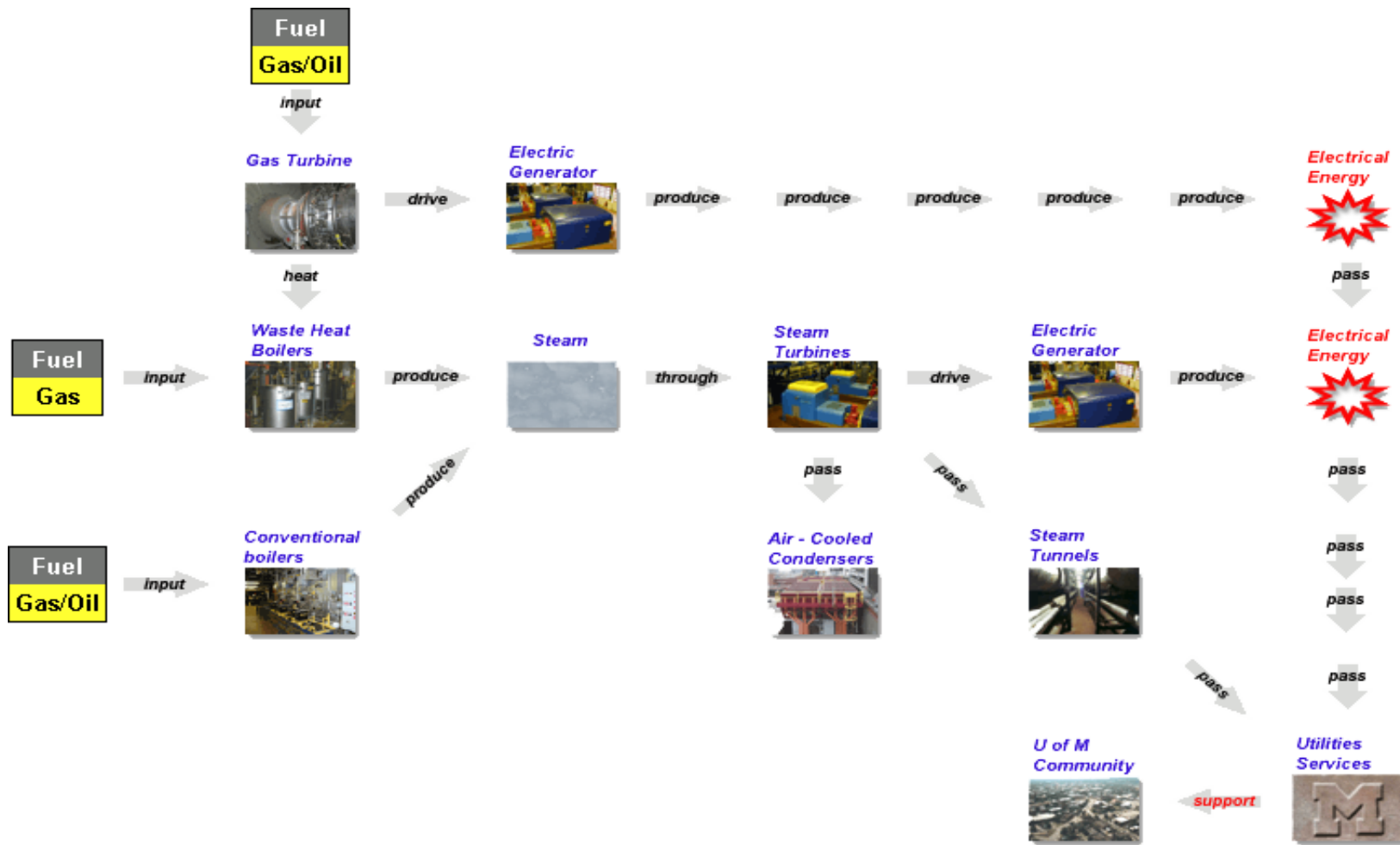
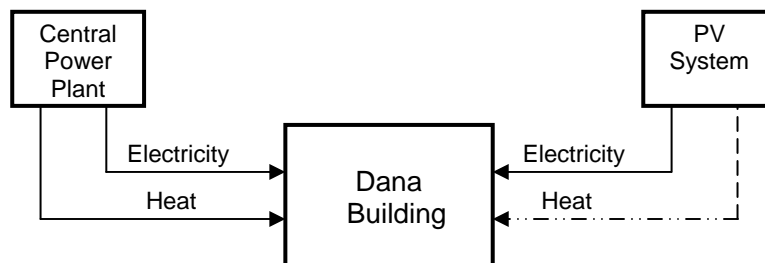


Figure 18: Central Power Plant Cogeneration Diagram⁴⁶

3.3.2. Compensatory Heating System for PV

The central power plant (CPP), whose primary function is the supply of heat to the buildings, also provides a certain fraction of electricity to the buildings. As mentioned before in the case of Dana Building, the central power plant contributes to 67% of the electrical load. In essence there are two types of services (heat and electricity) provided by the central power plant. About 42,555 kWh of electricity generated by the PV every year is supplied to Dana Building (after consideration of the 5% inverter losses). For the PV system to substitute for the central power plant i.e. to provide the same service as that of the central power plant, it also has to provide a certain amount of heat to the buildings. Thus the compensatory system supplies heat, in addition to the electricity generated by the PV system for both the system so that the PV system provides the same service as the CPP (Figure 19). The compensatory system is modeled based on the operation of the CPP.



To provide the same service as the central power plant, a certain amount of heat has to be produced in addition to the electricity generated. In essence, the environmental impacts of producing steam out of natural gas can be attributed to the PV system.

Figure 19: Compensatory System for Dana Building

In the calendar year 2003-2004, the central power plant generated 1.45×10^8 lbs steam (9.5 PSI) and 14,695 MWh of gross electricity. Using this heat to electricity ratio, the steam that has to be generated by the PV system corresponding to the annual electricity generated (42,555 kWh) was determined to be 4.19×10^5 lbs. Using a boiler efficiency of 83%⁴⁴, the natural gas required to generate the steam was calculated to be 5.70×10^5 ft³. The environmental impacts of producing this amount of natural gas can be attributed to the PV system. About 13,390 ft³ of natural gas was required to be produced

for every MWh generated by the PV system for the PV system to provide the same service as that of the central power plant.

4. Results and Discussion

The LCA of the PV system is used to quantify primary energy inputs in the system and its corresponding environmental impacts. These values are compared to the impacts caused by the traditional electricity generation sources that also supply power to the Dana building.

4.1. Primary Energy Consumption

The complete PV system consisting of 88 KC120 crystalline modules, 75 PVL62 thin film modules and 132 PVL136 thin film modules, balance of system, inverter installation and transportation energy, were modeled using the life cycle software SimaPro 6.0. Detailed level diagrams of the model built in SimaPro are included in appendix 11. The total primary energy consumption of the PV system was 9.07×10^5 MJ. Table 11 presents the breakdown of the energy input into the system and the percentage of total energy consumed by each one of its components. Out of the total primary energy consumption of 7.85×10^5 MJ, 86% (6.78×10^5 MJ) was for the production of the PV modules.

Table 11: Breakdown of the Total Energy Input into the PV System.

System Components	Energy Input MJ	% of Total Energy
Kyocera KC120 modules	3.63E+05	46%
UNI-SOLAR PVL136 modules	2.46E+05	32%
UNI-SOLAR PVL62 modules	6.43E+04	8%
Transportation	5.94E+04	8%
Balance of system	1.81E+04	2%
Installation	1.48E+04	2%
Inverter	1.51E+04	2%
Total	7.81E+05	

Table 12 presents the primary energy consumption per area (m^2) for three types of PV modules used. The PVL62 and PVL136 modules consumed approximately the same amount of energy per m^2 basis while the multi-crystalline module was 5.2 times as energy intensive as the thin film modules. It is necessary to mention here that the energy data for the thin film and multi-crystalline modules were obtained from different sources. The energy for the thin film modules was obtained from UNI-SOLAR where as the energy for the multi-crystalline modules was obtained from previous research literature (Alsema, Nieuwlaar, 2000; Phylipsen and Alsema, 1995)

Table 12: Primary Energy Consumption per Area for 3 PV Modules

Photovoltaic Module	Primary Energy per module MJ	Area per module m^2	Energy/Area MJ/m^2
PVL62	857	1.028	834
PVL136	1,860	2.160	861
KC120	4,120	0.929	4,435

Table 13 presents the primary energy consumption per peak power (W_p) for the three types of photovoltaic modules used. The PVL62 and PVL136 modules consumed approximately the same amount of energy per power (W_p) basis while the multi-crystalline module was 2.4 times as energy intensive to produce as the two thin film modules.

Table 13: Primary Energy Consumption per Peak Power (W_p) for 3 PV Modules

Photovoltaic Module	Primary Energy per module MJ	Power per module W	Energy / Peak Power MJ/W_p
PVL62	857	62	14
PVL136	1,860	136	14
KC120	4,120	120	34

4.2. Environmental Emissions and Impacts

Table 14 presents the mass of criteria air pollutants and greenhouse gases released at every stage of the life cycle of the PV system and its major components.

Table 14: Criteria Air Pollutants and Greenhouse Gas Emissions of the PV System

	Units	PVL136	PVL62	KC120	BOS	Installation	Transport	Inverter	Total
Air Pollutants									
Carbon Monoxide (CO)	kg	13.4	3.54	19.4	0.427	23.9	5.13	3.24	69.04
Particulate Matter (PM ₁₀)	kg	2.16	0.56	3.00	0.10	0	0	0	5.86
Nitrogen Oxides (NO _x)	kg	47.67	12.41	67.60	2.38	78.30	2.33	3.45	210.70
Sulfur Oxides (SO ₂)	kg	97.68	25.43	144.69	7.72	6.56	10.21	4.54	292.29
Lead (Pb)	kg	6.24E-04	1.69E-04	4.71E-03	5.66E-07	1.79E-04	1.70E-02	1.13E-03	2.27E-02
Hydrocarbons (HC)	kg	17.50	4.61	18.03	1.94	27.23	1.58	2.99	70.88
Greenhouse gases									
Carbon dioxide (CO ₂)	kg	12,934	3,379	19,745	1,110	4,350	881	669	12,934
Methane (CH ₄)	kg	26.9	6.98	39.7	0.292	5.3	1.93	1.66	26.9

For the criteria air pollutants, the production of the three photovoltaic modules contributed to 48% of the carbon monoxide emissions with the other significant contribution occurring during the transportation stage. The production of photovoltaic modules also contributed to 98%, 83%, 99% and 81% of PM₁₀, SO₂, lead and hydrocarbons, respectively. The transportation stage contributed to 37% of NO_x with the remaining NO_x emissions occurring during the production of the photovoltaic modules. The photovoltaic modules also contributed to 84% and 89% of the CO₂ and methane emissions, respectively. Thus it is evidently clear that except for NO_x, the production of photovoltaic modules emit the highest amount of air emissions among all life cycle stages. The potential net environmental benefits due to the installation of the PV system are calculated by comparing these emissions and the emissions from displacing the traditional electricity sources that previously supplied electricity to Dana Building. The environmental impacts due to the manufacture of the PV modules were calculated using the CML Baseline method (principle of the method explained later in section 4.8.2). The

global warming, smog formation and acidification impacts due to manufacturing were 4.47×10^4 kg CO₂ equiv, 32.3 kg C₂H₂ equiv and 452 kg SO₂ equiv, respectively.

The human health and ecological benefits, which consider the impacts of the electricity displaced, are presented in sessions 4.8.1 to 4.8.2. The baseline analysis was performed for a time period of 20 years which is the warranty life time for the thin film modules. Additionally, in relevant cases, results for the analyses for two time periods of 10 and 30 years are also provided.

4.3. Environmental Footprint of the Three PV Modules

The ecological footprint method evaluates the land area impacts exerted by the resource-energy consumption and greenhouse gas emissions associated with a process. In order to convert the release of CO₂ from a process, the molar carbon fraction (12 g of C per 44 g of CO₂) is applied. Further, using the factor of 1.8 metric tons of carbon / hectare / year⁴⁷ the land area required for the assimilation of CO₂ emitted from a process is determined. This factor means that an average forest area of one hectare can sequester 1.8 metric tons of carbon per year. In essence a hectare (10,000 m²) of forest area is thus used to sequester 1.8 metric tons of carbon emitted from a process or service. In this study, we calculated the land area impacts (in land area equivalents) exerted during manufacture of the three PV modules (due to the release of CO₂), added that value to the actual amount of land area (roof of Dana Building) occupied by the three PV modules. However the area due to resource extraction such as mining was not considered in the analysis.

As explained previously, the multi-crystalline modules consumed more energy (and consequently emitted more CO₂) during manufacturing than the thin film-modules. On the contrary the multi-crystalline Kyocera modules produce more than twice the amount of power than the two thin-film modules per unit area. Table 15 presents the amount of power generated by the three PV modules on an area basis. So, the ecological footprint impact results will provide a clear idea on the type of module exerting the higher overall environmental land area impacts in this case.

Table 15: Power to Area Ratio of the Three PV Modules

PV Modules	Power-Area ratio (W/m ²)
KC120	129
PVL62	60
PVL136	63

Figure 20: presents the total land area impacts (sequestration area due to CO₂ emissions during manufacturing added to the occupied area on the roof of Dana Building) per module, for the multi-crystalline and thin film PV modules. The multi-crystalline module exerts 4.9 times and 2.3 times the land area impacts as the PVL62 and PVL136 modules, respectively. This result demonstrates that even though the multi-crystalline module generates twice the amount of power for the same area (occupies less area to produce the same power) when compared to the thin-film modules, the fact that it is 5.2 times more energy intensive than the two thin film modules causes it to exert an overall higher footprint impact than the two thin-film modules.

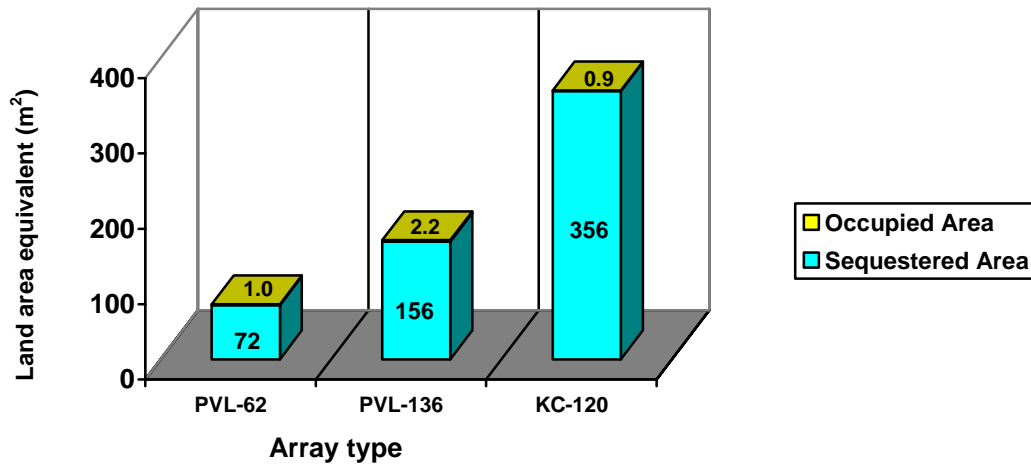


Figure 20: Total Land Area Impacts per Module of the Three PV Modules

Figure 21: presents the total land area impacts (occupied area+ sequestration area) for the three PV modules based on the life time (20 years) AC electricity output of the individual modules. The two thin film modules exerted approximately the same land area impact (10 m²/MWh for the PVL62 module and 7 m²/MWh for the PVL136 module).

The difference is due to higher average electrical output of the PVL62 array per unit of area when compared to the average for the PVL136 array. The better performance of the PVL62 array is because it is installed at a more favorable tilt angle compared to part of the PVL136 array that is placed on the rubber membrane. The multi-crystalline module exerted 2.5 times and 3.6 times the land area impact of the PVL62 and PVL136 modules, respectively. This result reflects the higher sequestration area needed for the multi-crystalline module due to the 5.2 times higher energy consumption during the manufacturing stage than the thin film modules coupled to its higher conversion efficiency compared to the PVL laminates (13% versus 6%).

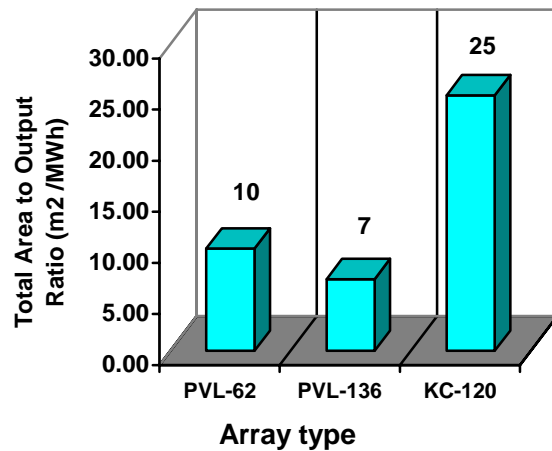


Figure 21: Total Land Area Impacts of the Three PV Modules Installed

4.4. Net Energy Ratio

The Net Energy Ratio (NER) can be defined as the ratio between the lifetime energy output of the system over the lifetime primary energy input into the systemⁱⁱ. In this case, it is expected that the PV system produces energy over a 20 year lifetime. The energy input to the system can be allocated to the manufacture of crystalline modules, two types of the thin film modules, balance of system components, inverter, and installation and transportation energy.

ⁱⁱ solar radiation is not included in the primary energy input of the system

$$\text{Net Energy Ratio (NER)} = \frac{\text{life cycle electrical energy output}}{\text{lifecycle primary energy input}} = \frac{E_{out}}{E_{in}}$$

$$= \frac{E_{KC-120} + E_{PVL-62} + E_{PVL-136}}{E_{KC-120} + E_{PVL-62} + E_{PVL-136} + E_{BOS} + E_{Installation} + E_{Transportation} + E_{Inverter}}$$

The annual DC energy output of the system using the *Bird Clear Sky Model* was 6,950 kWh (PVL62 modules), 23,528 kWh (PVL136 modules) and 14,370 kWh (KC120 modules) summing up to 44,848 kWh for a year. The annual energy output when combined with the inverter efficiency of 95%, total energy of 42,606 kWh is supplied to the building. The net energy ratio (NER) for the system is calculated for a period of 10, 20 and 30 years. The output from the PVL modules was calculated assuming a degradation of 1.1% in cell output efficiency per year²⁴

Figure 22 presents the net energy ratio (NER) of the complete system based on the AC electricity output from the system. The NER for 10, 20, 30 years was 1.9, 3.7, and 5.3, respectively, indicating that in the 10th, 20th and 30th year the cumulative energy generated from the system will be 1.9 times, 3.7 times and 5.3 times the energy input into the complete system. Further, the net energy ratio of the three individual PV modules was calculated for a time period of 20 years. The net energy ratio of the PVL62, PVL136 and KC120 modules for 20 years was 6.4, 5.7, and 2.7, respectively.

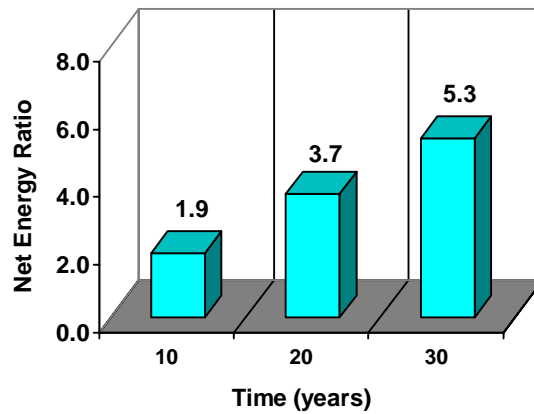


Figure 22: Net Energy Ratio of the PV System for 10, 20 and 30 Years

Figure 23 presents the net energy ratio of the three individual modules for two different cases: with and without the allocation of the inverter manufacturing energy to the individual modules. The total inverter manufacturing energy (1.51×10^4 MJ) was allocated to the three modules based on the fraction of the electrical output of their corresponding arrays. Accordingly 15.5% (2.34×10^3 MJ), 52.5% (7.92×10^3 MJ) and 32% (4.84×10^3 MJ) of the total inverter manufacturing energy was allocated to the PVL62, PVL136 and KC120 modules, respectively.

When the inverter energy was not allocated to the PV modules, the NER of the PVL62, PVL136 and KC120 modules generate 6.7, 5.9 and 2.7 times the energy that was consumed during the production of the modules, over a life time of 20 years. When the manufacturing energy of the inverter was allocated to the modules, the NER of the PVL62, PVL136 and KC120 modules was reduced by 0.24, 0.19 and 0.04, respectively.

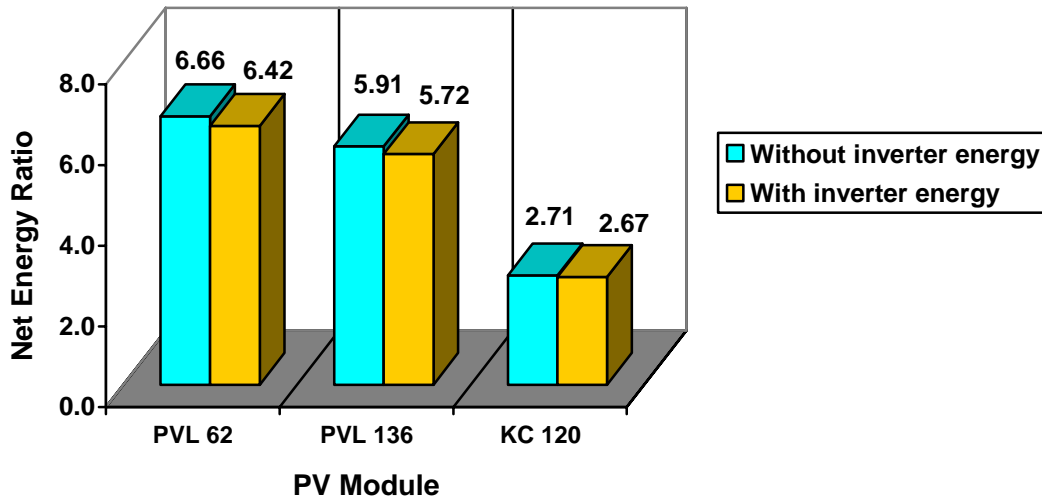


Figure 23: Net Energy Ratio (NER) of the PV Modules for Two Inverter Cases

4.5. Energy Pay Back Time

The energy pay back time (EPBT) indicates the number of years taken by the PV system to generate an equivalent amount of energy that was required to manufacture the

entire system. In this study, we calculated two different types of energy pay back times: energy pay back times for the crystalline and two types of thin-film modules, and the energy pay back time for the entire system.

The energy pay back time for three types Kyocera and UNI-SOLAR modules was calculated using the following ratio.

$$EPBT_{KC-120}(\text{years}) = \frac{\text{Energy input for the production of 88 KC - 120 modules}}{\text{Annual energy output of 88 KC - 120 modules}}$$

$$EPBT_{PVL-62}(\text{years}) = \frac{\text{Energy input for the production of 75 PVL - 62 modules}}{\text{Annual energy output of 75 PVL - 62 modules}}$$

$$EPBT_{PVL-136}(\text{years}) = \frac{\text{Energy input for the production of 132 PVL - 136 modules}}{\text{Annual energy output of 132 PVL - 136 modules}}$$

Figure 24 presents the energy pay back times for the three PV modules for the two cases of with and without allocating the manufacturing energy of the inverter to the individual modules. The E-PBT of the PVL62, PVL136 and KC120 modules without the allocation was 3.00 years, 3.38 years and 7.39 years, respectively. This is the energy breakeven point in years at which the exclusive energy output from the three modules is equivalent to the energy spent in manufacturing the respective modules. The E-PBT of the PVL62, PVL136 and KC120 modules increased, respectively, by 0.11 years, 0.11 years and 0.10 years when the inverter manufacturing energy was taken into consideration. Figure 25 presents the E-PBT of the three PV modules (inverter's allocation included) and for the entire system, including energy consumption associated with inverter, BOS, and installation.

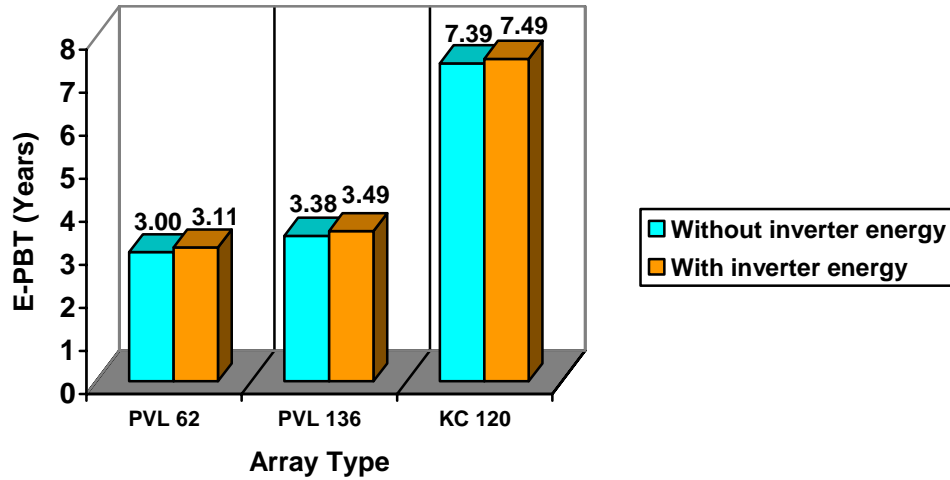


Figure 24: Energy Pay Back Time of PV Modules for the Two Inverter Cases

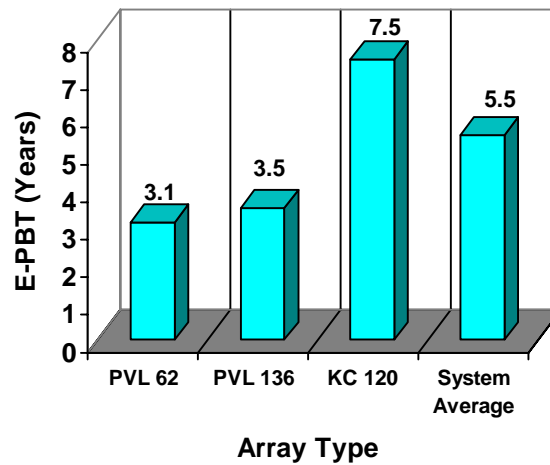


Figure 25: Energy Pay Back Time of the PV Modules and The Entire System

The total system energy pay back time is also calculated for the entire system and the ratio used in provided below.

$$EPBT_{\text{System}} (\text{years}) = \frac{E_{\text{KC-120}} + E_{\text{PVL-62}} + E_{\text{PVL-136}} + E_{\text{BOS}} + E_{\text{Installation}} + E_{\text{Transportation}} + E_{\text{Inverter}}}{E_{\text{KC-120}} + E_{\text{PVL-62}} + E_{\text{PVL-136}}}$$

When the entire system is taken into consideration the energy pay back time was 5.5 years (Figure 26) indicating that in 5.5 years the three types of PV modules will generate the amount of energy equivalent to the energy consumed during manufacture of the entire PV system. This time period also indicates the remaining time (14.5 years) for which net energy benefits can be realized from the PV system, expecting a 20 year life time for the PV modules.

4.5.1. Kyocera Modules' Pay Back Time With and Without the Frame

A single Kyocera KC120 module (0.93 m^2) is supported by a 2.35 kg aluminum frame. The total amount of aluminum required to support the 88 Kyocera modules (area: 81.7 m^2) is 206.8 kg. The primary energy required to manufacture the 206.8 kg of aluminum is 28,000 MJ, which is 7.7% of the total energy required to manufacture the Kyocera modules. As mentioned above, manufacturing aluminum is a highly energy intensive process, and in this section the impact of the aluminum frame on the final results is tested by calculating the energy pay back time (E-PBT) and the net energy ratio (NER) for the Kyocera modules without the aluminum frame.

Figure 26 presents the energy pay back time for both the Kyocera modules and the entire system with and without taking the frame into consideration. The energy pay back time was reduced by 8.1 % (7.40 years to 6.8 years) for the Kyocera modules and 4% (3.5 years to 3.4 years) for the entire system. Figure 27 presents the net energy ratio of the Kyocera modules with and without the frame for 10, 20 and 30 years. The input energy decreases by 28,000 MJ when the frame is not used. Consequently the net energy ratio slightly increased for all the time periods.

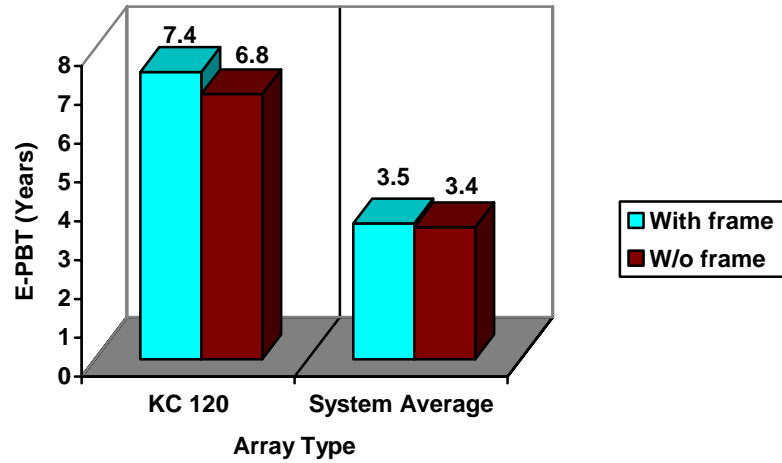


Figure 26: Impact of Frame on the E-PBT of Kyocera Modules and the System

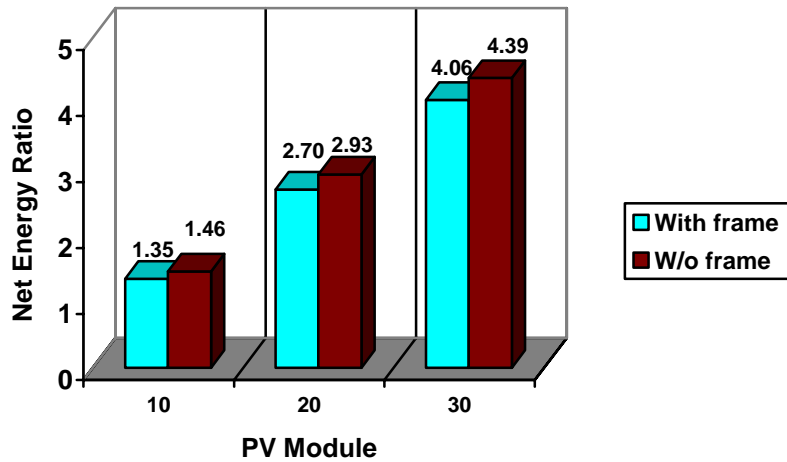


Figure 27: The NER of Kyocera Modules With and Without the Frame

The net energy ratio for the Kyocera modules were 1.46, 2.93 and 4.39 without the frame and 1.35, 2.70 and 4.06 with the frame included for 10, 20, and 30 years, respectively.

4.6. Pollution Prevention Benefits

The air pollution benefits (emissions avoided) due to the electricity generated from the PV system over 10, 20, and 30 years were calculated. As mentioned in the methods section, Dana Building receives 33% of its electricity from the ECAR grid and 67% from the CPP plant, which also delivers 9.5 psi steam to the building. Emissions from a compensatory system are subtracted from the average emissions from the traditional sources (CPP and ECAR). Emissions from a hypothetical compensatory system are estimated based on the same boiler efficiency of the CPP (83%) and typical emission factors.⁴⁸ Using the weighted emission factors (g/kWh) calculated, the total amount of electricity displaced by the PV system in 10 years (0.47 Million kWh), 20 years (0.93 Million kWh) and 30 years (1.4 Million kWh) the pollution prevention benefits were determined. Table 16 presents the CPP, ECAR, average emissions, and the net emissions factors.

Two different net emission factors are presented in Table 16. The ‘Net Emissions’ factors calculation assumes that for every kWh displaced, only 67% (670Wh) are associated with steam production because the remainder of the power 33% comes from the ECAR grid.

The ‘Net Emissions*’ factors present the values calculated for 100 % electricity displaced only from the ECAR grid. Therefore, this calculation does not take into account the compensatory system.

Since a combination of CPP and ECAR was used to model the electricity supplied to the Dana Building, the air pollution reduced was assumed to have occurred in the same region. Using photovoltaic energy to reduce conventional grid electricity becomes even more important in the ECAR region because the fossil fuels dominated fuel mix (89.5% coal and natural gas) emits higher quantities of air pollution. Policy makers should take notice to this fact when dealing with regions having problems in meeting the national ambient air quality standards (NAAQS) such as the metropolitan area of Detroit-Ann Arbor-Flint⁴⁹. It is also important to mention that displacement of a fraction of grid

electricity also reduces the consumption of exhaustible fossil fuel resources such as coal and natural gas.

According to EPA's criteria pollutant area summary report of 2005, the region comprising Detroit Ann Arbor and Flint was considered a non attainment area with respect to PM_{2.5} emissions and was marginal with respect to the 8 hour ozone standard. Therefore, reducing PM₁₀ emissions and reducing emissions of the precursors of ozone formation would contribute towards improving the regional environmental qualityⁱⁱⁱ.

Reductions of carbon dioxide emissions have an important global effect. Greenhouse gas emissions associated with electricity generation in 1999 in the US corresponded to 612 million metric tons of carbon.⁵⁰ The global average fossil fuel emissions, which include electricity generation, energy for transport and cement production corresponded to 5,762 million metric tons of carbon⁵¹. Thus electricity generation in the US is responsible for 11% of the global carbon emissions, and efforts that reduce emissions associated with electricity generation will help to alleviate the pressure exerted by the US on the global climate.

ⁱⁱⁱ PM₁₀ refers to particles with less than 10µm of diameter and includes PM_{2.5}, which refers to particles with less than 2.5µm of diameter . PM_{2.5} represents the fraction of particles of most concern in terms of human health impacts.

Table 16: Total Mass of Air Pollutant Emissions Reduced by the PV System

		UM CPP g/kWh	ECAR Grid g/kWh	Weighted Emission Factors g/kWh	PV system g/kWh	Compensatory System g/kWh	Net Emissions g/kWh	Net Emissions* g/kWh
Metals	Arsenic (As)	9.53E-07	3.30E-05	1.15E-05	2.24E-06	1.22E-06	8.47E-06	3.08E-05
	Cadmium (Cd)	5.24E-06	3.81E-06	4.77E-06	1.30E-06	6.69E-06	-1.02E-06	2.51E-06
	Chromium (Cr)	6.67E-06	4.28E-05	1.86E-05	2.87E-06	8.51E-06	1.00E-05	3.99E-05
	Mercury (Hg)	1.24E-06	2.99E-05	1.07E-05	1.05E-06	1.58E-06	8.58E-06	2.88E-05
Criteria Air Pollutants	Carbon Monoxide (CO)	0.64	0.22	0.50	0.081	5.11E-01	7.82E-02	1.39E-01
	Particulate Matter (PM ₁₀)	5.61E-02	1.29	0.46	0.007	4.62E-02	4.25E-01	1.28E+00
	Nitrogen Oxides (NO _x as NO ₂)	1.55	3.64	2.24	0.248	1.95E-01	1.86E+00	3.39E+00
	Sulfur Oxides (SO _x as SO ₂)	6.45E-03	6.22	2.06	0.343	3.65E-04	1.71E+00	5.88E+00
	Lead (Pb)	2.66E-06	4.32E-05	1.60E-05	2.67E-05	3.04E-06	-1.26E-05	1.65E-05
Greenhouse Gases	Carbon dioxide (CO ₂)	571.56	966.2	701.79	49.817	7.29E+02	1.63E+02	9.16E+02
	Methane (CH ₄)	0.01	2.10	0.70	0.095	1.40E-02	5.95E-01	2.00E+00
Air Toxics	Benzene (C ₆ H ₆)	1.00E-05	1.26E-05	1.09E-05	2.00E-04	1.28E-05	-1.97E-04	-1.87E-04

* assumes that PV system replaces 100% of ECAR grid electricity

4.7. Sensitivity Analysis of Pollution Prevention Benefits

The amount of air pollutant emissions reduced due to electricity generated from the photovoltaic system depends on the sources (University of Michigan Campus Power Plant (CPP) and ECAR Grid) that supply electricity to Dana Building. As mentioned previously, the University of Michigan currently receives two thirds of electricity from the campus power plant, and the rest is purchased from the ECAR grid (baseline scenario used for all other calculations). The air emissions of CO, PM₁₀, SO₂, NO_x, Pb and CO₂ were considered for the analysis. The emission factors of the two electricity sources, the composite (weighted) emission factors, and the net emission factors, considering the compensatory system, are presented in Table 16.

Except for carbon monoxide (CO) the campus power plant released lesser amounts of all other air emissions considered than the ECAR grid. The PV system is expected to generate 0.80 million kWh over a period of 20 years and consequently reduces the air emissions by displacing electricity generated from the two above-mentioned sources. Due to the fact that electricity supplied to Dana Building by the central power plant does not have significant distribution-transmission losses the amount of electricity displaced in 20 years was considered to be equivalent to the amount of PV electricity generated in 20 years. As far as the ECAR grid is concerned, a transmission-distribution loss of 10% has been reported.¹² So, the actual amount of grid electricity displaced by the PV system in 20 years is expected to be 110% of the PV electricity generated in 20 years. Figure 28 presents the share of avoided air emissions from each of the displaced sources. Since the campus power plant released a comparatively higher amount of CO on a per kWh basis than the ECAR grid, highest amounts of CO will be reduced if 100% of electricity is supplied by the campus power plant than if 100% electricity is supplied by the ECAR grid. For all the other substances considered, the highest reduction in emissions occur due to the displacement of electricity supplied by the ECAR grid because of its comparatively higher emission factors than the ones from the campus power plant. Thus from an environmental standpoint, except for CO, it makes more sense to reduce the amount of electricity purchased from the grid to derive the maximum benefits from generating electricity from the PV system (Figure 28).

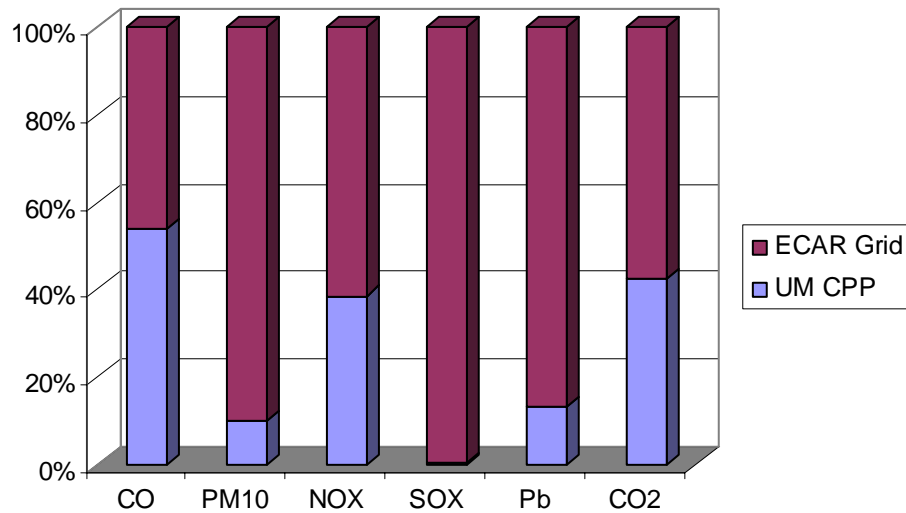


Figure 28: Share of Avoided Air Emissions from Each of the Displaced Sources

4.8. Life Cycle Impact Assessment Results

In this session, certain midpoint indicators are used to characterize the impacts reduced due to displaced electricity by the PV system. The impacts reduced are calculated by combining the two net emission scenarios, which are presented on Table 16, with the CML, and TRACI impact methodologies.

4.8.1. Human Health Benefits:

After determining the net air emissions, subsequent life cycle impact analyses were run to determine the impacts reduced. To determine the human health impacts reduced, the human toxicity cancer potential (HTP) method was used. This method calculates the human cancer risks due to air emissions by normalizing the cancer potency of each carcinogen emitted to that of benzene (C_6H_6) known as the HTP factor. Once the HTP factor is determined for each carcinogen, the mass of the corresponding carcinogen released is then multiplied by the HTP factor of that carcinogen to arrive at a final human toxicity cancer potential value expressed in mass benzene equivalents ($kg C_6H_6 equiv$)⁵². For example, the HTP factor of Arsenic is $3,300 C_6H_6 equiv / kg$ ⁵³. This in essence means that release of 1 kg of Arsenic has a 3,300 times higher human cancer potency

when compared to the release of 1 kg of benzene. This value further multiplied by the mass of arsenic released from the process analyzed provides the human toxicity cancer potential due to the emission of arsenic from the process. The same methodology is applied to all the carcinogens released from the process and added together to arrive at a final impact value. In this case, the human cancer potential reduced due to the reduction in the emissions of metal carcinogens (As, Cd, Cr, Pb) and non-metal carcinogens (benzene) were analyzed for a time period of 10, 20 and 30 years and the results are provided below.

Figure 29 presents the cumulative human cancer impacts reduced as a result of generating solar electricity in Dana Building for the next 10, 20 and 30 years. Using the ‘Net Emissions’ scenario 13.5, 27.0, and 40.5 kg of benzene equivalent of human cancer impacts are reduced for the next 10, 20 and 30 years due to 0.47 Million kWh, 0.93 Million kWh and 1.4 Million kWh of electricity being displaced, respectively. Using the ‘Net Emissions*’ scenario 50.8, 101.5, and 152.3 kg of benzene equivalent of human cancer impacts are reduced for the next 10, 20 and 30 years due to 0.47 Million kWh, 0.93 Million kWh and 1.4 Million kWh of electricity being displaced, respectively.

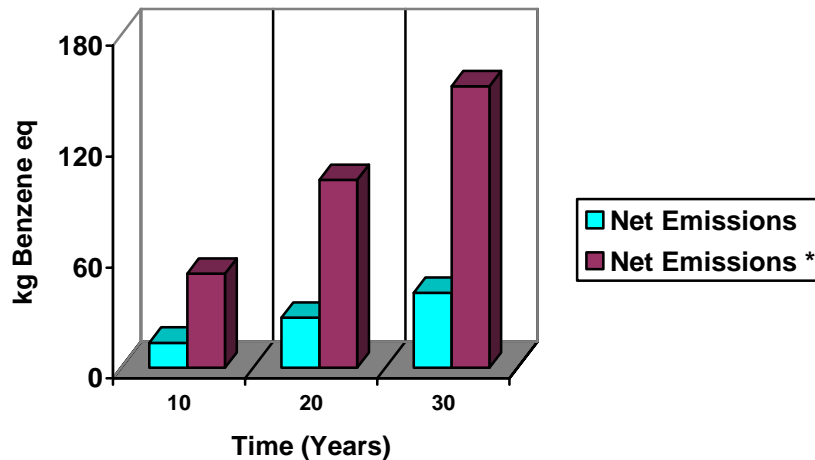


Figure 29: Human Cancer Impacts Reduced Due to Generation of PV Electricity

4.8.2. Ecological Benefits:

In this section the ecological benefits involving the reduction in global warming, smog formation and acidification impacts are calculated and presented for a time period of 10, 20 and 30 years. The CML Baseline 2000 methodology developed by the Center of Environmental Studies in University of Leiden was used to analyze the impacts reduced. This method is a midpoint approach that expresses environmental impacts in terms of global warming potential, smog formation potential, and acidification potential, which are typical midpoint indicators. This method is modeled based on the environmental phase modeling approach. This approach is based on the principle that if more than one stressor contributes to the same impact, the impact of the different stressors is normalized to the impact of a base element/compound chosen for that particular category (e.g. SO₂ is chosen as the baseline compound for acidification impact and the acidification impact of NO_x is expressed in terms of SO₂ equivalents). Acidification Potential is expressed in kg of SO₂ equiv. The acidification potential factor of NO_x is 0.5 SO₂ equiv; this means that release of one kg of NO_x has half the acidification impact of that of one kg of SO₂. The location of the emissions, which affects the magnitude of regional impacts caused by acid rain and smog, is not considered in the final computation of the potential impacts.

Figures 30, 31, and 32 present the cumulative global warming, smog and acidification impacts reduced respectively for three time periods. As expected, the impacts reduced for all the three categories increase progressively with time. When the total impacts reduced are expressed in terms of per kWh, 176 g CO₂ equiv./kWh of global warming impact, 0.09 g C₂H₂ equiv./kWh of smog impact and 2.05 g SO₂ equiv./kWh of acidification impact are reduced for the life time of 30 years based on the 'Net Emissions' scenario. About 957 g CO₂ equiv./kWh of global warming impact, 0.30 g C₂H₂ equiv./kWh of smog impact and 7.06 g SO₂ equiv./kWh of acidification impact are reduced for the life time of 30 years based on the 'Net Emissions*' scenario.

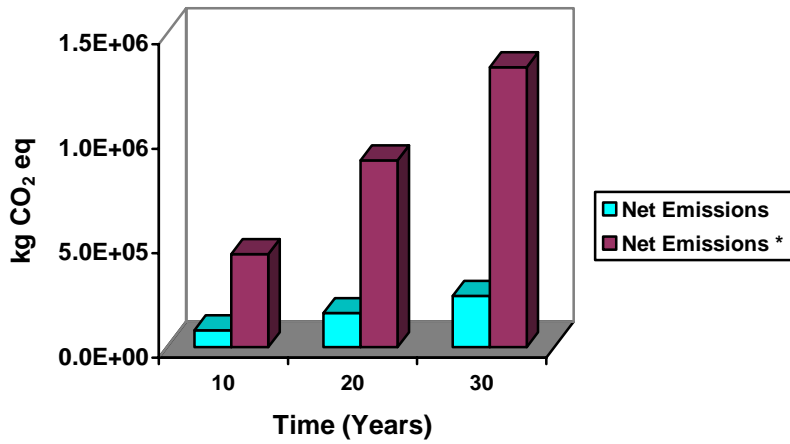


Figure 30: Global Warming Impact Reduced Due to Generation of PV Electricity

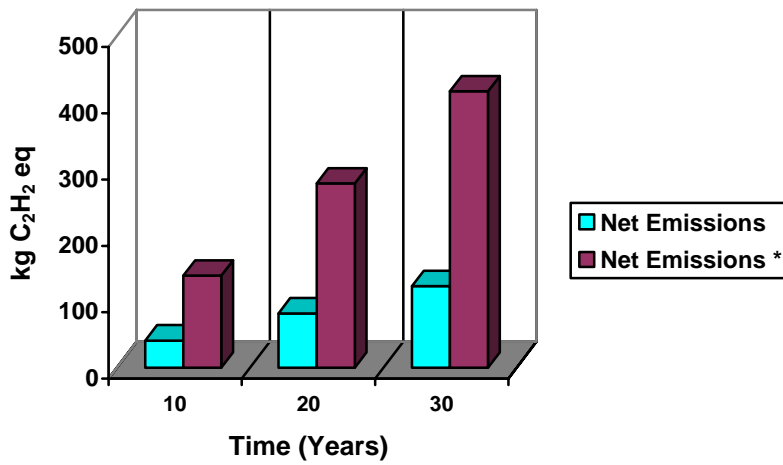


Figure 31: Smog Formation Impact Reduced Due to Generation of PV Electricity

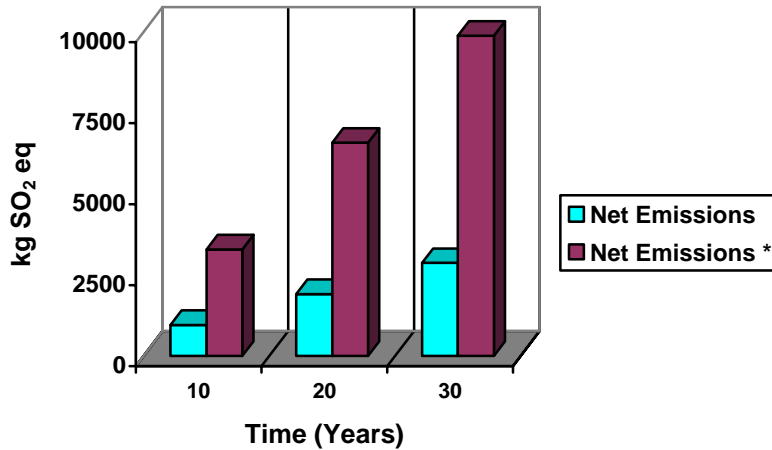


Figure 32: Acid Rain Impact Reduced Due to Generation of PV Electricity

In addition to the CML baseline method, the U.S. EPA Tool for Reduction and Assessment of Chemical and other Environmental Impacts (TRACI)⁵⁴ impact method, which was specifically built for U.S. conditions, was also used to calculate the ecological benefits of the PV system. Figures 33, 34 and 35 present the global warming, smog formation and acid rain impacts avoided for three time periods of 10, 20 and 30 years and for the two scenarios presented on Table 16. Both the CML and TRACI impact methods express global warming potential in units of CO₂ equivalents. However, the smog formation potential and acid rain potential are expressed in units of NO_x equiv and H⁺ mol equiv respectively by TRACI when compared to the CML method that expresses the same impact categories in units of C₂H₂ equiv and SO₂ equivalent respectively. When the impacts reduced are expressed on the basis of energy output, 176 g CO₂ equiv/kWh of global warming impact, 2.31 g NO_x equiv/kWh of smog formation impact and 161 g H⁺ mol equiv/kWh of acid rain impacts are reduced due to the electricity output from the PV system, considering the ‘Net Emissions’ scenario. About 964 g CO₂ equiv/kWh of global warming impact, 4.21 g NO_x equiv/kWh of smog formation impact and 434 g H⁺ mol equiv/kWh of acid rain impacts are reduced due to the electricity output from the PV system, considering the ‘Net Emissions*’ scenario.

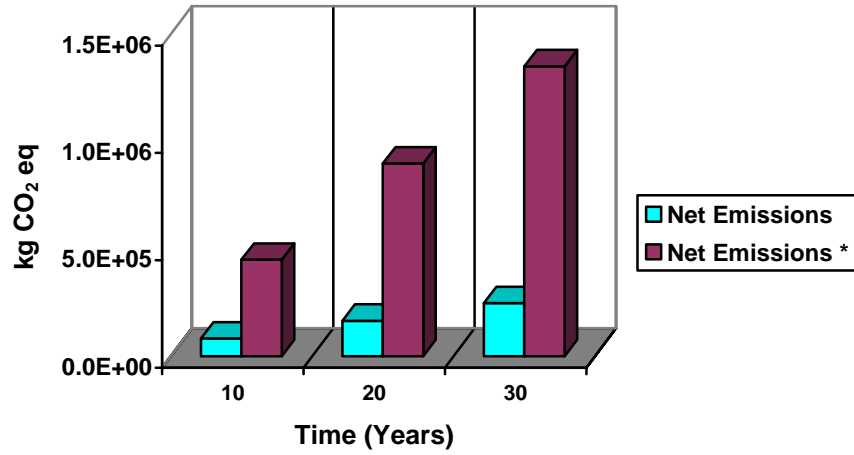


Figure 33: Global Warming Impact Reduced Due to Generation of PV Electricity

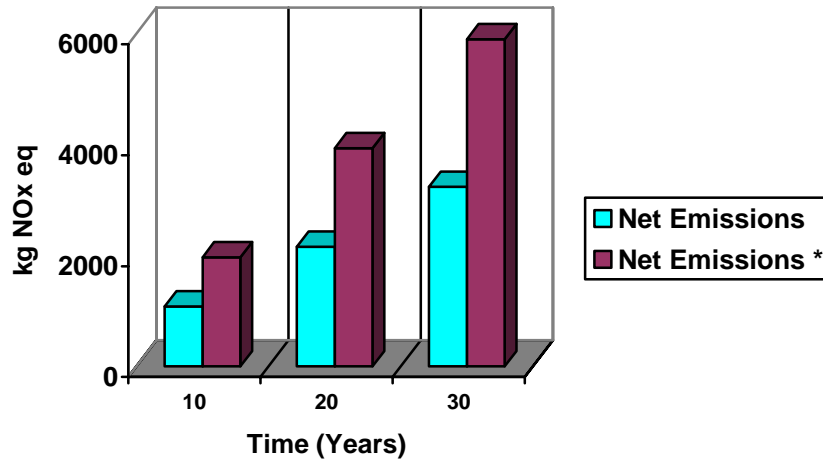


Figure 34: Smog Formation Impact Reduced Due to Generation of PV Electricity

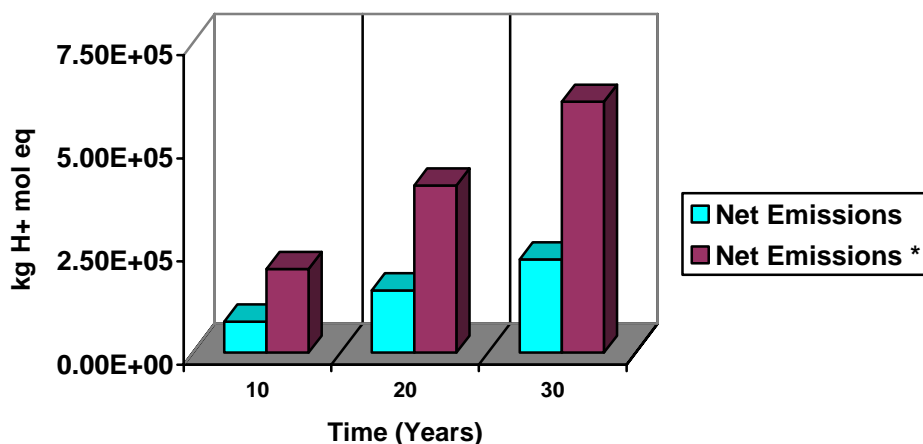


Figure 35: Acid Rain Impact Reduced Due to Generation of PV Electricity

4.9. Unique Scenario

In this section the NER of the PV system is analyzed for the scenario in which the electricity consumed for manufacture of the PVL62 and PVL136 laminates is derived from another similar set of PVL laminates instead of the conventional grid. The primary energy required to generate the electricity for manufacture of the PVL62 and PVL136 laminates is 1,428 MJ and 651 MJ respectively. Multiplying these values by the primary energy to electricity ratio of 0.29, the electricity required is thus calculated to be 415 MJ and 189 MJ respectively. Finally, dividing these values by the NER of the PVL62 (6.4) and PVL136 (5.7), the total fossil resources inputs to both the PVL laminates were calculated. In the case of the PVL136, the fossil fuel energy input associated with electricity supply corresponds to 72 MJ. Figure 36 presents the NER for the two scenarios analyzed for the PVL136 laminate. The NER of the PVL62 and PVL136 laminates for the scenario in which PVL laminates generate the required electricity was 23.4 and 21.1 respectively. The NER for this scenario increased by 3.7 for both the laminates when compared to when the energy was generated from fossil based resources.

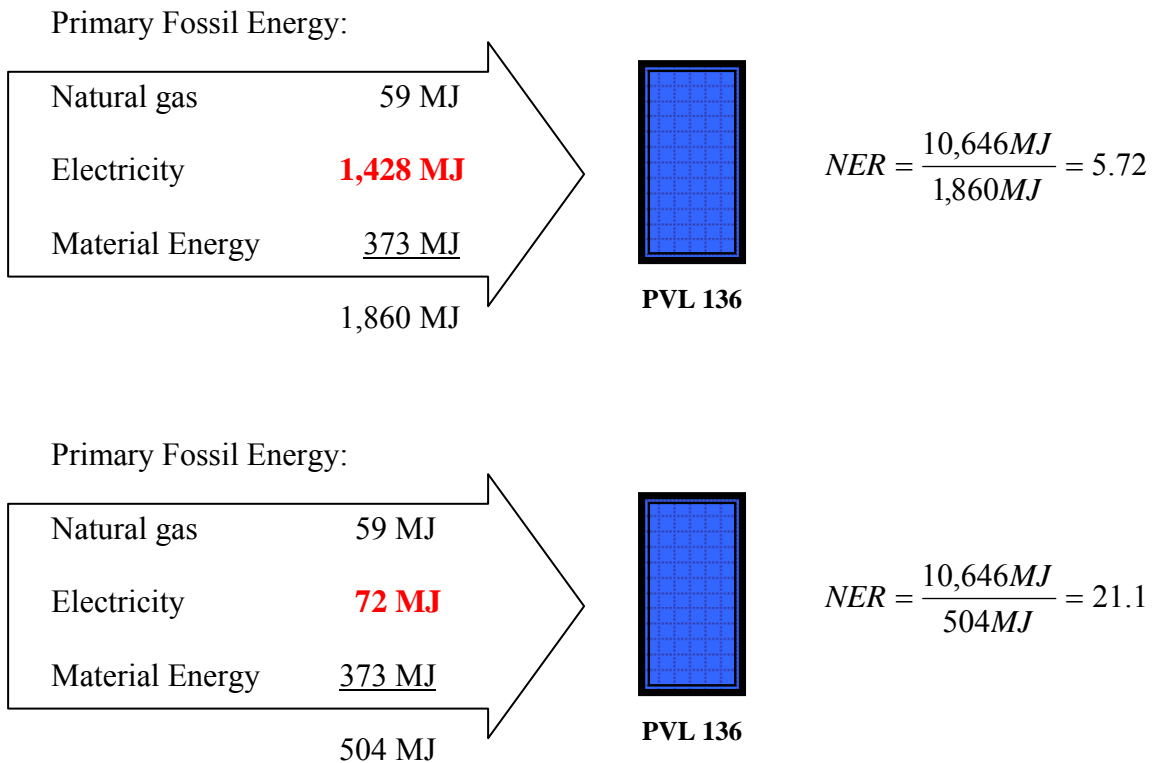


Figure 36: NER of PVL136 Considering Two Alternative Energy Sources.

4.10. Cost Comparison of PV Technologies

A comparative analysis requires the assessment of the costs associated with each of the alternatives. Although the comparison involves two different technologies (multi-crystalline KC120 modules and PVL136 laminates), because they both supply the same service the comparison offered here is done based on the cost of the individual pieces and their total AC energy output, which is based on comparable arrays (same tilt angle). In addition, the annualized cost of the inverter is calculated based on the total system output.

The market cost of each KC120 module is \$499.00⁵⁵ and the market cost of each PVL136 is \$864.99⁵⁶. The cost of the Ballard Ecostar 30 kW inverter is \$15,000.⁵⁷ The annualized electricity cost was calculated based on different annual discount rates (Figure 37).



Figure 37: Cost Comparison of Major Components of the PV System

The cost estimates do not take into account installation costs such as labor, transportation, materials and other BOS components that are also part of the system such as cables, cable housings, combiner boxes, meteorological station and sensors, DAS, etc.

5. Conclusions

The total primary energy consumption of the whole PV system consisting of the manufacture energy of the three PV arrays, balance of system components, and inverter in addition to the transportation and installation energy was 7.81×10^5 MJ. About 86% (6.73×10^5 MJ) of the total primary energy was consumed in the production of the three types of PV modules: 46% for the 88 KC120 modules, 32% for the 132 PVL136 modules and 8% for the 75 PVL62 modules. On a per area (m^2) and per peak power basis (W_p), the multi-crystalline KC120 modules consumed respectively 5.2 times more primary energy than the thin film PVL62 and PVL136 laminates. These results demonstrate that multi-crystalline modules are more energy intensive when compared to thin film laminates.

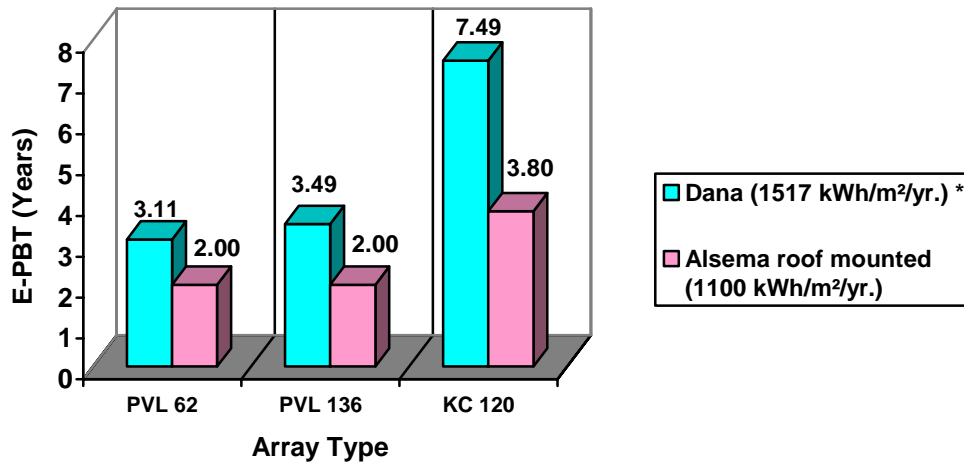
The manufacturing life cycle stage of the three types of the PV modules exerted the highest environmental impact potential (air emissions) among all stages and components of the whole PV system. The production of modules contributed more than 90% of PM_{10} and lead emissions, more than 80% of SO_x and hydrocarbon emissions, 53% of carbon monoxide and 61% of NO_x emissions. In addition, the production also contributed to 85% of CO_2 and 91% of methane emissions.

Subsequently, the net energy and environmental benefits due to grid electricity displaced by the electricity generated from PV were calculated. The total electricity generated from the PV system after inverter losses was 42,555 kWh per year, 0.9 million kWh (for 20 years) and 1.3 million kWh (for 30 years)⁴. The net energy ratio (NER) of the entire PV system was 1.9, 3.7 and 5.3 for a period of 10, 20 and 30 years respectively. This result demonstrates the potential energy benefits of generating photovoltaic electricity. The PV system generates 3.7 times (in 20 years) and 5.3 times (in 30 years), the input energy that was consumed during the production of the whole PV system.

The net energy ratio (NER) of the individual KC120, PVL62 and PVL136 modules are 2.7, 6.4 and 5.7 respectively, for a period of 20 years and with the allocation

⁴ Cumulative energy production takes into account the expected degradation in the conversion efficiency of the thin film modules, which corresponds to 1.1% per year as noted on session 6.3.

of the manufacturing energy of the inverter. The KC120, PVL62 and PVL136 modules have energy pay back times of 7.4, 3.1 and 3.5 years respectively. The pay back time for the entire system is 5.5 years. When compared to the net energy ratio of a typical conventional electrical grid of 0.3, these results demonstrate the potential of PV electricity to decrease the consumption of exhaustible fossil fuel resources and consequently drive society towards sustainable energy generation. In the system studied the NER is higher for the two thin film laminates than for the multi-crystalline modules. The thin film laminates also pay back the energy that was consumed during their production earlier than the multi-crystalline modules. These results are compared to previously published results based on the same technologies ⁷ (Figure 38). It is however essential to mention here that these results are specific to the PV system on the roof of Dana Building, and the two distinct inventory methods used in the research. In addition, the multi-crystalline modules need a supporting structure which is also energy intensive. The lack of supporting structure decreases the pay back time of the Kyocera modules by 0.6 years.



* including inverter manufacturing energy

Figure 38: Comparison of E-PBT Results in this Report and Previous Assessment

The environmental benefits due to the use of the PV system are much more noticeable when the system substitutes for electricity supplied by the ECAR grid than when the PV system, now coupled to a hypothetical compensatory system, substitutes for

the actual energy service supplied to the Dana Building. For example, the human cancer risks reduced due to displaced grid electricity was determined to be 0.030 g benzene equivalent per kWh of electricity displaced based on the 'Net Emissions' scenario and 0.109 g benzene equivalent per kWh of electricity displaced based on the 'Net Emissions*' scenario. Thus, for a lifetime of 20 and 30 years, 27 and 40.5 kg benzene equivalent human cancer risks will be reduced due to PV electricity generation based on the 'Net Emissions' scenario and 102 and 153 kg benzene equivalent human cancer risks will be reduced due to PV electricity generation based on the 'Net Emissions*' scenario respectively. When the total impacts reduced are expressed in terms of per kWh, 176 g CO₂ equiv./kWh of global warming impact, 0.09 g C₂H₂ equiv./kWh of smog impact and 2.05 g SO₂ equiv./kWh of acidification impact are reduced for the life time of 30 years based on the 'Net Emissions' scenario. About 957 g CO₂ equiv./kWh of global warming impact, 0.30 g C₂H₂ equiv./kWh of smog impact and 7.06 g SO₂ equiv./kWh of acidification impact are reduced for the life time of 30 years based on the 'Net Emissions*' scenario. Thus, for a life time of 20 years, 1.64 x 10⁵ kg CO₂ equiv global warming impacts, 81.8 kg C₂H₂ equiv smog formation impacts and 1910 kg of SO₂ equivalent acidification impacts will be reduced due to a system that comprises a 33 kW PV installation coupled to a boiler, and offers the same level of service as the CHP facility on campus. These results reveal the potential of PV electricity to reduce human health risks and ecological impacts. These results should be strongly considered in future policymaking and environmental decision making, for issues concerning reducing human cancer risks and maintaining federal air quality standards.

6. Outreach Resources

This session aims to explore some possible educational facets of the PV project. Initially we discuss the technology and in the sub-sessions 6.2 and 6.3 we discuss the significance of renewable energy in the US and its relevance. We present in session 6.4 the data acquisition system, which is coupled to the PV system, and the layout of the display that is installed in the lobby of SNRE. Finally, in session 6.5 we compare the actual output of the system with the theoretical output modeled with data available at the NREL website.

6.1. PV Technology Description

Photovoltaic (PV) modules convert solar energy directly into electricity, and the availability of solar radiation in the US is site dependent (Figure 39). The phenomenon that explains electricity generation by PV modules is known as the photoelectric effect, and Einstein won the 1921 Nobel Prize in Physics for his description of the photoelectric effect.

The photoelectric effect is possible because light can behave as a stream of particles that knock electrons out of a metallic surface, which is usually made of silicon. Electricity is produced through a stream of electrons flowing from a photovoltaic module that is exposed to light. The number of electrons ejected from the module's surface is proportional to the intensity of the light. Thus, the higher the light intensity more electricity is produced. Temperature has minor effects in the electrical output of PV modules, and actually some modules are more efficient under lower temperatures.

The PV modules produce direct current (DC) that can be easily stored in batteries; however, usually electricity consumed in buildings is alternating current (AC). An inverter converts DC into AC, and allows the electricity to go into the building electrical network. Thus, electricity produced by the PV system can be consumed by all electrical equipment in Dana.

Silicon, which is also used in the electronic industry, is the most common material used in the manufacture of photovoltaic cells. Two distinct technologies are used to fabricate silicon PV modules. Crystalline modules require the production of crystals of

silicon in the form of ingots, which are later sawed to produce the cells that are assembled in a module. This process is very energy intensive and expensive but results in modules with high energy conversion efficiencies. Thin film modules do not require the production of silicon crystals. They are fabricated through the deposition of gaseous silicon on a flat substrate. They are less expensive than crystalline modules and more versatile because fewer materials are required for their installation on existing buildings.

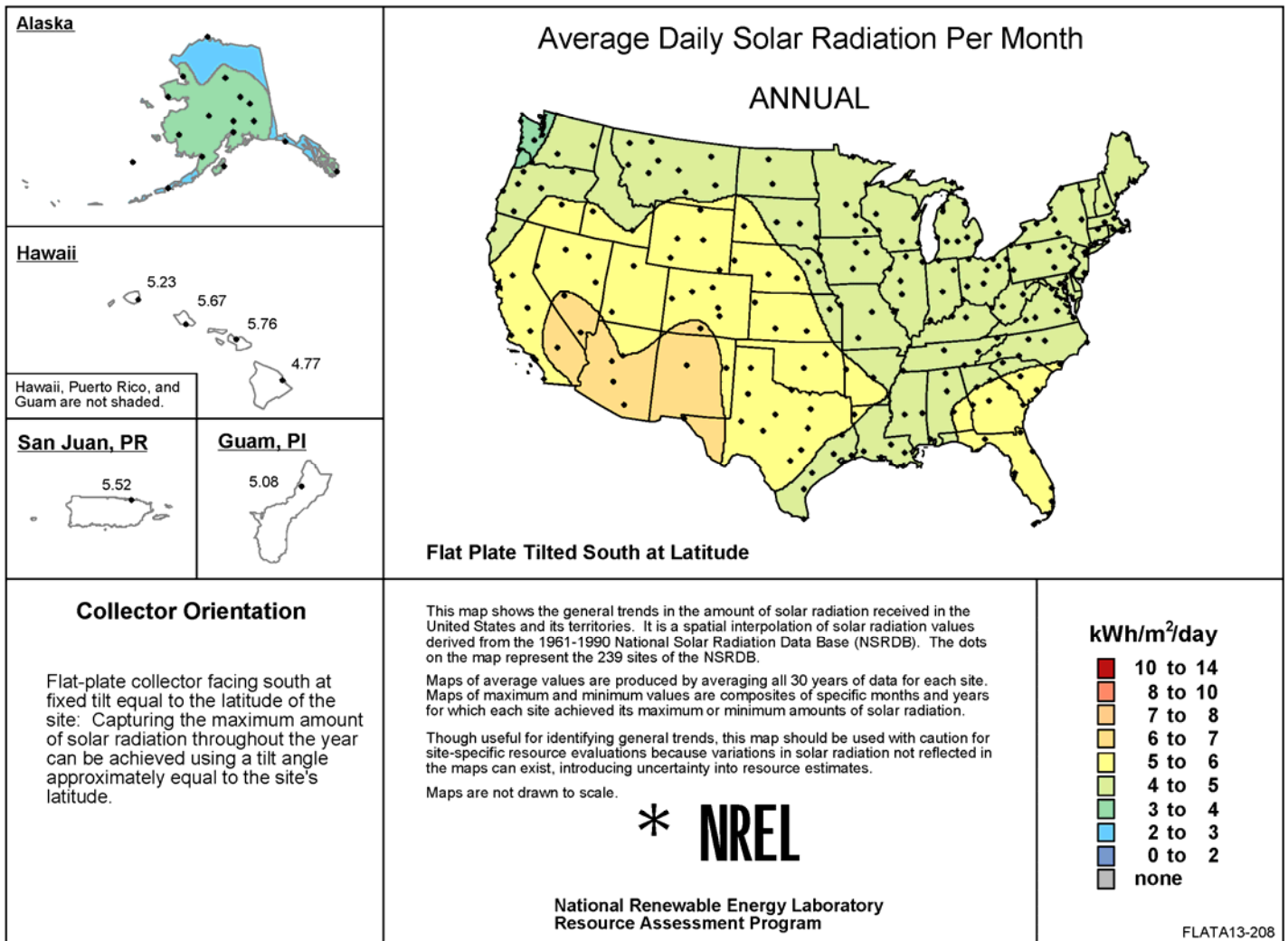


Figure 39: Direct Solar Radiation Map⁵⁸

6.2. Renewable Energy in the US

The United States currently relies heavily on coal, oil, and natural gas for its energy. Fossil fuels are *nonrenewable* because they draw on finite resources that will eventually dwindle, becoming too expensive or too environmentally damaging to retrieve. In contrast, *renewable energy* resources—such as solar energy—are constantly replenished and will never run out.

Most renewable energy comes either directly or indirectly from the sun, such as hydropower, biomass, and wind. Sunlight, or solar energy, can be used directly for heating and lighting homes and other buildings, for generating electricity, and for hot water heating, solar cooling, and a variety of commercial and industrial uses. Despite the benefits of using renewable energy sources its participation in the US energy matrix is still timid (Figure 40).

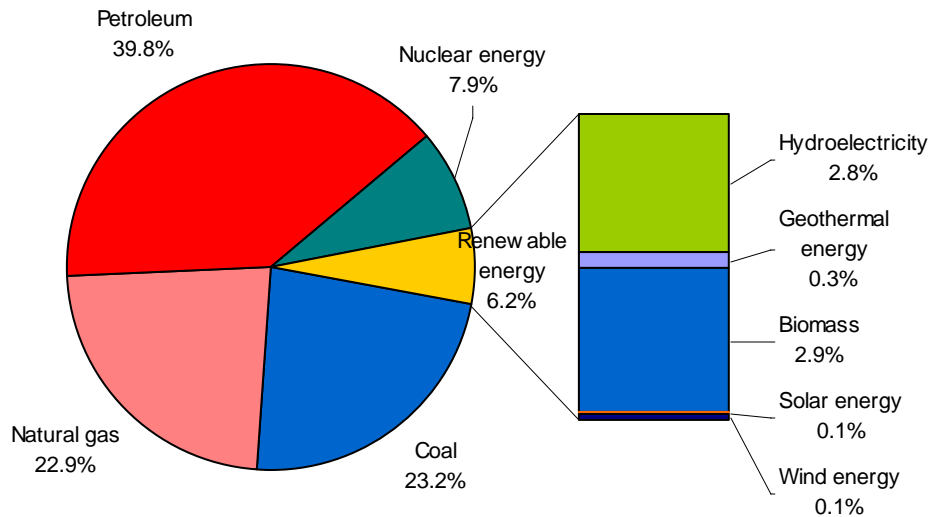


Figure 40: The Role of Renewable Energy Consumption in the US Energy Supply⁵⁹

6.3. Benefits of Renewable Energy Use

Electric power plants that burn fossil fuels emit several pollutants linked to the environmental problems of acid rain, urban ozone (smog), and global climate change.

The use of a renewable energy system such as the PV system on the roof of this building leads to a series of tangible environmental benefits. These benefits include avoided emissions and also the fossil fuel leverage due to the decreasing consumption of resources in the ground.

The following environmental benefits associated with the operation of the PV system can be quantified:

- CO₂ emissions
- NO_x emissions
- SO₂ emissions
- Pb emissions
- Hg emissions
- Uranium consumption
- natural gas consumption
- Coal consumption

In addition to these quantitative benefits, the use of decentralized renewable energy sources is also beneficial because of its reliability when compared to centralized sources that depend on a potential faulty grid. Renewable sources could play a major role in the future energy self-sufficiency of the US, while reducing the expenditures with imported energy, creating jobs, and providing energy security.

6.4. Data Acquisition System and Lobby Display

The PV system is also used as an educational tool, and various sensors are integrated in the system to portrait its operational conditions, which help on the future prediction of its electrical output. Figure 41 shows various components of the system and information flows that are monitored by the data acquisition system (DAS).

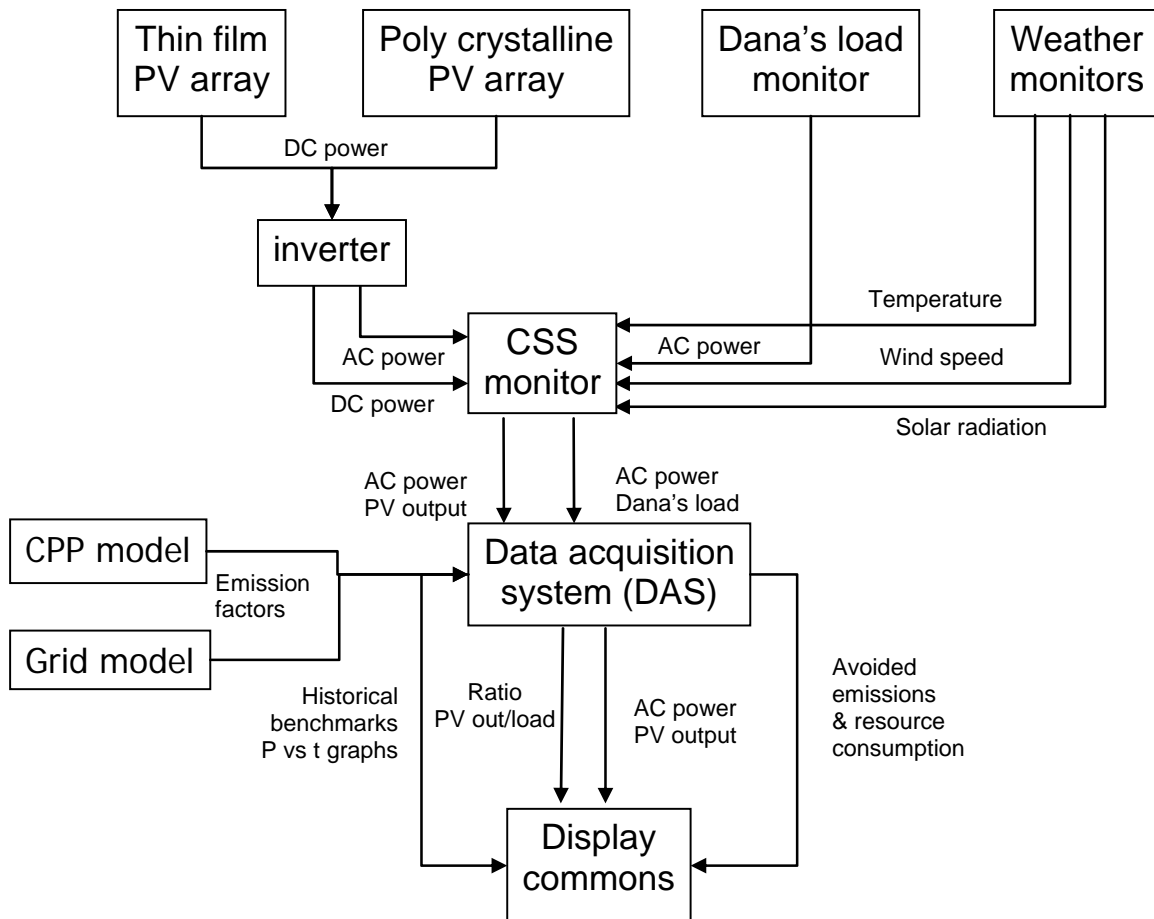


Figure 41: PV System Data Flow Chart

The DAS monitors and displays the following parameters:

- **Air Temperature:** indicates the outdoor air temperature according to the sensor located at weather station.
- **Wind Speed:** measures wind speed through the sensor located at the weather station.
- **Solar Radiation:** shows the value measured by the silicon-photodiode pyranometer located at the weather station.
- **Solar Array DC Current:** shows the PV array DC current input in the inverter.
- **Solar Array DC Voltage:** shows the PV array DC voltage input in the inverter.
- **Inverter AC Current:** shows the inverter's AC current output.

- **Inverter AC Voltage:** shows the inverter’s AC voltage output.
- **Environmental Impact:** these values are calculated based on the factors determined in session 6
 - CO₂ emissions
 - NO_x emissions
 - SO₂ emissions
 - Hg emissions
 - Uranium consumption
 - natural gas consumption
 - Coal consumption
- **DC power Input:** shows the power of PV system before the inverter.
- **AC power output:** shows the power of PV system after the inverter.
- **Total output Today:** indicates the total electrical energy supplied to the grid in that day.
- **System Total output:** indicates the cumulative electrical output of the system that is supplied to the grid.

All the information is stored and made available in CSS for future research. The DAS has also an interface that is presented on a display located in the lobby of SNRE (Figure 42).

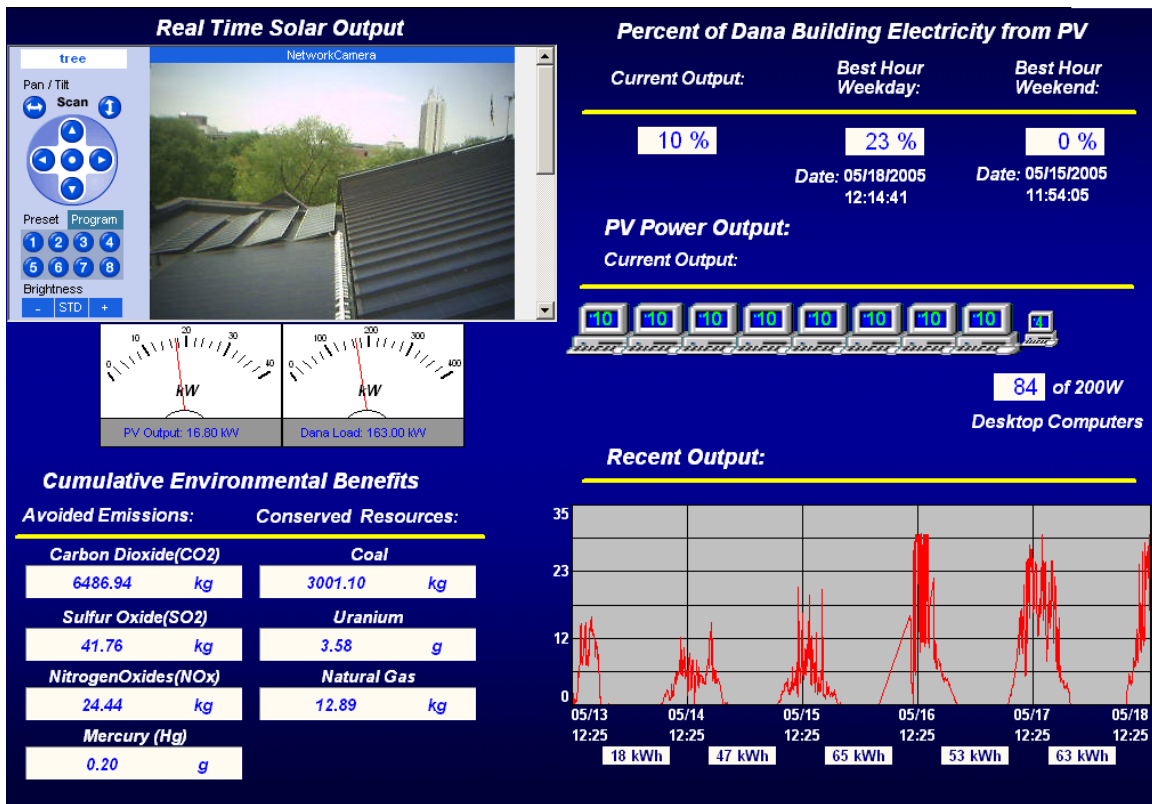


Figure 42: Layout of the Display in the SNRE’s Lobby

The cumulative environmental benefits calculation is based on the total electrical (AC) system output. Equation 7 shows the calculation.

$$CEF = EL_p * EF_p + EL_i * (EF_p + EF_i) \quad (7)$$

Where:

CEF is the cumulative environmental benefit,

EL_p is the present electricity (AC) output,

EF_p is the present emission factor or resource consumption factor,

EL_i is the initial electricity output until the EFs last change,

EF_p + EF_i is the adjustment to reflect the savings until the EFs last change. EF_i may represent a time weighted EF average to account for the savings in the past.

The term EL_i * (EF_p + EF_i) can serve as a correction factor to change the cumulative savings shown on the display.

6.5. Theoretical vs. Actual Data Comparison and Comparison with NREL Data

After the installation of the PV Data Acquisition System (DAS) in the Center for Sustainable Systems in Dana Building the preliminary comparison of the following data was made

- 1) The energy output calculated from the NREL solar radiation data for 05/18/1990 versus the energy output as recorded by the PV DAS for 05/18/2005
- 2) Actual energy output data obtained from the PV DAS versus the theoretical energy output calculated by the *Bird Sky Model* used in this study, both for 05/18/2005

Figure 43 presents the theoretical DC energy output calculated from the two sets of solar radiation data mentioned above for the PV modules on the roof of Dana Building. As one can observe, the energy output for the solar radiation in 1990 was comparatively

less than that for 2005. The DC energy output for the 1990 solar radiation data was calculated to be 160 kWh for the entire day when compared to 214 kWh energy output in 2005. Both energy output curves followed pathways very similar to that of their respective solar radiation curves.

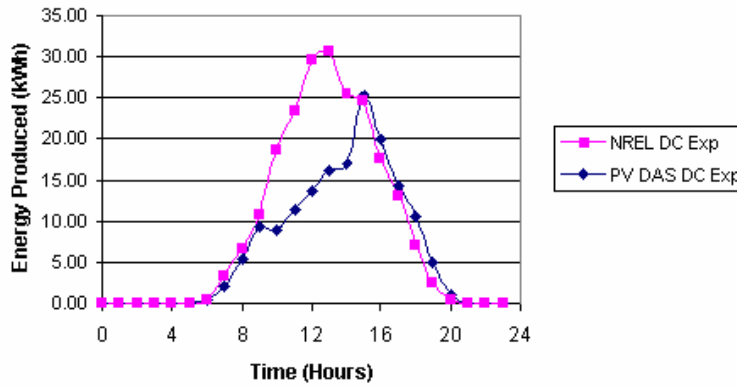


Figure 43: Energy Output Comparison : NREL vs. PV DAS

The final data comparison was done between the theoretically calculated energy output from the solar radiation available for May 18th, 2005 and the actual cumulative energy output for the same day as reported by the PV DAS. Figure 44 presents the two energy output curves. Quite expectedly the theoretical energy output (214 kWh) was slightly higher than the actual output (184.5 kWh). The actual energy output was 86.1% of the theoretical energy output. This might possibly be because of the inverter, as it would start converting DC to AC power only above a certain voltage conditions.

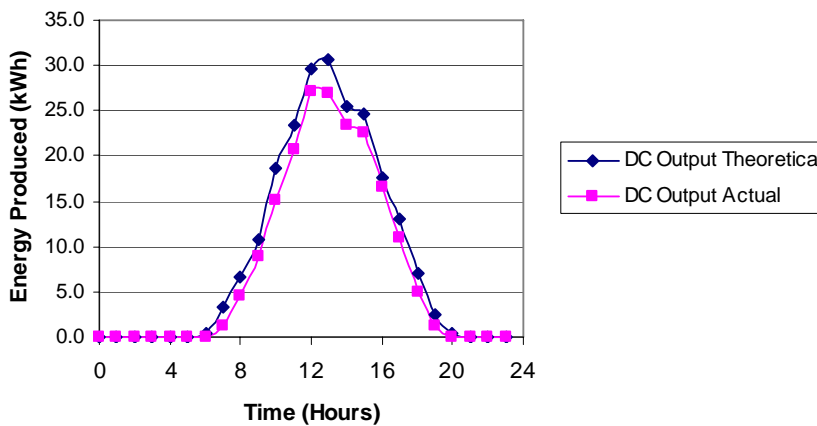


Figure 44: Theoretical vs. Actual Energy Output for May 18th, 2005

7. References

1. Pacca, S. Global Warming Effect Applied to Electricity Generation Technologies. PhD Dissertation. University of California, Berkeley, 2003.
2. Komiyama, H. Yamada, K. Inaba, A. Kato, K. 1996. *Energy Conversion and Management* 37(6-8): 1247-52.
3. Lewis G.McD. Keoleian, G.A. Moore, M.R. Mazmanian, D.L. Navvab, M. 1999. PV-BILD: A Life Cycle Environmental and Economic Assessment Tool for Building-Integrated Photovoltaic Installations. Technical Report No. CSS99-02R2Center for Sustainable Systems. 20 December 1999.
4. Alsema, E.A., "Energy Pay-back Time and CO₂ Emissions of PV Systems", *Progress in Photovoltaics: Research and Application*, 8, pp. 17-25, 2000.
5. Frankl, P., A. Masini, M. Gamberale, D. Toccaceli, "Simplified Life-cycle Analysis of PV Systems in Buildings: Present Situation and Future Trends", *Progress in Photovoltaics: Research and Applications*, 6(2), pp. 137-146, 1998.
6. Dones, R. and R. Frischknecht, "Life Cycle Assessment of Photovoltaic Systems: Results of Swiss Studies on Energy Chains", *Progress in Photovoltaics: Research and Applications*, 6(2), 117-125, 1998.
7. Alsema, E.A. and E. Nieuwlaar, "Energy Viability of Photovoltaic Systems", *Energy Policy*, 28, pp. 999-1010, 2000.
8. Duke, R., Kammen, D.K. "The Economics of Energy Market Transformation Programs", *The Energy Journal*, 20(4), pp. 15-64, 1999.
9. Keoleian, G.A., G. Lewis, "Application of Life-cycle Energy Analysis to Photovoltaic Module Design", *Progress in Photovoltaics: Research And Applications*, 5, pp. 287-300, 1997.
10. Keoleian, G.A., G. Lewis, "Modeling the life-cycle Energy and Environmental Performance of Amorphous Silicon BIPV Roofing in the US", *Renewable Energy*, 28, pp. 271-293, 2003.
11. Pearce, J.M. "Photovoltaics - A Path to Sustainable Futures", *Futures*, 34, pp. 663-674, 2002.
12. EGRID 2002 (Emissions and Generation Resource Integrated Database). U.S. EPA. (www.epa.gov/cleanenergy/egrid).
13. Fthenakis, V.M. "End-of-life Management and Recycling of PV Modules", *Energy Policy*, 28, pp. 1051-1058, 2000.
14. Schmela, M. "World's largest PV system in Bavaria", *Photon International: The Photovoltaic Magazine*, January 2003 http://www.photon-magazine.com/news/news_03-01_eu_ger_bavaria.htm, Accessed May 2003.
15. Eikelboom, J.A. and Jansen, M.J. June 2000. *Characterisation of PV Modules of New Generations - Results of tests and simulations* the Netherlands Energy Research Foundation, report ECN-C-00-067. <http://www.ecn.nl/docs/library/report/2000/c00067.pdf>
16. Staebler, D.L. and C.R. Wronski, "Reversible Conductivity Changes in Discharge-Produced Amorphous Si", *Applied Physics Letters*, 31(4), pp. 292-294, 1977.
17. The Bridge. National Academy of Engineering. Link: [http://www.nae.edu/NAE/bridgecom.nsf/weblinks/MKEZ-6LUM4Y/\\$FILE/Bridge-v35n4.pdf?OpenElement](http://www.nae.edu/NAE/bridgecom.nsf/weblinks/MKEZ-6LUM4Y/$FILE/Bridge-v35n4.pdf?OpenElement) Link accessed on February 26th 2006.
18. Unisolar: Field Applied Roofing PV Laminates for Steel Roofs. Data Sheet
19. Oliver, M. and T. Jackson "The Evolution of Economic and Environmental Cost for Crystalline Silicon Photovoltaics", *Energy Policy*, 28, pp. 1011-1021, 2000.

20. Greijer, H., L. Karlson, S.E. Lindquist, A. Hagfeldt “Environmental Aspects of Electricity Generation From a Nanocrystalline Dye Sensitized Solar Cell System”, *Renewable Energy*, 23, pp. 27-39, 2001.
21. Izu, M and Ovshinsky, H.C. 1984. Method for continuously producing tandem amorphous photovoltaic cells *United States Patent 4,485,125* November 27, 1984.
22. Nath, P. et al. 1995. Photovoltaic module fabrication process United States Patent 5,457,057 October 10, 1995.
23. Mr. Spitzley – CSS personal communication (3/7/2005)
24. Dr. Guha – United Solar personal communication (3/7/2005)
25. Lewis, G. and Keoleian, G.A. 1997. Life cycle design of amorphous silicon photovoltaic modules. Technical report EPA/600/R-97/081. National Risk Mangement Research Laboratory. Office of Research and Development. US EPA. August 1997.
26. <http://www.kyocerasolar.com/dxf/70030449-1-A.dxf>
27. Phylipsen, G.J.M. and Alsema, E.A. Environmental life-cycle assessment of multicrystalline silicon solar cell modules. Report n° 95057. Department of Science, Technology and Society. Utrecht University. Utrecht, Netherlands.
28. <http://www.kyocerasolar.com/dxf/70030449-1-A.dxf>
29. http://www.kyocerasolar.com/news/news_detail.cfm?key=153
30. <http://www-rohan.sdsu.edu/~irsc/tjreport/tj3.html>
31. <http://www.world-aluminium.org/production/processing/properties.html>
32. Atlanta Solar. Connect Energy Combiner Box. Link: http://www.atlantasolar.com/product_info.php/name/High%20Voltage%20PV%20Array%20Combiner%20Box%20-%208%20inputs/products_id/173 Link accessed on 05-31-05
33. <http://www.ballard.com/resources/powergen/EPC-PV%2030kW%20Final%207.2.4.pdf>
34. Personal Communication MSc.. Bernhard Dietz. Center for Sustainable Systems, University of Michigan
35. Personal communication with sales representative <http://www.lem.com/>
36. MapQuest Road Distances. Link: <http://www.mapquest.com/directions/main.adp> Link accessed on 04-19-05
37. http://www.volvo.com/NR/rdonlyres/E8FD3F6B-B06B-4EBE-BA7D-A529AFE0BFD0/0/euro3_03.pdf
38. Kreith, F. 1978. Principles of solar engineering. Hemisphere Publishing Co.
39. Bird, R. E., and R. L. Hulstrom, *Simplified Clear Sky Model for Direct and Diffuse Insolation on Horizontal Surfaces*, Technical Report No. SERI/TR-642-761, Golden, CO: Solar Energy Research Institute, 1981.
40. <http://zipinfo.com/search/zipcode.htm> (accessed 04/18/2005)
41. Walraven, R. 1978. Calculating the Position of the Sun. *Solar Energy* 20: 393-397.
42. Daryl Myers - Personal communication
43. <http://rredc.nrel.gov/solar/pubs/redbook/PDFs/MANUAL.PDF>
44. Personal Communication. William Weakley. University of Michigan Central Power Plant (3/7/2005)
45. http://www.plantops.umich.edu/utilities/CentralPowerPlant/summary/Mass_Bal0304.html
46. <http://www.plantops.umich.edu/utilities/CentralPowerPlant/cogeneration/>
47. Wackernagel, M. and Rees, W. 1996. Our Ecological Footprint: Reducing Human Impact on Earth. Page 121.
48. <http://www.epa.gov/ttn/chief/ap42/ch01/final/c01s04.pdf>
49. <http://www.epa.gov/oar/oaqps/greenbk/anc12.html>
50. http://www.eia.doe.gov/cneaf/electricity/page/co2_report/co2emiss.pdf
51. http://cdiac.esd.ornl.gov/trends/emis/tre_glob.htm

52. McKone, T.E and Hertwich, E.G. 2001. The Human Toxicity Potential and a strategy for evaluating model performance in life cycle impact assessment. *Int. J.LCA* 6 (2) 106-109
53. Hertwich, E.G. Mateles, S.F. Pease, W.S. McKone, T.E. 2001. Human Toxicity Potential for life cycle assessment and toxic release inventory risk screening. *Environ. Toxicol and Chem* 20 (4) 928-939
54. U.S. EPA TRACI Link: http://epa.gov/ORD/NRMRL/std/sab/iam_traci.htm Link accessed on 07-10-05
55. <http://www.affordable-solar.com/1027.html>
56. <http://www.altersystems.com/catalog/unisolar-136-watt-pv-laminate-module-p-367.html>
57. Personal communication Glenn Kowalske, Ballard Power Systems.
58. <http://www.eere.energy.gov/consumerinfo/pdfs/130.pdf>
59. <http://www.eia.doe.gov/cneaf/solar.renewables/page/trends/trends.pdf>
60. <http://rredc.nrel.gov/solar/pubs/redbook/PDFs/MI.PDF>
61. <http://www.kyocerasolar.com/pdf/specsheets/KC35-120Install.pdf>
62. <http://www.dynamicfastener.com/specifications.html>

Appendix 1: Bill of Materials

9/28/2004

BILL OF MATERIALS FOR U of M PROJECT, ANN ARBOR, MI									
PROJECT NUMBER 62014									
Item	Supplier	Description	Manufacturer (Vendor)	Part Number	Qty	PO Number	Wt/pc	Total Wt	Notes
1	Uni-Solar	136 Watt Solar Electric Laminate Applied in 11-panel arrays	UNI-SOLAR	PVL-136	131	TIJ WHSE	20	2620	5 pallets
2	Uni-Solar	68 Watt Solar Electric Laminate Applied in 11-panel arrays	UNI-SOLAR	PVL-68	68	TIJ WHSE	10	680	5 pallets
3	Uni-Solar	Wire Tray, Extruded CPVC, White, 20' long	UNI-SOLAR	AA44291	6	ABH WHSE	10	60	20' long
4	Uni-Solar	Wire Tray Cover, Extruded CPVC, White, 20' long	UNI-SOLAR	AA44293	6	ABH WHSE	10	60	20' long
5	Uni-Solar	Base Channel, Wire Tray Support, White w/Seam Tape	UNI-SOLAR	AA44292	55	ABH WHSE	0.25	13.75	Boxed
6	Uni-Solar	Data Acquisition System with Camera option	UNI-SOLAR		1		25	25	Boxed
7	Kyocera	120 Watt Crystalline Solar Panel, Framed	Kyocera	KC-120	88	240666LDH	26.3	2314.4	Boxed
8	Two Seas Metalworks	Mounting Assembly for mounting Crystalline Panel Arrays to low-slope membrane roof	Two-Seas	GR-11/KC-120	8	240696LAG	125	1000	one pallet
9	Connect Energy	8A Fuses for Combiner box	Littelfuse	KLKD8	24	240805LAG			
10	Connect Energy	Solar String Combiner Box, 8 input, 10A ea, 1 Output, 600 VDC, UL Listed	Connect Energy	PCBHV8	3	240805LAG	20	60	Boxed
11	Xantrex	AC Circuit Breaker, Molded Case 125A for 208 Vac Installation	Xantrex	1-151432-06	1	240806LAG	3	3	Boxed
12	Xantrex	Enclosure for 125A circuit breaker, NEMA 3R	Xantrex	1-151433-01	1	240806LAG	3	3	Boxed
13	Graybar	60A, Lockable, 3-pole, 600Vdc, Fused, Disconnect Switch, External Handle, NEMA 3R Enclosure	Square D	H362RB	3	240808LAG	12	36	Boxed
14	Graybar	Fuse Puller set	Square D	H60FP	1	240808LAG	1	1	Boxed
15	Graybar	Fuse, 60 A, 600VDC	Square D	FRS-R-60	6	240808LAG	1	6	Boxed
16	Graybar	Ground Bar for DC Disconnect Switches	Square D	GTK0610	3	240808LAG	1	3	Boxed
17	Graybar	Carlton LT20E 90 Degree 3/4" Conduit Fitting	Carlton	LT20E	10	240808LAG	1	10	Boxed
18	Graybar	Carlton LT43E Straight 3/4" Conduit Fitting	Carlton	LT43E	10	240808LAG	1	10	Boxed
19	Dynamic Fastener	S-5-U Clamp	S-5I	S-5-U	75	Credit Card Purchase - NO PO#	1	75	Boxed
Total								6905.15	

Confidential

Page 1

Appendix 2: UNI-SOLAR Shingle ASR128 Specifications



UNI-SOLAR[®] Architectural Standing Seam

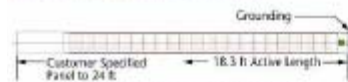
For Residential and Commercial Solar Power Systems

UNI-SOLAR Architectural Metal Panels are building integrated photovoltaic panels. They are reliable, attractive, and cost-effective design options for creating sustainable and energy self-sufficient buildings.

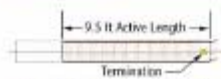
Aesthetically-pleasing, solar architectural roofing panels are integrated into the roof following the specifications of conventional architectural standing seam panels.

Solar electric power is collected through terminations located on top of the panel under the ridge cap. No deck penetrations are required.

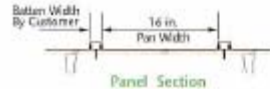
All UNI-SOLAR systems are installed on a National Association of Home Builders (NAHB) 22x24 Century Bowdoin or 30x40 panel. The 22x24 panel system is preferred. A 30x40 batten layout.



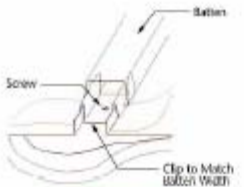
Panel Plan View: 16.3 ft Active



Panel Plan View: 9.5 ft Active



Panel Section



Batten Seam Detail

- Standard Laminate Length: 9.5 ft or 16.3 ft, active solar length bonded to conventional flat metal roof panel.
- Laminate Width: 15.75 in.
- Metal Panel: GALVALUME[®] steel, painted or unpainted.
- Pan Width: 16 in. (In-situ width per batten size).
- Customer Specified Panels: From 9.5 ft to 24 ft.
- Electrical Connections: Standard-potted top termination, hidden and protected by ridge cap (see previous page).
- Roof Slope: Minimum 3:12 slope.
- Installation: Per panel supplier's specification.
- Ideal Roof Orientation: Open southern exposure.
- Wind Load: Per panel supplier's specification.
- Array: Size dependent on power demands. See table below.
- System: Typical systems range from 1 kW to 10 kW.

Specification & Performance

Product	Rated Power (W)	Voltage (V _{mp})	Current (I _{mp})	Voltage (V _{oc})	Current (I _{sc})	Length (ft)	Width (in.)	Weight (lbs/ft ²)	Area (ft ²)	Energy Per Day (Wh/ft ²)
ASR-60	60	16.5	3.6	23.8	4.5	9.5	16	2	12	20-30
ASR-64	64	16.5	3.9	23.8	4.8	9.5	16	2	12	20-30
ASR-120	120	17	3.6	47.6	4.5	16.3	16	2	23	20-30
ASR-128	128	17	3.9	47.6	4.8	16.3	16	2	23	20-30

GALVALUME is a Registered Trademark of Bethlehem Steel.

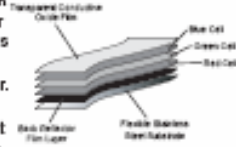
Appendix 3: UNI-SOLAR PVL Specifications

Field Applied Roofing PV Laminate For Steel Roofs



Triple Junction Technology

The foundation of the new UNI-SOLAR PVL is the Triple Junction silicon solar cell unique to UNI-SOLAR. Each cell is composed of three semiconductor junctions stacked on top of each other. The bottom cell absorbs the red light, the middle cell absorbs the green light and the top cell absorbs the blue light. This spectrum splitting capability is the key to higher efficiency.



United Solar Ovonic

United Solar Ovonic is the world leader in thin-film technologies. It's a company with years of experience in photovoltaics and is backed by a U.S. technology leader, Energy Conversion Devices, which holds 350 U.S. patents and 800 foreign patents. Our technology has proven itself over decades under the most extreme conditions imaginable, including satellites, ocean buoys and military applications. We offer a proven product, a proven technology, from a proven company.

Dimensions & Specifications

Physical:

Model Number	Laminate Length	Laminate Width	Laminate Thickness	Weight	Minimum Slope	Maximum Slope
PVL-31	4 ft. 7 1/2 in.	15 1/2 in.	0.12 in.	4.1 lb	1:12 (5°)	21:12 (60°)
PVL-62	8 ft. 6 1/2 in.	15 1/2 in.	0.12 in.	8.2 lb	1:12 (5°)	21:12 (60°)
PVL-68	9 ft. 4 1/4 in.	15 1/2 in.	0.12 in.	9 lb	1:12 (5°)	21:12 (60°)
PVL-93	12 ft. 6 1/2 in.	15 1/2 in.	0.12 in.	12.3 lb	1:12 (5°)	21:12 (60°)
PVL-124	16 ft. 5 1/2 in.	15 1/2 in.	0.12 in.	16.5 lb	1:12 (5°)	21:12 (60°)
PVL-136	18 ft.	15 1/2 in.	0.12 in.	17 lb	1:12 (5°)	21:12 (60°)

Electrical:

Performance	PVL - 31	PVL - 62	PVL-68	PVL-93	PVL-124	PVL-136
Rated Power (Watts)	31	62	68	93	124	136
Normal Operating Voltage	6	12	12	18	24	24
Operating Voltage (Volts)	7.5	15	16.5	22.5	30.0	33.0
Operating Current (Amps)	4.13	4.13	4.13	4.13	4.13	4.13
Open-Circuit Voltage (Volts)	10.5	21.0	23.1	31.5	42.0	46.2
Open-Circuit Voltage (Volts) at -10°C and 1250 W/m ²	12.0	23.9	26.3	35.9	47.9	52.7
Short-Circuit Current (Amps)	5.1	5.1	5.1	5.1	5.1	5.1
Short-Circuit Current (Amps) At 75°C and 1250 W/m ²	6.7	6.7	6.7	6.7	6.7	6.7
Series Fuse Rating (Amps)*	8	8	8	8	8	8
Min. Blocking Diode (Amps)	8	8	8	8	8	8

NOTES:

Overlight: And-3 (series) operation, electrical specifications specifications. Power output may be higher by 15%, operating voltage may be higher by 11% and operating current may be higher by 4%.

Electrical specifications (15%) are based on measurements performed at standard test conditions of 1000 W/m² irradiance, Air Mass 1.5, and Cell Temperature of 25°C after long-term stabilization. Actual performance may vary up to 13% from rated power due to low temperature operation, spectral and other related effects. Maximum system open-circuit voltage not to exceed 800 VDC.

*Refer to section 690.6 of the National Electric Code for an additional factor of 125%, which may be applicable.

Corporate Sales & Marketing Office:

United Solar Ovonic
5800 Lapar Rd., Auburn Hills, MI 48326
Tel: 248.475.0100
Toll Free: 800.843.3892
Fax: 248.364.0510
Email: info@uni-solar.com

North American Sales Office:

United Solar Ovonic
4520 Vantage Ave., San Diego, CA 92123
Tel: 858.514.1435
Toll Free: 800.397.2083
Fax: 858.514.8694
Email: west@uni-solar.com

European Sales Office:

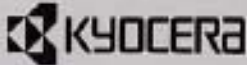
United Solar Ovonic Europe GmbH
Dennward Str. 25-27
52068 Aachen - Germany
Tel: +49.241.9631130
Fax: +49.241.9631138
Email: europ@uni-solar.com

www.uni-solar.com

©Copyright 2008 United Solar Ovonic - All Rights Reserved



Appendix 4: KC120 Specification Sheet



KC120-1

HIGH EFFICIENCY MULTICRYSTAL PHOTOVOLTAIC MODULE

TYPICAL OUTPUT 120 Wp

MODEL KC120-1



HIGHLIGHTS OF KYOCERA PHOTOVOLTAIC MODULES

Kyocera's advanced cell processing technology and automated production facilities have produced a highly efficient multicrystal photovoltaic modules.

The conversion efficiency of the Kyocera solar cell is over 14%.

These cells are encapsulated between a tempered glass cover and an EVA potant with PVF back sheet to provide maximum protection from the severest environmental conditions.

The entire laminate is installed in an anodized aluminum frame to provide structural strength and ease of installation.

APPLICATIONS

- Microwave/Radio repeater stations
- Electrification of villages in remote areas
- Medical facilities in rural areas
- Power source for summer vacation homes
- Emergency communication systems
- Water quality and environmental data monitoring systems
- Navigation lighthouses, and ocean buoys

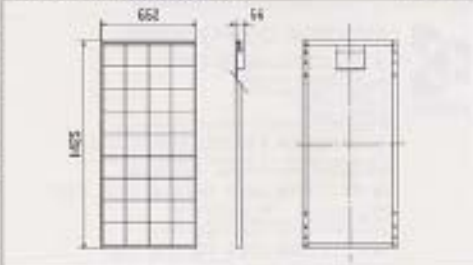
- Pumping systems for irrigation, rural water supplies and livestock watering
- Aviation obstruction lights
- Cathodic protection systems
- Desalination systems
- Recreational vehicles
- Railroad signals
- Sailboat charging systems

SPECIFICATIONS

■ Electrical Specifications

MODEL	KC120-1
Maximum Power	120 Watts
Maximum Power Voltage	15.6 volts
Maximum Power Current	7.10 Amps
Open Circuit Voltage	21.5 volts
Short-Circuit Current	7.45 Amps
Length	1425mm (56.1in.)
Width	652mm (25.7in.)
Depth	59mm (2.2in.)
Weight	11.9kg (26.3lbs.)

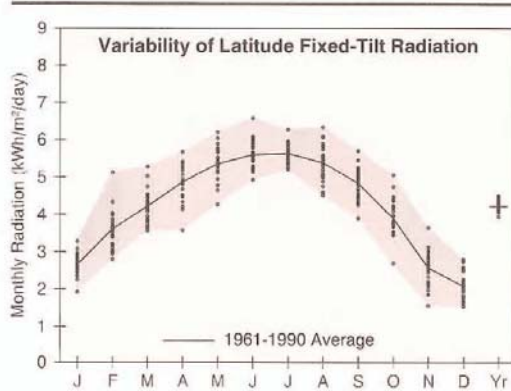
■ Physical Specifications (Unit: mm)



NOTE: The electrical specifications are under test conditions of irradiance of 1000W/m², spectrum of 1.5 air mass, and cell temperature of 25°C.

Kyocera reserves the right to modify these specifications without notice.

Appendix 5: Solar Radiation in Detroit, MI⁶⁰



Detroit, MI
WBAN NO. 94847

LATITUDE: 42.42° N
LONGITUDE: 83.02° W
ELEVATION: 191 meters
MEAN PRESSURE: 992 millibars

STATION TYPE: Secondary

Solar Radiation for Flat-Plate Collectors Facing South at a Fixed Tilt (kWh/m²/day), Uncertainty ±9%

Tilt (°)		Jan	Feb	Mar	Apr	May	June	July	Aug	Sept	Oct	Nov	Dec	Year
0	Average	1.6	2.5	3.4	4.6	5.6	6.2	6.1	5.3	4.1	2.8	1.7	1.3	3.8
	Min/Max	1.3/1.9	2.1/3.2	3.1/4.0	3.6/5.2	4.6/6.5	5.5/7.3	5.7/6.8	4.6/6.1	3.5/4.7	2.2/3.4	1.3/2.1	1.1/1.5	3.6/4.0
Latitude -15	Average	2.4	3.3	4.1	5.0	5.7	6.1	6.1	5.6	4.8	3.7	2.4	1.9	4.3
	Min/Max	1.8/2.9	2.7/4.6	3.5/5.1	3.7/5.8	4.6/6.7	5.4/7.2	5.6/6.8	4.8/6.6	3.9/5.6	2.6/4.7	1.5/3.3	1.4/2.5	4.0/4.5
Latitude	Average	2.7	3.6	4.2	4.9	5.4	5.6	5.6	5.4	4.8	3.9	2.6	2.1	4.2
	Min/Max	1.9/3.3	2.8/5.1	3.6/5.3	3.6/5.7	4.3/6.2	4.9/6.6	5.2/6.3	4.5/6.3	3.9/5.7	2.7/5.1	1.6/3.7	1.5/2.8	4.0/4.5
Latitude +15	Average	2.8	3.7	4.1	4.5	4.8	4.9	4.9	4.9	4.6	3.9	2.6	2.2	4.0
	Min/Max	2.0/3.5	2.8/5.4	3.5/5.2	3.3/5.3	3.8/5.5	4.3/5.7	4.6/5.5	4.1/5.8	3.7/5.5	2.6/5.1	1.5/3.8	1.6/3.0	3.7/4.2
90	Average	2.6	3.3	3.2	3.0	2.8	2.7	2.8	3.1	3.3	3.2	2.3	2.0	2.9
	Min/Max	1.8/3.4	2.5/5.0	2.7/4.1	2.2/3.6	2.3/3.1	2.5/3.0	2.6/3.0	2.6/3.6	2.6/4.0	2.1/4.2	1.3/3.5	1.4/2.9	2.7/3.1

Solar Radiation for 1-Axis Tracking Flat-Plate Collectors with a North-South Axis (kWh/m²/day), Uncertainty ±9%

Axis Tilt (°)		Jan	Feb	Mar	Apr	May	June	July	Aug	Sept	Oct	Nov	Dec	Year
0	Average	2.2	3.3	4.5	5.9	7.2	8.0	7.9	6.9	5.5	3.8	2.2	1.7	4.9
	Min/Max	1.6/2.7	2.6/4.6	3.8/5.7	4.3/7.1	5.6/9.0	6.7/9.8	7.1/9.1	5.8/8.3	4.3/6.4	2.6/5.0	1.4/3.1	1.2/2.2	4.6/5.3
Latitude -15	Average	2.8	4.0	5.0	6.3	7.4	8.0	8.0	7.3	6.0	4.5	2.7	2.1	5.3
	Min/Max	1.9/3.5	3.0/5.7	4.1/6.5	4.4/7.5	5.7/9.2	6.7/9.8	7.2/9.3	6.0/8.8	4.7/7.2	3.0/5.9	1.6/4.0	1.5/2.9	4.9/5.8
Latitude	Average	3.0	4.2	5.1	6.2	7.1	7.7	7.7	7.1	6.1	4.7	2.9	2.3	5.3
	Min/Max	2.0/3.8	3.2/6.1	4.2/6.6	4.3/7.5	5.5/8.9	6.4/9.4	6.9/9.0	5.8/8.6	4.7/7.3	3.0/6.2	1.6/4.3	1.6/3.2	4.9/5.8
Latitude +15	Average	3.1	4.3	5.0	5.9	6.7	7.1	7.2	6.8	5.9	4.7	2.9	2.4	5.2
	Min/Max	2.1/4.0	3.2/6.3	4.1/6.6	4.1/7.2	5.1/8.4	5.9/8.8	6.4/8.4	5.5/8.2	4.5/7.1	3.0/6.3	1.6/4.4	1.7/3.3	4.8/5.6

Solar Radiation for 2-Axis Tracking Flat-Plate Collectors (kWh/m²/day), Uncertainty ±9%

Tracker		Jan	Feb	Mar	Apr	May	June	July	Aug	Sept	Oct	Nov	Dec	Year
2-Axis	Average	3.1	4.3	5.1	6.3	7.5	8.2	8.2	7.3	6.1	4.7	3.0	2.4	5.5
	Min/Max	2.1/4.0	3.2/6.3	4.2/6.7	4.5/7.6	5.8/9.3	6.8/10.1	7.3/9.4	6.0/8.8	4.7/7.3	3.0/6.3	1.6/4.4	1.7/3.4	5.1/6.0

Direct Beam Solar Radiation for Concentrating Collectors (kWh/m²/day), Uncertainty ±8%

Tracker		Jan	Feb	Mar	Apr	May	June	July	Aug	Sept	Oct	Nov	Dec	Year
1-Axis, E-W Horiz Axis	Average	1.5	2.0	2.2	2.7	3.2	3.7	3.6	3.2	2.8	2.3	1.5	1.1	2.5
	Min/Max	0.9/2.1	1.2/3.3	1.2/3.5	1.2/3.6	2.0/4.6	2.6/5.1	2.9/4.6	2.3/4.4	1.7/3.7	1.1/3.5	0.4/2.6	0.6/1.9	2.2/2.9
1-Axis, N-S Horiz Axis	Average	1.0	1.7	2.4	3.4	4.3	4.8	4.8	4.2	3.3	2.2	1.1	0.7	2.8
	Min/Max	0.6/1.4	1.0/2.7	1.4/3.8	1.7/4.6	2.7/6.2	3.4/6.7	3.9/6.2	3.1/5.7	2.0/4.3	1.0/3.4	0.3/2.0	0.4/1.2	2.5/3.3
1-Axis, N-S Tilt=Latitude	Average	1.6	2.4	2.9	3.7	4.2	4.6	4.6	4.3	3.7	2.9	1.7	1.2	3.2
	Min/Max	1.0/2.3	1.4/3.9	1.6/4.6	1.8/4.9	2.6/6.1	3.2/6.4	3.7/5.9	3.2/5.9	2.3/4.9	1.3/4.4	0.5/3.0	0.6/2.0	2.7/3.6
2-Axis	Average	1.8	2.5	2.9	3.7	4.4	5.0	5.0	4.5	3.8	3.0	1.7	1.3	3.3
	Min/Max	1.0/2.5	1.4/4.0	1.6/4.6	1.8/5.0	2.8/6.4	3.5/6.9	4.0/6.4	3.3/6.1	2.3/4.9	1.4/4.5	0.5/3.1	0.7/2.2	2.9/3.8

Average Climatic Conditions

Element	Jan	Feb	Mar	Apr	May	June	July	Aug	Sept	Oct	Nov	Dec	Year
Temperature (°C)	-5.1	-3.7	2.1	8.5	14.7	19.8	22.4	21.4	17.3	10.7	4.6	-2.1	9.2
Daily Minimum Temp	-9.1	-8.0	-2.8	2.7	8.4	13.5	16.3	15.3	11.4	4.9	0.1	-5.9	3.9
Daily Maximum Temp	-0.9	0.7	6.9	14.3	20.9	26.1	28.5	27.4	23.3	16.4	8.9	1.8	14.5
Record Minimum Temp	-29.4	-26.1	-20.0	-12.2	-3.9	2.2	5.0	3.3	-1.7	-8.3	-12.8	-23.3	-29.4
Record Maximum Temp	16.7	18.3	27.2	31.7	33.9	40.0	38.9	37.8	36.7	32.8	25.0	20.0	40.0
HDD, Base 18.3°C	725	616	504	295	135	21	0	9	57	242	413	632	3649
CDD, Base 18.3°C	0	0	0	0	21	64	128	103	27	4	0	0	348
Relative Humidity (%)	75	73	70	66	65	67	69	72	73	72	75	77	71
Wind Speed (m/s)	5.4	5.1	5.3	5.2	4.6	4.2	3.8	3.7	3.9	4.4	5.0	5.1	4.6

Appendix 6: System Layout



Appendix 7: PVL Installation and Cable Connections



Modules glued on the rubber membrane of the roof



Modules installed on the metallic seam of the roof



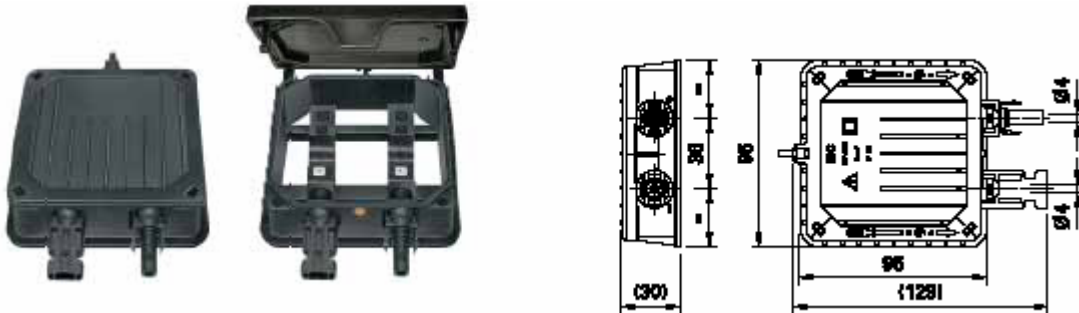
Quick connectors and cable housing




PVL Modules on Rubber Membrane

Appendix 8: Junction Box and BOS for Kyocera Modules

Each KC120 module has an M type junction box with 2 diodes⁶¹



Stainless steel nuts volume calculation

Nuts (stainless steel)		
	Number of nuts for T-connectors	400
	Number of nuts for inside connectors	384
	Total no. of nuts	784
	Volume per nut (cm ³)	2
	Density of Stainless steel (g/cm ³)	7.74
	Mass per nut, bolt, and washers (g)	15.48
	Mass for 784 nut sets (kg)	12.14

Connect energy high voltage PV array combiner box – 8 inputs



Two Seas Metalwork dimensions of vertical struts for the east side

East Side							Total length (in.)	Volume (LxBxT) (In³)
Row 1 - one assembly	Top support height	6.0	6.0	10.0	29.5	46.0	97.5	60.94
	Bottom support height	0.0	0.0	0.0	17.0	34.0	51.0	31.88
Row 2 - one assembly	Top support height	6.0	6.0	6.0	16.0	32.0	66.0	41.25
	Bottom support height	0.0	0.0	0.0	0.0	19.0	19.0	11.88
Row 3 - one assembly	Top support height	6.0	6.0	6.0	6.0	17.0	41.0	25.63
	Bottom support height	0.0	0.0	0.0	0.0	0.0	0.0	0.00
Row 4 - one assembly	Top support height	6.0	6.0	6.0	6.0	6.0	30.0	18.75
	Bottom support height	0.0	0.0	0.0	0.0	0.0	0.0	0.00
							304.5	190.31

Two Seas Metalwork dimensions of vertical struts for the west side

West Side							Total length (in.)	Volume (LxBxT) (In³)
Row 1 - one assembly	Top support height	33.5	18.0	6.0	6.0	6.0	69.5	43.44
	Bottom support height	21.0	6.0	0.0	0.0	0.0	27.0	16.88
Row 2 - one assembly	Top support height	18.5	6.0	6.0	6.0	6.0	42.5	26.56
	Bottom support height	7.5	0.0	0.0	0.0	0.0	7.5	4.69
Row 3 - one assembly	Top support height	6.0	6.0	6.0	6.0	6.0	30.0	18.75
	Bottom support height	0.0	0.0	0.0	0.0	0.0	0.0	0.00
Row 4 - one assembly	Top support height	0.0	0.0	0.0	0.0	0.0	0.0	0.00
	Bottom support height	0.0	0.0	0.0	0.0	0.0	0.0	0.00
							176.5	110.32

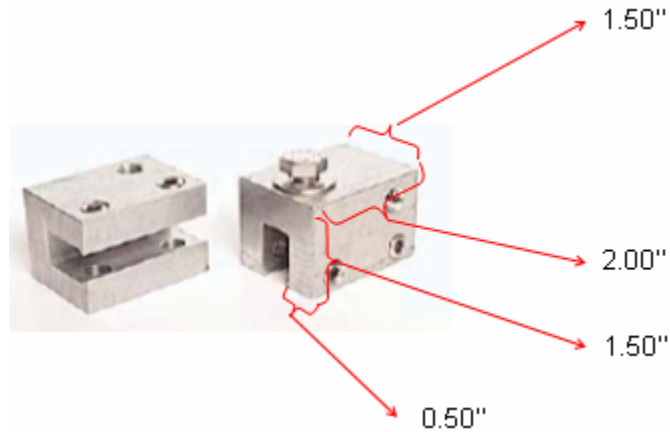
Aluminum requirements for the Two Seas Metalwork mounting structure

Vertical supporting struts	Arrays	Struts/Array	No. of struts		
Struts on the left side	4	10	40		
Struts on the right side	4	10	40		
Thickness (T)	0.125				
Breadth (B)	2.25				
Depth (D)	1.375				
Total Length (L) left	176.5				
Total Length (L) right	304.5				
Total Volume (In3)	300.63				
Total Volume (cm3)	4926.66	6.65 kg			
Diagonal struts					
Struts on the left side	3				
Struts on the right side	2				
Length(L) / strut	46				
Thickness (T)	0.125				
Breadth (B)	2				
Depth (D)	1.25				
Total length (L)	230				
Total Volume (In3)	129.38				
Total Volume (cm3)	2120.21	5.72 kg			
T-Connectors					
	Arrays	T-connectors /Array	No. of T-connectors	Nuts / Tconnector	No. of nuts
T connectors on the left side	4	10	40	5	200
T connectors on the right side	4	10	40	5	200
Length (L)	10				
Thickness (T)	0.125				
Breadth (B)	1.875				
Depth (D)	1.625				
Total Volume (In3)	512.50				
Total Volume (cm3)	8398.89	22.68 kg			
Inside Connectors (I-C)					
	Arrays	I-C / Array	No. of I-C	Nuts / IC	No. of nuts
IC on the left side	4	6	24	8	192
IC on the right side	4	6	24	8	192
Length (L)	10				
Thickness (T)	0.125				
Breadth (B)	1.8125				
Depth (D)	1.3125				
Total Volume (In3)	285.47				
Total Volume (cm3)	4678.28	12.63 kg			
			TOTAL MASS = 47.68 kg		

Appendix 9: UNI-SOLAR BOS Components

S-5-U Aluminum clamp

Clamps are manufactured from certified 6061 T6 aluminum, in strict conformity with "The Aluminum Association, Incorporated's, "Aluminum Standards and Data" and ASTM standard B-221. Dimensions of the S -5-U is 1.5" x 1.5" x 2" long. S-5-Z is 1.8" x 1.9" x 2" long⁶².



Aluminum clamp

Aluminum is modeled based on production of aluminium ingots from 75% virgin aluminium and 25% scrap by re-melting and casting of plain scrap from production waste (extrusion discards, sheet edge trim, turnings and millings) or plain post consumer scraps. Data derived from EAA (1993). Data for virgin aluminium are based on 40% production in Canada and 60% production in Western Europe and are representative for Switzerland.

Appendix 10: Energy Requirement for Hoisting Equipment

Loading:

$$27 \text{ hoists} \times \frac{45 \text{ s}}{\text{hoist}} \times \frac{1 \text{ hour}}{3600 \text{ s}} \times \frac{15.1 \text{ gal}}{\text{hour}} \times \frac{125 \text{ kBtu}}{\text{gal.}} = 632.8 \text{ kBtu}$$

Idling:

$$= 1.5 \text{ hours} - \left(27 \text{ hoists} \times \frac{45 \text{ s}}{\text{hoist}} \times \frac{1 \text{ hour}}{3600 \text{ s}} \right) = 1.1625 \text{ h}$$

$$1.1625 \times \frac{15.1 \text{ gal}}{\text{hour}} \times \frac{125 \text{ kBtu}}{\text{gal.}} = 2180 \text{ kBtu}$$

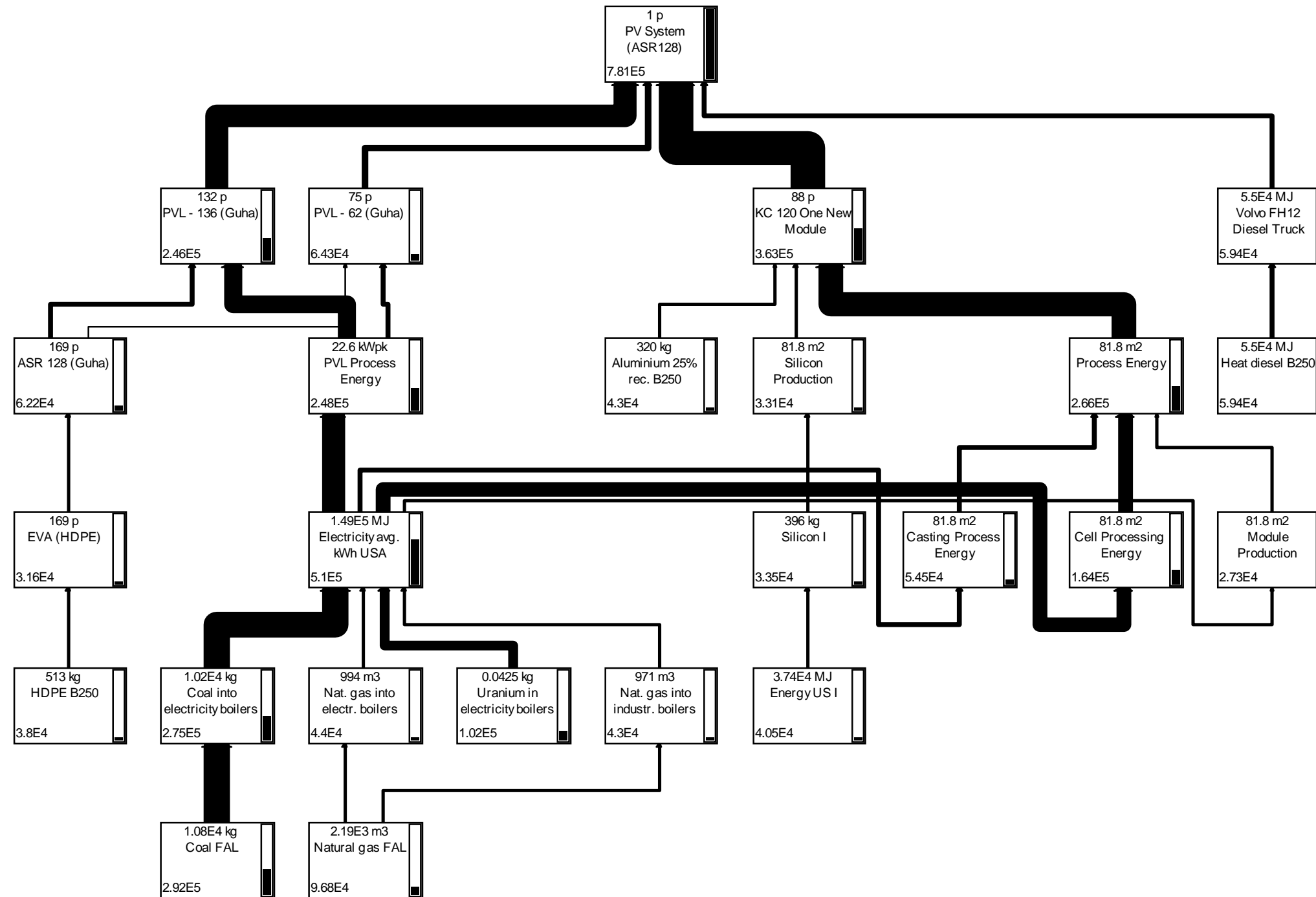
Total energy consumption so far:

$$= 632.8 + 2,180 = 2,812.8 \text{ kBtu}$$

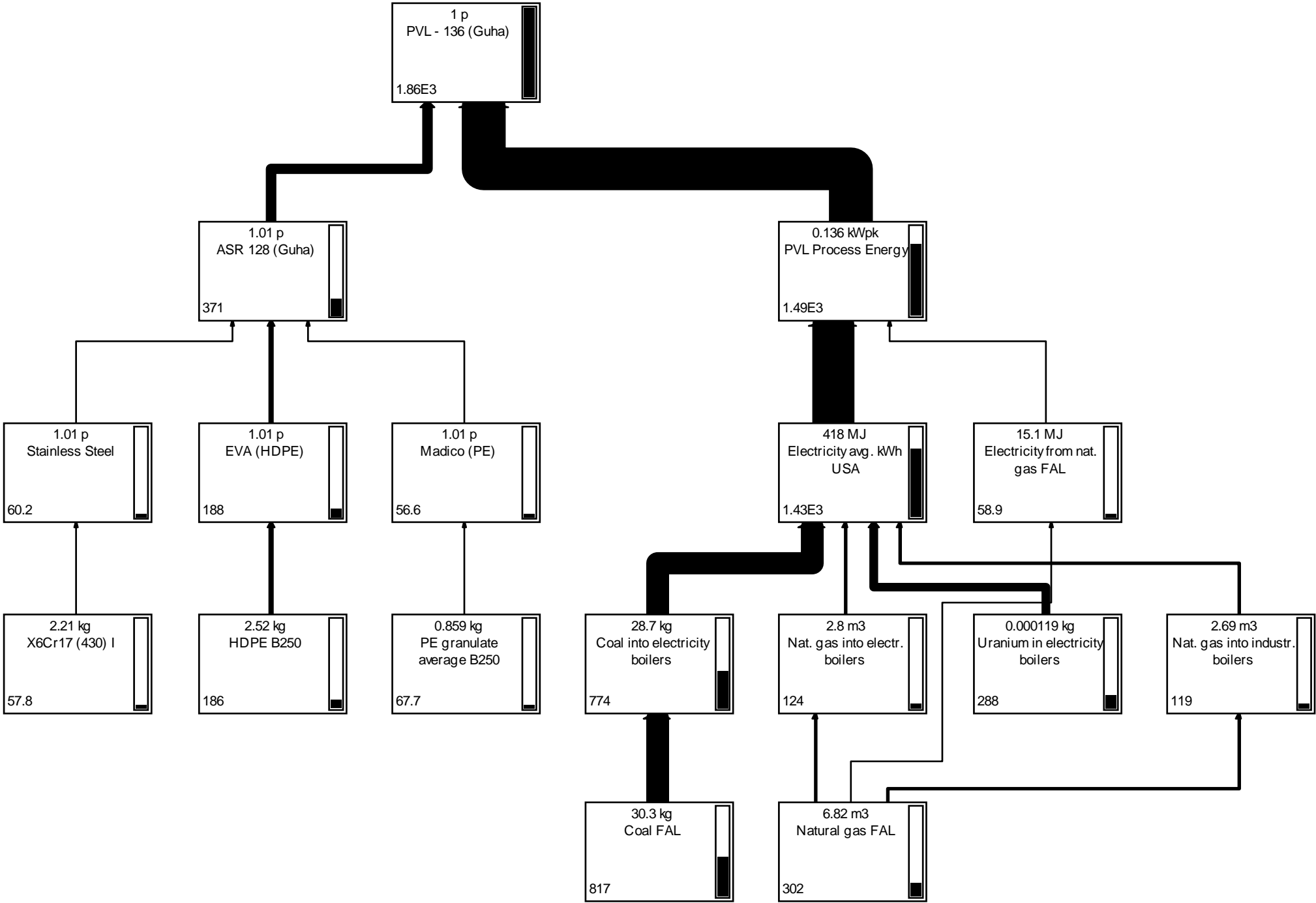
~ 3,000 MJ

Appendix 11: Level Diagrams

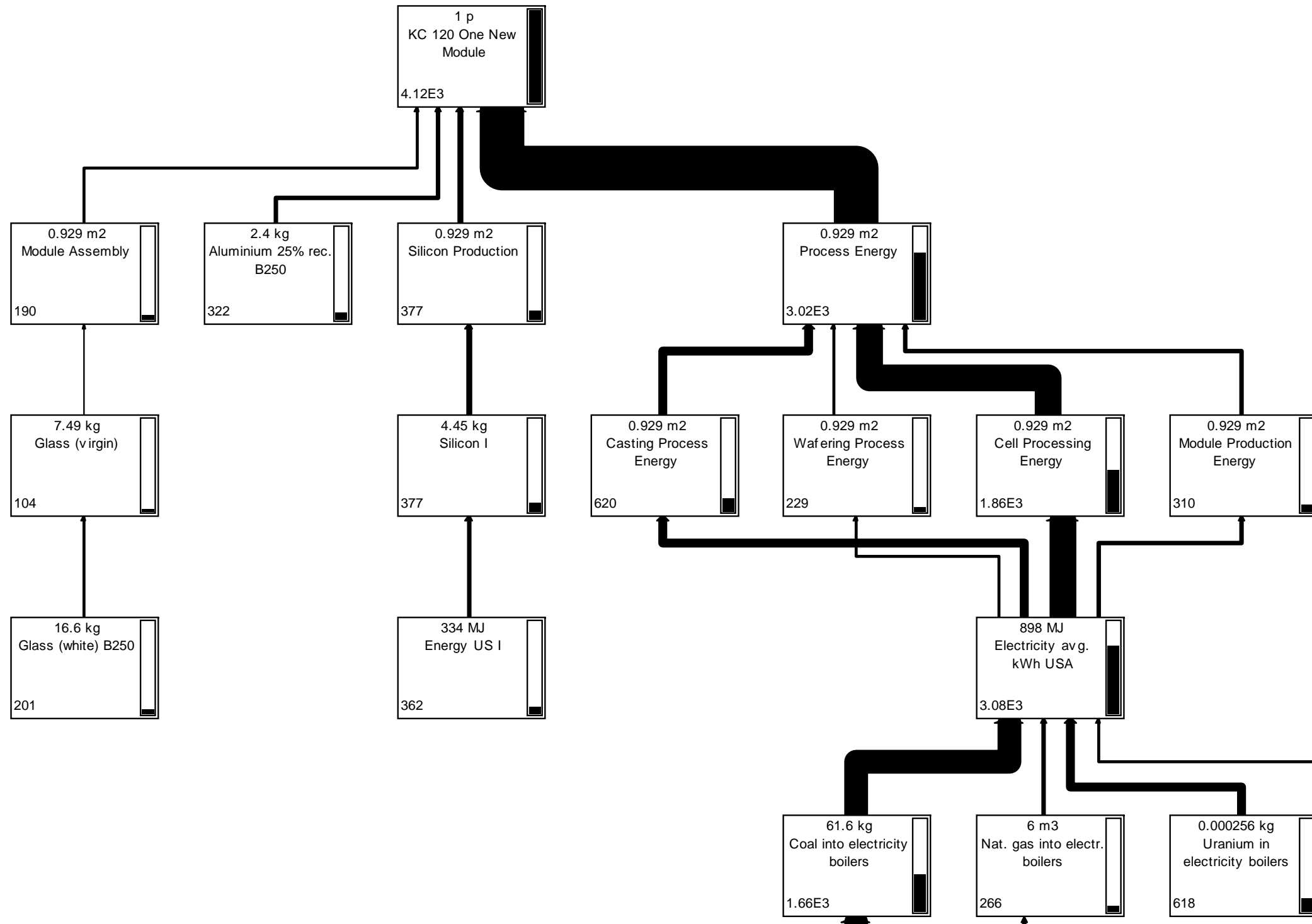
Level Diagram of the PV System at the University of Michigan



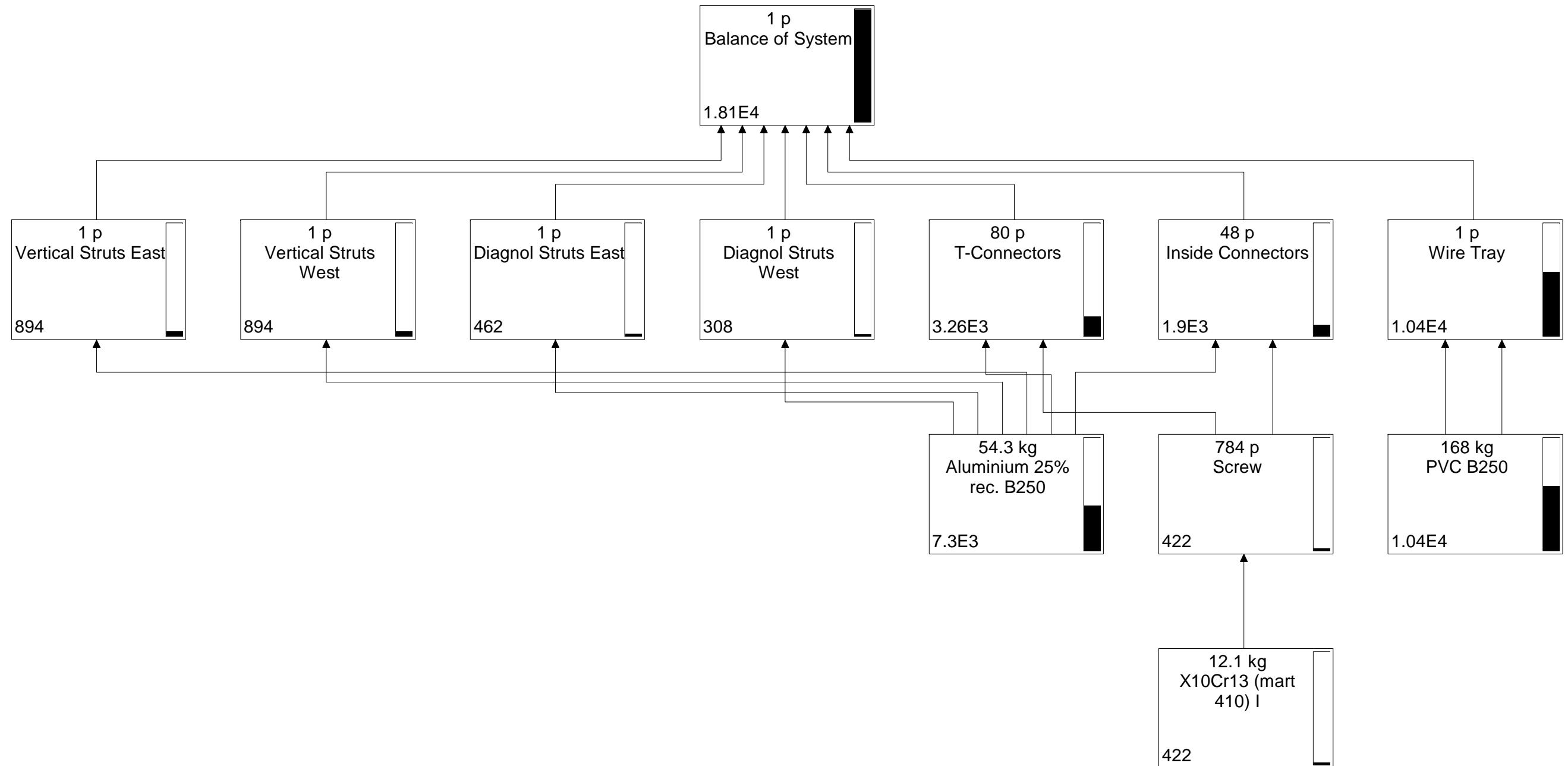
Level Diagram of the Unisolar PVL 136 Amorphous PV Module



Level Diagram of the Kyocera Multi-Crystalline Module



Level Diagram of Balance of System Components (BOS)



Level Diagram of Ballard Inverter

